FINAL REPORT

to

National Aeronautics and Space Administration

under the

Sustaining University Program

Project Grant NGL 34-001-005

Multidisciplinary Aeronautics and Space-Related Research - Urban Transportation Systems

DME/TR-72-07

DUKE UNIVERSITY

Durham, North Carolina

June, 1972

FINAL REPORT

to

National Aeronautics and Space Administration

under the
Sustaining University Program
Project Grant NGL 34-001-005

MULTIDISCIPLINARY AERONAUTICS AND SPACE-RELATED RESEARCH - URBAN TRANSPORTATION SYSTEMS

DME/TR-72-07

DUKE UNIVERSITY
Durham, North Carolina

June 1972

Jack B. Chaddock
Project Director

FOREWORD

On February 1, 1965, a scientific research program under the NASA Sustaining University Program was initiated at Duke University. The program entitled, "Multidisciplinary Space-Related Research in the Physical, Engineering, and Life Sciences," received an initial grant of 200,000 dollars, step-funded over three years. It was conceived as a seed type grant to establish new group research activities, particularly ones that would promote multi-disciplinary projects. A primary objective was to focus attention on some significant problems where developments in space technology could be related to their study and solution.

Four supplements to the initial grant were approved in response to proposals submitted in 1966, 67, 68, and 69. Each supplementary grant was in the amount of 100,000 dollars which, through step-funding extended the grant to January 31, 1972. A no cost extension to June 30, 1972 was requested to complete the research and prepare this final report.

Thirty-five Duke University faculty members, and a larger number of graduate students, have benefited through this grant. It has been a pleasant and rewarding experience for me to have served as Chairman of the Space Studies Committee, which supervised the program, since 1967. We acknowledge with thanks the support and cooperation of the NASA Sustaining University Grant Office. In particular, we express our appreciation to W. A. Greene, Herbert B. Quinn, and Francis Smith of the Office of University Affairs.

Jack B. Chaddock
6/29/72

CONTENTS

I. OUTLINE OF THE DUKE PROGRAM

OUTLINE OF THE DUKE PROGRAM

A. Objectives

In its proposal of September 1964, initiating the NASA Sustaining University Program at Duke University the objectives were given as:

1. The establishment of a broad space-oriented program of research, to become an integral part of the University's spectrum of activities in furthering basic knowledge and in the production of research personnel with advanced degrees.
2. Through a formal "Space" program, focus attention on some of the unsolved problems related to space exploration and, thereby, serve as a source of enrichment for research output and research potential.
3. Establish a means of initiating research in areas of mutual interest to NASA and the University.
4. Assist in laying the foundation for the development of a broadly based multidisciplinary research program.

B. Administration

The program was directed by a Space Studies Committee consisting of five senior faculty and administrative officers appointed by the Provost. Those who served on the committee are as follows:

1. John J. Gergen, Professor and Chairman, Department of Mathematics (Member 1964-66, Chairman Oct. 1965 to July 1966)
2. Harold W. Lewis, Professor of Physics, Vice Provost and Dean of Faculty (Member 1964-72, Chairman July 1964 to Oct. 1965)
3. James L. Meriam, Professor of Engineering Mechanics, Dean of the School of Engineering, 1963-69, (Member 1964-66)
4. Richard L. Predmore, Professor of Romance Languages, Dean of Graduate School, 1962-69, (Member 1964-69)

5. Daniel C. Tosteson, James B. Duke Professor and Chairman, Department of Physiology and Pharmacology (Member 1964-70)
6. Charles R. Vail, Professor of Electrical Engineering and Associate Dean of School of Engineering (Replaced J. L. Meriam and served as Chairman July 1966 - June 1967)
7. Jack B. Chaddock, Professor and Chairman, Department of Mechanical Engineering (Replaced C. R. Vail and served as Chairman June 1967 to June 1972)
8. John C. McKinney, Professor of Sociology and Dean of the Graduate School, 1969- , (Replaced R. L. Predmore as member from 1969-72)
9. Jacob J. Blum, Professor of Physiology, (Replaced D. C. Tosteson as a member 1970-72)

C. Operation

The program was initiated on February 1, 1965 under a grant of 200,000 dollars, step-funded for three years. It was conceived as a seed-type program under the title "Multidisciplinary Space Related Research in the Physical, Engineering, and Life Sciences". The overall objective was to focus attention on some problems where scientific developments in space technology could be related to their study and solution.

The administrative "Space Studies Committee" solicited proposals from the faculty in the disciplinary areas relevant to the proposed program, and acted as a review panel in selecting projects for funding. It did not attempt to be innovative in organizing a broad interdisciplinary program, though it made clear its encouragement for cooperative endeavors that cut across traditional disciplines. For the most part, in the first four years of the program, 1965-68, the funds were expended on projects of individual faculty members. The criterion used in selection was: a) the quality of the proposed research; b) the initiation of a new area of research which has potential for expansion and long-range contribution to the University and the Nation; c) the qualifications of the investigator, and, if a younger faculty member, his potential for research contribution in the proposed field; d) the supplementing of

research laboratories or faculty with proven excellence to direct their attention and capabilities to space-related problems; and e) the broad distribution of projects among disciplines in physical, engineering, and life sciences.

Proposals for continuation of the Sustaining University Program as a seed grant for space-related research were approved for the years 1966, 1967, and 1968 in the amounts of 100,000 dollars. Over the initial four year period of the program 1965-68 a total of nineteen projects were established through subgrants made by the Space Studies Committee. A listing of these projects is given in Table I. Details of the objectives and results of these projects have been reported in the prior annual reports on this project.

In 1968 a NASA study of the effectiveness of the Sustaining University Program was completed and documented in a report, SP-185, "A Study of NASA University Programs". That report gave the following statement on goals of the SUP: The broad goals include acceleration of the transfer of technology between segments of the economy, development of a capability for multidisciplinary research on societal problems, development of sensitivity to real-world problems, and development of capability to respond institutionally to societal problems.

In response to these goals the proposal for continuation of the Duke SUP Grant in 1969 was for the development of a multidisciplinary team research effort on Urban Transportation Systems. The relatedness of NASA's missions in aeronautics and space exploration, and in exploiting the technological, and project management developments of NASA to the solution of national problems in transportation was cited. Supporting evidence for initiating this research effort at Duke University was in terms of the following activities:

1. Project Mountainwell - This research project on pneumatic tube propulsion as a high speed ground transportation system, was an outgrowth of an Army Research Office (Durham) study of missile vacuum propulsion. Faculty from the Civil and Mechanical Engineering departments participated in this research.

TABLE I

PROJECTS RECEIVING SUPPORT
under the program

MULTIDISCIPLINARY SPACE RELATED RESEARCH IN THE PHYSICAL, ENGINEERING AND LIFE SCIENCES

1965-70

No.	Active Years	Principal Investigator	Department
1	'65-68	G. W. Pearsall	Mechanical Engineering
	(Title: "An Investigation of Vibration Forming")		
2	'65-67	D. W. Hill	Civil Engineering
	(Title: "Effects of Intersections on the Distribution of Stresses in Thin Elastic Shells")		
3	'65-68	H. G. Robinson	Physics Department
	(Title: "Experiments on the Properties of Atoms and Ions by Radiofrequency and Microwave Spectroscopy")		
4	'65-67	D. C. Tosteson	Department of Physiology and Pharmacology
	(Title: "The Architecture of Physiological Systems")		
5	'65-67	D. S. Burdick	Mathematics Department
		G. T. Williams	Mathematics Department
	(Title: "Research in Stochastic Processes and Other Areas of Statistics")		
6	'66-69	R. B. Kerr	Electrical Engineering
		L. W. Nolte	Electrical Engineering
	"Title: "Informational Processing of Signals for Advanced Control Processes")		
7	'66-67	F. W. Barton	Civil Engineering
	(Title: "A Study of Human Response to Dynamic Loads")		
8	'67-69	S. Vogel	Zoology Department
	"Title: "Heat Dissipation by Organisms through Free and Forced Convection")		
9	'67-69	D. B. Chesnut	Chemistry Department
	(Title: "Electron Paramagnetic Resonance Studies of Organic Materials")		

Table I (Continued)

No.	Active Years	Principal Investigator	Department
10	'67-68	J. V. Baxley	Mathematics Department
	(Title: "Numerical Methods for Singular Differential Operators")		
11	1968	R. W. Wheat	Microbiology Department
	(Title: "Studies on the Pathogenic Fungus, Coccidioides Immitis")		
12	'68-70	J. W. Moore	Physiology and Biomedical Engineering
	(Title: "Hybrid Delay Line Filters")		
13	'68-70	W. R. Krigbaum	Chemistry Department
	(Title: "X-Ray Diffraction Studies of Orientation in Drawn and Worked Materials")		
14	'68-70	R. A. Palmer	Chemistry Department
	(Title: "Structure and Bonding in Metal-Containing Inorganic Heterocycles")		
15	'68-69	D. G. Herr	Mathematics Department
	(Title: "Statistical Inference Based on a General Stochastic Model")		
16	1968	M. Weisfeld	Mathematics Department
	(Title: "Studies in the Analytic Theory of Differential Equations")		
17	'68-70	W. T. Joines	Electrical Engineering
	(Title: "A Study of Materials and Fields Associated with Microwave Integrated Circuits")		
18	'68-70	J. J. Murray	Mechanical Engineering
		C. M. Harman	Mechanical Engineering
	(Title: "The High "G" Instantaneous Acceleration Apparatus")		
19	'68-70	J. N. Macduff	Mechanical Engineering
	(Title: "Determination of Human Dynamic Characteristics by Impulse Testing")		

2. Urban Planning and Transportation - an expanding area of instruction and research in Civil Engineering.
3. Engineering Research in Materials, Dynamic Systems and Controls - Some eight research projects that are transportation related were noted.
4. Business Administration - A newly approved MBA and Ph.D. program in Business Administration in 1968 brought to the Duke Community a new group of faculty. Their curriculum and research programs are devoted to a rigorous analytic approach to decision problems. In particular, strong interest was expressed in dealing with problems of design of complex socio-economic systems, as exemplified by transportation systems.

Approval for the Transportation Systems Study in the form of an additional 100,000 dollars of grant support was given in April, 1969. Under the step-funding nature of the SUP, the research has been conducted over the three year period to June 30, 1972. A listing of the research projects supported is given in Table II. Part II of this report presents the results of those projects.

TABLE II

PROJECTS RECEIVING SUPPORT
under the program

MULTIDISCIPLINARY AERONAUTICS AND SPACE-RELATED RESEARCH
- URBAN TRANSPORTATION SYSTEMS

1969-72

No.	Active Years	Principal Investigator	Department
1	'69-72	H. H. Baligh	Graduate School of Business Administration
		D. C. Dellinger	Graduate School of Business Administration
		L. D. Volpp	Graduate School of Business Administration
	(Title: "Systems Analysis of Transportation")		
2	'69-72	J. F. Wilson	Civil Engineering
		D. Wright	Mechanical Engineering
	(Title: "Guideway and Vehicle Dynamics for High Speed Ground Transportation")		
3	'69-72	J. B. Chaddock	Mechanical Engineering
		B. R. Munson	Mechanical Engineering
		D. Wright	Mechanical Engineering
	(Title: "Tube Transportation")		

II. RESEARCH PROJECT SUMMARIES

A. SYSTEMS ANALYSIS OF TRANSPORTATION

1. "A Model for the Systems Analysis of Transportation Problems," Helmy H. Baligh, David C. Dellinger, and Louis D. Volpp, Graduate School of Business Administration (For Presentation at the First Conference on Management Sciences, Computer Applications, and Industrial Development, Cairo, Egypt, July 3-6, 1972.)

2. "An Algebra for the Analysis and Design of Transportation Networks," Helmy H. Baligh, David C. Dellinger, and Louis D. Volpp. (A summary of a paper to be published in TRANSPORTATION SCIENCE, v. 6, no. 6, Nov. 1972.)

A MODEL FOR THE SYSTEMS ANALYSIS OF TRANSPORTATION PROBLEMS

H. H. Baligh, D. C. Dellinger, and Louis D. Volpp
Graduate School of Business Administration, Duke University

Introduction

Effective application of systems analysis to transportation planning depends on development of a rigorous theoretical foundation. An approach to developing that foundation is the subject of this paper. "In many respects the (applications of systems analysis to transportation planning) are narrow in focus, primitive in theory, and limited in effectiveness."[1] The theoretic underpinnings for systems analysis in the field of transportation are sought in this paper through development of theory with a broad focus capable of being applied effectively.

A Conceptual View of the Transportation Problem

All transportation problems derive from the preferences of people concerning their geographic location in time, and concerning the geographic locations of other people and economic goods. People desire to change the location of goods and people, including themselves. In addition, people care about the kind of experience associated with place transformations and about the resource cost of those transformations. The transportation problem, then, can be described in terms of peoples' preferences over: (a) possible place-time points of people and goods, (b) possible experiences related to alteration in the place-time space, (c) the cost, or resource requirements, for possible place transformations, and (d) the indirect effects of possible place transformations.

Place-Time Preferences

One, unique geographic position defines the geographic state of any person or thing at any instant in time. This state can be modified in an infinite number of ways for some future time, and people have preferences over such possible future states. The preference a given person has for his or others' positions is influenced by the location of other people, by the location of things, and by time. Such a change of location or geographic state is transportation, and the capacity to make such place alterations is an essential component of the definition of a transportation system.

Quality-of-Experience Preferences

The change in the place of any person or thing necessarily requires a change in time. People care about that span of time and the preference a person holds for "stay-put time" as opposed to "travel time" depends on the quality of experiences pertinent to the use of time. Since the length of time required for a place-to-place alteration may affect the quality of the "transportation experience", people should be expected to show some quality-of-experience versus time preference. Very simply, whether or not a person chooses a place alteration for himself, another person, or some good, depends on the available quality of events over the related span of time, while stationary or in transit.

Resource Preferences

Place-to-place change requires time, has associated with it some quality of experience, and absorbs resources. Since transportation can be accomplished only through use of valuable resources, people care about the relative value of the place-time alteration and about the resources used in the change. People would, therefore, be expected to choose transportation in a manner that would maximize their satisfaction from the resources expended.

Indirect Effect Preferences

Preferences pertinent to a transportation system include those over the side effects of possible systems. These side effects include: changes in the value of land in areas served or not served; the effects on the "natural environment"; the demographic pattern in and around cities; the effects on the national, regional, and local economies from both the building and the use of transportation systems. The quantity and quality of some side effects can be affected by variation in the physical system and, in turn variation in resources used. Obviously, preferences over these side effects and resources are a critical part of some transportation problems today.

Criteria for Structuring the Transportation Problem

Ideally, the transportation problem should be described carefully in order to lead to the best solution, where both the solution at the planning horizon and the path to that point in time are considered. Since choice of the "best" transportation system for any given time is affected by the social and economic conditions and goals existing at that time, the transportation problem should be described in a way that facilitates a continual process of solution.

In contrast to the ideal, frequently we are forced to solve sub-problems of the general transportation problem with little or no orderly concern devoted either to other sub-problems associated with the first or to the problems that will be caused by the solution. Even though undesirable, this approach is made necessary by the pressing nature of some transportation sub-problems, and the lack of a well developed structure for making adjustments in the general transportation system to meet

the requirements of a changing environment.

The results desired from a model designed to structure the transportation problem are those which overcome the above problems. That is, a proper structure ought to preserve, and perhaps enhance, our ability to solve short period sub-problems in the transportation system. It ought to facilitate forecasting the effects of possible solutions to the sub-problem and to facilitate selecting the solution that will tend to improve the general system.

To achieve these ends, the general transportation problem should be structured so that it can be broken into component problems. Provision in the general model for this decomposition needs to be pointed toward achieving three specific characteristics: tractability, completeness, and connectedness.

Tractability Characteristic

The general transportation problem should be structured so that its decomposition produces components or sub-problems that are amenable to solution. Obviously, this involves seeking an effective balance between the types and quantities of intellectual effort available, and the points of reasonable segmentation of the general problem. This characteristic is not difficult to achieve when considered alone, but meeting the need for tractability while achieving completeness and connectedness is the requirement for a proper structure of the general transportation problem.

Completeness Characteristic

The proper structure of the general transportation problem ought to be decomposable into sub-problems which, taken together, omit none of the important transportation issues. Just as above, this criterion is easy to meet when considered alone, but to achieve tractability in the components while focusing on vital issues is both more difficult and more worthwhile.

Connectedness Characteristic

Possible solutions to the sub-problems must be recomposable so that the general transportation system can be evaluated in light of the general transportation problem. This requires that the solutions to the sub-problems be expressed in terms of variables that permit connecting these sub-problem solutions into a potential solution to the general transportation problem.

Notice that if the characteristics of tractability, completeness, and connectedness were achieved, the general transportation problem could be decomposed into sub-problems that could be solved, the component problems would be complete enough to represent all of the important issues in the general transportation problem, and the possible solutions to the sub-problems could be fitted together into potential general transportation problem solutions.

A Decomposition of the General Transportation Problem

The criteria for structuring the general transportation problem are applied in this section by identifying segments into which the general problem can be decomposed. These segments or components ought to meet the criteria of tractability and completeness, or ought to be decomposable themselves into components that meet these two criteria. In the following section on Transformations some of the relationships between the components are examined in an attempt to move toward proper recomposition and, therefore, connectedness.

The four segments into which the general transportation problem is decomposed are the basic resource inputs, the physical components, the network, and people and their preferences. The role of each of these in a study of transportation follows.

Basic Resource Inputs

A transportation system can be created only through use of resources. These resources may be used in quantities so great that an appreciable effect on the economy results. In order to examine these effects, and in order to keep price changes over time in perspective, these resources should be treated in their "natural" form and quantities, rather than in some common numeraire such as dollar cost. The basic resource inputs lead both remotely (in the case of resources used in research) and proximately (in the case of transportation machine materials) to the creation of the second of the four main segments.

The Physical Components

The physical system comprises all of the physical components and their relationships. These components are identified physically in classical engineering form and have physical capacities and relationships that limit and define the ways in which the physical system can be operated. This physical system needs to be defined and analyzed in a manner that specifies actual and potential physical components and their actual and potential relationships. The variables in whose terms the physical components are described include both those that are necessary to relate the physical components to the use of resources and those which are necessary to relate the physical components to each other in the various feasible physical systems.

In order both to analyze the broad transportation problem (i.e., decompose the broad problem into workable components) and to recompose the conclusions or solutions developed into a workable solution to the broad problem, the engineering technology must be expressible in terms of either (a) the possible variations in the resource input that would be required to produce a given set of physical component outputs, or (b) the possible variations in the physical component output that could

be produced from a given set of resource input, or preferably both. This view of the form in which engineering technology might be expressed is neither new nor innovative but it is a view to which the performance does not always conform.

Finally, the definition of the physical system must provide for identification of any general relationships that may exist between the physical system and users. As explained in the following section, the link between the physical system and users is the network, so the physical system needs to be described in a manner that will permit specification of the various networks that are feasible from a given physical system, and to specify the various physical systems which may be used to produce any given network. Obviously, given a physical system we wish to produce the "best" network from it. Given a network to be created, we wish to do so by selecting the "best" physical system for that task.

The Network

Any physical transportation system, however defined, has associated with it a set of networks that are physically feasible. For each such physical system there exists a set of possible operating rules, each of which defines a subset of the set of feasible networks associated with that physical system. The choice is among pairs, each of which is a physical system and a set of operating rules. Thus, a set of operating rules applied to a physical system defines the capacity of this system in terms of the place-time transformations, the quality of those transformations, and the side effects from the system. These are the terms in which preferences of people for transportation can be expressed.

The potential or actual place-time alterations and the potential or actual quality of the transformations form a network. Notice that the purely physical segment plus a set of operating

rules create a network. The network, then, reflects the capacity to provide movement of people and things from place to place, over time, along with some specifiable quality of experience for the movements. The side effects mentioned earlier are not an element of the network, but are one of the outputs of it.

The term network in the context of transportation is applied to any group of place-time transformations and an associated group of vectors that express measures of quality and capacity of each transformation. These vectors do not specify anything relating to the physical system, but they do specify the output which may be obtained from a physical system. The concept of a network is an abstract description of some group of potential changes in the state of a person or thing. That state is defined in terms of origin and destination in place and time, and includes some description of the quality and capacity associated with these changes. The development of such an abstract concept is essential for the analysis of the general transportation problem. This point is brought out briefly in the paper by Baumol and Quandt [2].

This abstract concept of a network also needs to be developed formally, so that existing or new analytic tools of logic and mathematics may be employed in the analysis and design of transportation systems. Whatever detailed form the definition of a network is given, one can specify at this point those characteristics the definition must have if it is to be analytically useful and practical. First, the definition of a network should enable us to identify those properties of the network which affect its "value", and to identify the manner in which variations in these properties in combination will alter such "value". Second, the definition should provide that any change of property in a network produces what is in effect another

network. These variations in the characteristics of a network need to be described in a form that permits analysis of just how "value" or "resource usage" varies with changes in the network.

These characteristics of the definition of a network are needed for efficient analysis and treatment of the transportation problem. Without these qualities, conclusions on either the value or the resource usage of one network cannot be obtained from a knowledge about such value and resource usage for any given set of other networks. Research on any particular network will add nothing but hunches to our knowledge of another network unless we can somehow compare networks on the basis of their individual properties. A proper network definition lets the analyst avoid a complete search of all networks in his attempt to obtain an idea of how close any choice of network might be to that which is optimum. With a proper definition, he can develop procedures that indicate where next to look to obtain a "better" network. A large number of transportation research efforts have ignored this point with the result that they are unable to evaluate more than a finite number of networks, and that they never have any basis in the evaluation for judging how one more network may be designed that is conceptually guaranteed to be more valuable than those specifically studied. The definition must provide for analysis of the important problems, and must provide for connections to the other major components in this first stage of decomposition of the general transportation problem. To achieve tractability, and to provide completeness and connectedness within the major component "network", special attention needs to be devoted to the problems of composition and decomposition.

The definition of a network must permit one to "compose" two networks and get a third network. This property is needed

because we do not always have the capacity to analyze any network directly without first analyzing individually other networks which, when put together, somehow give us the initial network. Thus, we need to be able to decompose networks into more simple ones. But if one network is analyzed, then another is analyzed, we should expect to have developed some conclusions to some third network. That third network is the one which would have been obtained if the two networks previously studied had been combined. We need therefore a definition that permits us to make this combination. In simple terms, if we analyze the network or railroads, then the network of airlines, we may from this analysis obtain general concepts regarding the analysis of the network of rail and air.

If the conditions to relate properties of networks to the value of those networks are available, then we would like in a simple process to be able to "compose" the value of two networks into a value of the network which is a composition of the two. The composition of value may not be simple, but in the analysis of one network some use may come from the analysis of networks which together compose it. This whole idea is essential in that the value of any network depends on other existing networks. Some concept of the value of the total network with a new added network and the total network without this new added network is necessary before we can evaluate the added network. For example, of what value would a Metroliner be if those who want to use it cannot find adequate transportation to the embarkation point? Complete enumeration of existing networks is the only avenue available unless we can compose and decompose networks. Even where general relationships of network properties and value of networks may not be available because of the weakness in the definition or because of difficulties in estimating such relationships, composition and decomposition of networks permits us

to learn something about the value of one network from knowledge of the values of some other networks related to it. Composition and decomposition of networks also permits us to define rigorously the relationships that must exist between networks before any such knowledge may be transferred from the value of one network to that of another.

We have developed formally this concept of a network in a companion paper entitled "An Algebra for the Analysis and Design of Transportation Networks."[3]

People

The transportation capacity of a transportation system is merely potential until the network is used to accomplish a transportation task. The most direct impact people have on the system is as users but they also express preferences for certain networks in non-user roles such as individuals who like or dislike noise, pollution, or the physical appearance of particular physical systems; as investors who buy automobiles or operate transportation services; as non-users who relocate their homes or businesses to avoid or use transportation; or as social groups (governments) which finance, research and develop projects, subsidize physical systems or constrain operating rules. The actual consequences of selecting any network can be estimated only through the consideration of people (and their preferences over resources), the networks that can be created by using these resources, and the side effects from use of those networks.

Transformations Between Major Segments

We have decomposed the general transportation problem into four major components (resources, physical systems, networks,

and people). With the exception of people (whose role will be discussed later), these components describe sets which can be related one to the other by transformations, or functions in a mathematical sense. The alternatives from which decision makers choose are sets of possible transformations. One can by a choice of operating rules, transform a physical system to a network; by choice of an engineering design, transform a set of resources into a physical system. People can, by a choice to utilize certain links in the network, transform a potential trip into a real trip. These possible transformations make up the decision alternatives.

Physical Components to Network Through Management Technology

The "end points" of this transformation process are physical components and networks. Any set of transportation capacities, or any network, can be made available for service only through use of physical components. However, most conceivable sets of physical components could be operated according to more than one set of rules. Hence, a given set of physical components might be used to produce any one of many networks, the determining factor being the operating rules.

The knowledge we have available for use in the design of operating rules can be considered to be the managerial technology. The design of a set of operating rules is restricted by the available managerial technology at the time, and the managerial technology used is, in turn, restricted by what is physically feasible. Further, the range of physically feasible alternatives is limited most generally by the "laws of nature" and the characteristics of the physical components for creation of the network. In general, operating rules are defined in a very broad sense to include such things as operating speeds, maintenance policies, crew training, schedules, etc.

Resources to Physical Systems Through Engineering Technology

The transformations of resources (material, land, manpower) into physical transportation systems are familiar ones. In this case, the term engineering technology is used in a very broad sense to include all the activities (design, production, construction, etc.) which are necessary to produce the elements of physical transportation systems (highways, automobiles, aircraft, etc.) from common resources. This set of decision alternatives usually receives a great deal of attention and a great deal of public debate.

It should be noted that it is inappropriate to consider either the set of transformations from resources to physical systems or the set of transformations from physical system to network in isolation. Taken together, they define the relationships between resources and networks, the elements essential to decision makers. In isolation, they define only partial relationships. Efforts to choose these transformations can be expended in two basically different ways: to select directly from existing technology, or to engage in research to increase the set from which the choice is to be made.

Network to "State of the World" Through Preferences of People

Preferences of people over combined networks, physical systems, and resources are based in the final analysis on their preferences for the place-time states of people and things, which might be called the "state of the world". The preferences for different states of the world are fundamental to the changes which are brought about in these states. Such preferences are the bases for the preferences on networks, physical systems, and resources. These derived preferences are expressed in two basically different ways, individual and group responses or choices. The individual responds to an existing network in the short run by using some or none of the capacity offered. This

form of the response determines the output of the systems, which can be called user output. The individual can also respond in the long run by changing his life style or the location of his home or office, by purchasing an automobile, or taking some other action which changes the demographic, social, physical, economic, or political character of the area. The first of these forms of individual response is normally associated with transportation demand studies while the second type is associated with studies of the economic impact of transportation systems.

The individual preferences which are expressed through groups (frequently some level of government) are of a different character. These preferences are based not so much on the user characteristics of networks as on a combination of (2) the non-user characteristics of the network, such as noise, pollution and beauty, and (b) the demographic, social, physical, economic, and political characteristics which result from individual preferences and networks. The group preferences are expressed as governmental actions which tend to limit the set of networks from which people, as individuals, can choose.

Once again, a network is defined in terms of the alteration in place-time locations of people or things and in terms of both the quality and capacity of any such place-time alterations. Whether or not any transporting is accomplished depends on whether or not the capacity is used. The actual use of the capacity results in an actual place-time alteration, a user output. Notice that if a network moves a person in time only, while in the same location, it can be considered output. For example, a transfer point in a network may provide for waiting capacity, and use of that capacity constitutes output.

The relationship between a network and the user output from that network depends on both the preferences of the actual and potential users on the one hand and on the economic opportunities

available to those actual and potential users on the other hand. The economic opportunities open to users include both transportation alternatives and other economic alternatives. The reason the latter should be included is that use of the place-time alteration capacity of a network may require the user to make some payment for use of the service. That problem of choice can be considered in the classical economic terms of the user preferences and the user budget of economic resources. This "consumer behavior" aspect of the transportation problem is analogous to the problems of choosing engineering or managerial technology.

The long run effects of the non-user, individual preferences are not very well understood, but there is ample evidence to indicate that the selection of a transportation system is to some extent a cause, rather than a pure result of, demographic, social, and economic growth. The location of railroads, for example, to a large extent determined population patterns in the development of the West. Good highway systems have stimulated economic growth in many regions. Improved urban transportation systems have fostered the development of suburban residential areas. These effects are generally more relevant to group preferences, expressed through governmental action, than those network characteristics which are particularly relevant to individual users. Consequently, even though these effects result from individual preferences as do user outputs, they are treated as a separate class of transportation system "outputs".

In the same sense that individual preferences defined over physical systems alone are inadequate for analysis, group preferences expressed over networks alone are also inadequate for analysis. In the case of individual users, the properties or attributes of a transportation system relevant to his choice were described in a network. In the case of group preferences, the relevant properties are defined in terms of non-user output

effects (the demographic, social, economic, physical, and political effects), the network (pollution, noise, beauty, etc.), physical system (political interest in certain modes), and resource requirements. The choice is not the simple problem of choosing a single transformation, such as from resources to physical system or physical systems to networks. It is a choice over all these alternatives, and the choice depends on individual responses, both users and non-users. This is the essence of the problem facing the government in its role as interpreter of group preferences.

Effects and Feasibility of the Model

We have tried to indicate what a general model of a transportation problem ought to look like. In so doing we relied on our concepts of how such a model would help us solve a large number of highly similar yet non-identical politically and administratively localized transportation problems. That such a model is even conceivable is a direct result of the concept of a generalized transportation problem, one in which the specific nature of the environmental conditions are ignored. This concept is useful precisely because it is postulated that the essential nature of all localized transportation problems is the same, and efforts directed at the solution of one of these ought to be in part directed by their contributions to the solutions of others. The presence of such a model could greatly reduce the duplication of the efforts of those engaged in the solution of specific localized transportation problems. It would also greatly increase the usefulness of the knowledge obtained from the solution of one localized problem to the solution of another. It would do so, very simply, because the model would indicate

those characteristics of a generalized transportation problem shared by the two localized problems.

It is apparent from the literature on transportation that there is a need for the development of a greater degree of coordination of the research efforts on transportation. Such coordination does not necessarily come from the direction of such effort alone. In whatever way it is attained, however, it is necessary that a general model with the properties we have identified exist before coordination is attained. Whether a coordinated effort is worthwhile depends upon the cost of developing such a model. It does not take much analysis to show that the payout to coordinated research effort is sufficiently great in this case to more than justify the creation of this model.

The need for such a general model has been repeatedly mentioned in the literature of transportation. What has not been specified are the properties that such a model ought to have if it is to be useful. That is the subject of this paper. It should be noted that we have not at this stage restricted outselves to linear models or even to models in which the values of all variables lie in Cartesian real-number space. Such decisions cannot be made correctly until an attempt is made to develop the actual model. Only then will the requirements of operationally and use of the model in the context of available or feasible data indicate what the costs and returns to such simplifications are. What we have so far suggested is the nature of a general framework for the solution of transportation problems that needs to be developed in a rigorous form.

References

1. Steiger, Wilbur A., "Systems Analysis in Transportation Planning," Cost-Effectiveness Newsletter, Vol. 4, No. 2, April 1969, Operations Research Society of America.

2. Baumol, William J. and R. E. Quandt, "The Abstract Mode Model: Theory and Measurement," Studies in Travel Demand, Vol. II, Mathematics, New Jersey, 1966.

3. Baligh, Helmy H., David C. Dellinger, and Louis D. Volpp, "An Algebra for the Analysis and Design of Transportation Networks," Transportation Science, forthcoming issue.

AN ALGEBRA FOR THE ANALYSIS AND DESIGN OF TRANSPORTATION NETWORKS*

H. H. Baligh, D. C. Dellinger, and L. D. Volpp
Graduate School of Business Administration, Duke University

Introduction

The transportation system in our society has been developed piecemeal. The existing system is marked by good and bad components put together through trial and error into a collection that is strained to meet the perceived needs in the economy. The complexity of transportation requirements, and the investment necessary to make major alterations or additions to the transportation system, make a rigorous analytic framework for improved design of the transportation system necessary. "In many respects the (applications of systems analysis to transportation planning) are narrow in focus, primitive in theory, and limited in effectiveness."[1] The needed framework, or useful theory, is not available.

A physical transportation system has the potential for producing any one of a large number of sets of movements of people and things. Unfortunately, this potential for movement cannot be appropriately characterized in the same way that the potential output of most manufacturing systems is characterized, i.e., the numbers of things which can be produced. Measures of potential output which have been reduced to numerical expressions, such as ton-miles or passenger-miles, do not capture

---

*This is a descriptive summary which omits essentially all the algebra development. The development is presented in the full paper published in Transportation Science, v 6. n. 6, Nov. 1972

the significant potential of a transportation system. They do not indicate, for example, the particular points in time and space between which movements can be made, the quality of the movements, nor other characteristics which determine the value of the system to potential users.

The purpose in this paper is to develop a set of useful definitions and some rules of logic that can be used to create an integrated theory on which improved transportation system design will be based. More specifically, the focus in this paper is on the problem of design of the transportation network, and the approach is to develop an algebra for solution of this problem.

A design of a network, and therefore an algebra developed for that purpose, is valuable only if it is expressed in terms that can lead to production and use of the network. As a result, the algebra eventually must permit linkage to the physical system from which it can be produced and to potential users whose preferences determine its actual use.

The Transportation Network

Any physical transportation system, however defined, has associated with it a set of networks that are physically feasible. For each such physical system, a set of possible operating rules exists, each of which defines a subset of the set of feasible networks associated with that physical system. The choice is among pairs, one element a physical system and the other a set of operating rules. Thus, a set of operating rules applied to a specific physical system determines the capacity of this system in terms of the place-time transformations it can make, and the quality of those transformations. These are

terms in which preferences of people for transportation can be expressed.

A collection of potential or actual place-time alterations and the potential or actual quality of the transformations form a network. The network, then, reflects the capacity to provide movement of people and things from place to place, over time, along with some specifiable quality of experience for the movements.

The abstract concept of a network needs to be developed formally, so that existing or new analytic tools of logic and mathematics may be employed in the analysis and design of transportation systems. Whatever detailed form the definition of a network is given, it should enable us to identify those properties of the network which affect its "value", and to identify the manner in which variations in these properties in combination will alter such "value". These variations in the properties or characteristics of a network need to be described in a form that permits analysis of just how "value" and "resource usage" vary with changes in the network.

An algebra of transportation networks should include the fundamental building blocks for the development of intellectual and computer models, for the generation of different networks for evaluation, and for a systematic procedure for generating one network from another, i.e., a useful search procedure. To serve these purposes the algebra should include an abstract form of a network, the rules for intellectual operations on networks, and the functions which assign certain relevant properties to networks, thereby making it possible to evaluate systematically on the basis of clearly defined properties rather than on a non-directed evaluation of every network. The assignment of these properties also facilitates evaluation by allowing sequential determination of the effects

of each property on the network's value. Such an algebra has been developed.

A Transportation Network Algebra

An abstract space of transportation networks is needed for development of the algebra. Let

X = the set of all people x_i

x_i = a person

G = the set of all geographic locations g

g = a geographic location

T = the set of all points in time t

t = a point in time

S = the set of all single trips s for x_i

s = a single trip for x_i in geography and time, or time only

C = the collection of sets of trips γ

c = a set of direct trips which contains

1) no trips in which geography is changed in zero or negative time

2) for every trip in the collection for which geography is changed, trips which represent waits at the geographic origin and destination

c_v = trips in γ which change grography

c_w = trips in γ which are waits, i.e., stations in the network

M = set of all indirect trips m

m = an indirect trip

N = the set of all subsets of indrect trips

n = a collection of indirect trips, a subset of M

H = a function which relates any set of direct trips c to the set of indirect trips n_s

n_s = the set of indirect trips which can be composed from the direct trips in c

h = a network

h^o = the null network

X x G x T is the "relevant" state-space and thus, (x_i,g,t) defines the location of x_i at time t. A particular function s can be written as the set

$$\{((x_i,g,t),(X_j,g'xt'))\}$$

This can be interpreted as a single trip for x_i either in geography or time, or in time only (such as a wait in a station).

The collection C is of particular sets of trips c as defined above. For any set c it is possible to identify the set of all stations, i.e., the set of geographic points from which some individual may choose to start in his way to a different geographic point, and also those points to which he may choose to be taken. The set c identifies what could be called a set of direct trips which a group of people are permitted to take.

In order to identify indirect trips from the set c it is necessary to establish a formal process of building up an indirect trip from a series of direct trips. The key to this process is the composition of the functions that describe direct trips. For example a set $m = \{(((x_i,g,t),(x_i,g',t')),((x_i,g',t'),(x_i,g',t")),((x_i,g',t"),(x_i,g",t''')))\}$ describes a trip which x_i may take. It is made up of three direct trips in the order listed.

The set c has associated with it by the function H a unique element n_s. The pair (c,n_s) defines a transportation network. Thus $H = \{(c,n_s) = h \text{ such that } H(c) = n_s)\}$ is the set of all transportation networks obtained once X, G, T, and C are specified. The pair (c,n_s) can be shown to describe the transportation system's potential performance with respect to some set of individuals within the set of all people X.

In summary, the pair (c,n_s) is in general written as

$$(\{s,s'\ldots\ ,\ m,m',\ldots\})$$

where s is a set with one element and m is a set with one element. We note that the pair (c,H(c)) uniquely defines a network since, given c and the function H applied to it, $n_s = H(c)$ is unique. Thus (c,H) is a network in its general form, and (c,n_s) is a network in its extensive form. Describing a network by (c,n_s) is not redundant, i.t., c alone won't describe the network by itself, but only with H will it do so.

This completes the definition of the first element of the algebra, the abstract form of a network. Now, the operation which permits adding two or more networks is developed.

Any two networks may be "combined" to produce another network, and we define this addition operation by the function A as follows:

$$(c,n_s) + (c',n_s') = A((c,n_s),(c',n_s') = (c'',n_s''))$$

This is a network space. Before it can be used in the design and evaluation of transportation networks, its formal properties need to be examined. Before doing that, an example is shown.

The following simplified example illustrates how two schedules can be expressed in network form and added to obtain a new network. To avoid sets with infinite numbers of elements, only discrete points in time are considered, i.e., 0, 1, 2, ... Waits in stations must not exceed 2 time units.

Direct	Departure		Arrival	
Trip N.	Point	Time	Point	Time
		Schedule A		
1	a	0	b	10
2	b	11	c	20
3	c	21	a	30
		Schedule B		
1	d	0	b	9
2	a	31	d	40

Schedule A maps into a set of 3 direct moving trips, 24 waiting trips in stations, and 27 indirect trips. The direct moving trips are

$$\{\{((x,a,0),(x,b,10))\}\ \{((x,b,11),(x,c,20))\}\ \{((x,c,21),(x,a,30))\}\}$$

The waiting trips in stations include the following waits at a

$$\{\{((x,a,-2),(x,0,0))\}\{((x,a,-1),(x,a,0))\}\{((x,a,-1),(x,a,1))\}\{((x,a,0),(x,a,1))\}\{((x,a,0),(x,a,2))\}\},$$

and the set of indirect trips include, for example:

$$(\{((x,a,-2),(x,a,0))\},\{((x,a,0),(x,b,10))\},\{((x,b,10),(x,b,11))\})$$

The network representing Schedule B contains 2 direct moving trips, 20 waiting trips in stations, and 16 indirect trips. When the two networks are added by the rules defined above, the new network contains 5 direct moving trips, 38 waiting trips in stations, and 121 indirect trips. The addition of the two networks produced 54 indirect trips which were not contained in either of the two original networks.

Though the new definition is more complicated than the old one, it is in a form that simplifies greatly the identification of indirect trips, and is much more efficient for intellectual and computer operations. It is analogous to the use of binary numbers in computer operations rather than the base ten system.

Properties of the pair $\{H,+\}$.

The pair $\{H,+\}$, i.e., the set H and the binary operation on it meets the associativity and identity requirements of the definition of a group, but fails to meet the requirement of an inverse and is therefore not a group.

The binary operation defined above identifies a relationship between the elements which abstractly stand for transportation networks. It is essential to specify this relation if

one seeks a systematic and efficient way to think about a network to be evaluated once one specifies another network and evaluates it. The binary operation permits one to create network by modifying an existing network in a prescribed manner. It is applicable to any of the networks in the total set of networks. It meets a condition necessary to develop rules for searching for networks to evaluate once we have a starting point. In addition, the particular properties of the binary operation help determine the search rules which we may employ, and tell us something about the systematic manner in which we may now generate networks.

Three theorems give the properties of this binary operation: The pair {H,+} is 1) associative, 2) has a right identity, and 3) is commutative.

Some Properties of Networks

Many properties of transportation networks are valuable in the analysis and design of transportation systems. Their most basic value is in permitting us to develop a systematic and efficient network generating and search rule. Without specifying network properties no such non-random rules are possible, and we must rely on a random procedure or complete evaluation of all networks. If network values (costs and benefits) are tied to network properties properly defined, then our conceptual efficiency of analysis is much improved. If, as we suggest, the transportation system should be viewed as three interrelated segments, then the properties relevant in the analysis in one of them depends on how those properties affect the other two segments. For example, how a physical system is related to the networks which may be created by its use will determine those properties of networks that are relevant. Those properties of networks that change with changes in the physical systems from which they may be created are

obviously of relevance to the analysis, providing they also are related to the value of the network as determined by users.

In the absence of such a complete treatment the relevant properties of networks cannot be determined. However, within the context of this paper, a number of transportation network properties appear at this stage to be of relevance to any reasonable analysis and design of a transportation system.

One property of our abstract definition of transportation networks is that these networks can be said to "include" other networks. Thus we are able to look at only a "part" of the network at a time, and are sure that any general network properties also apply to this part since it itself is a network. The efficiency of a procedure for generating, searching and evaluating networks does not depend on application to some initial whole network, but can be applied sequentially to parts of that network. This inclusiveness property is captured by the concept of a subnetwork.

Two properties of the subnetwork, as developed, are stated in the following theorems:

Theorem 1: If $h' = (c', n_s')$ is a subnetwork of $h = (c, n_s)$, then $n_s' \_\_ n_s$.

Theorem 2: If h' is a subnetwork of h then $h + h' = h$

In order to identify other transportation network properties it is useful to define two major functions. The first function permits the identification of the "stations" in a network. The second identifies the set of direct trips which would produce the same effect as the set of indrect trips in the network. The first function is important since it identifies the entry and exit points to the network and is critical in terms of the value of the network. This function identifies a property of a network which is related to the generation,

search, and evaluation procedures used in the design of networks or the improvements of existing ones.

The second function identifies a property which is important since a major segment of the value of a network to people is related to what transformations in the time-geographic space the network makes possible. That is, the value is in large measure dependent on the changes permitted independently of the "routes".

The value of a network to a person or a group depends upon whether the network is capable of meeting their presently unknown requirements for trips. One network property which helps the determination of this capability is connectedness, which tells the individual whether he can get from any station in the network to any other. This all-or-none property may be applied to subnetworks, and can be used to measure how closely a total network comes to having the property by measuring which of its subnetworks have it, or by identifying the connected subnetwork which contains the most stations. The property is a measure on the completeness of the network given its specified points of entry and exit.

Another property which contributes to the value of a network identifies the minimum time necessary to get from any station to any other station, and the minimum of these times. This capability is measured in terms of time and not just geography, and since time is valuable and reducing trip time is costly, this property which we call t-connectedness (t for time) is related to the total value of a network. Both properties are directly related to economic value, so their definitions and the definitions of the functions which assign specific measure of the properties to networks are useful in analysis. They permit systematic design and improvements on the basis of the search for properties that networks need to have instead of

complete enumeration and evaluation.

Eight additional theorems have been developed relating to the algebra of networks analysis. These theorems are concerned with the time-connectedness properties mentioned above; coalescence properties of two networks; the properties of "stations" in a network, (including the concept of a central critical station, and the effect of removal and addition of stations (which has the effect of adding or removing "trips").

Network Equivalence Relations

Networks and Equivalence

The first equivalence relation for networks can be stated as: $(c,n_s) = (c',n_s')$ if and only if $C = c'$ and $n_s = n_s'$. The specification of an equivalence relation of the set of networks defined produces a partition of the set. The equivalence classes of networks so created are extremely useful in network analysis and design if the relation producing them is relevantly defined. Such classes permit the analysis of networks to proceed in a systematic, and more easily done, sequential manner. One may ascribe properties of networks to whole classes and thus, in a first cut at the problem, search only within those classes holding desirable properties. For more careful analysis one may specify equivalence relations that will partition each of these classes and then ascribe more comprehensive kinds of properties to each of these new equivalence classes. This narrows the search for networks to those within classes with desirable properties. In view of the complexity of networks, such a procedure in analysis and design is likely to have important effects on the efficiency of the procedure. Equivalence classes produce one mechanism for the specification of operational search rules of greater efficiency. They also

provide a means of operational specification of constraints, i.e., allow one to evaluate only those networks which have the same station sets, or the same points of origin and destination. Many equivalence relations may of course be specified depending upon the needs and details of our analysis or design. Those developed in this work deal with the following subjects:

a) Station equivalence of two networks

b) Station-pair equivalence of two networks

c) People-station-pair equivalence of two networks

The types or classes of networks and their related types of sets of trips should be of great value in our attempts to relate networks to their value to potential users and to the physical systems which "produce" the networks. Since the long run aim of this algebra is its use in the design or analysis of total transportation systems, it would be of great value to be able to say that any given physical system may produce a network of some given type rather than list all these networks. Again in terms of pragmatic usage of a computer to generate networks from a physical system of some given form and to evaluate those networks, a concept of classes gives us the tools for structuring computer programs so that they search and design purposefully within a subset of the set of all networks, rather than to search randomly in the whole set. Equivalence classes give us the means to produce efficiencies in our intellectual procedures of analysis and design of networks and transportation systems.

Generalizing the Network Concept

The model presented here can be extended to include capacity and quality of a trip and the movement of many classes of

things and people. Thus one can set,

$$R = S \times Y \times Q$$

where

- Y = the set of all capacities y
- y = the capacity of a trip, i.e., the number of things it can accommodate
- Q = the set of all quality vectors q
- q = a vector of trip quality indicators
- R = the set of all points $r = (s,y,q)$
- r = a trip whose description includes its capacity and quality

Further one can let

$$R^* = S \times Y^b \times Q^b$$

for b classes of quality on a trip. The maximum number of classes b is determined by the absolute total variations in quality of ride permissible for all networks. Therefore, in the addition of networks we can always obtain this by having arbitrarily many classes available.

References

1. Helmy H. Baligh, David C. Dellinger, and Louis D. Volpp, "A Model for the System Analysis of Transportation Problems," forthcoming in the Proceedings of the First Conference on Management Sciences, Computer Applications, and Industrial Development (Institute of Management Sciences, et al), Cairo, 1972.

2. Robert G. Busacker and Thomas L. Saaty, Finite Graphs and Networks, McGraw-Hill Book Company, New York, 1965.

3. Hiram Paley and Paul M. Weichsel, A First Course in Abstract Algebra, Holt, Rinehart and Winston, Inc., New York, 1966.

B. GUIDEWAY AND VEHICLE DYNAMICS

1. "Dynamics of Beams with Moving Loads," James F. Wilson and B. Inan Alpay, Civil Engineering Department, Duke University.

2. "Design Optimization of Prestressed Concrete Spans for High Speed Ground Transportation," Andre' Touma and James F. Wilson (paper presented at the National Symposium on Computerized Structural Analysis and Design, George Washington University, Washington, D.C., March 27-29, 1972. To be published in the Journal of Computers and Structures.)

3. "Active Suspension Systems: Experimentation and Simulation Studies," John Beattie and Donald Wright, Mechanical Engineering Department, Duke University.

DYNAMICS OF BEAMS WITH MOVING LOADS

James F. Wilson and B. Inan Alpay
Civil Engineering Department, Duke University

Abstract

The paper consists of two parts: first, an investigation of the dynamic deflections of high speed trains as they pass over simply supported, elevated spans; and, second, dynamic effects for passage over a guideway on an elastic foundation. An existing digital computer program was modified and used to study span deflections resulting from the passage of a single pressure segment associated with air cushion vehicles traveling at both constant and changing speeds between 0 and 400 mph. Explicit results for the double pressure segment case were derived. The boundedness of guideway deflections to both traveling pressures and traveling masses were compared. The mathematical models of the guideway were kept as general as possible where pressure length, stiffness, and subgrade support were the basic parameters. Results are evaluated and presented in such a way that it will be of help to both researchers and designers who are pursuing more detailed investigations in high speed ground transportation.

Introduction

The mathematical model for this study is the Bernoulli-Euler beam equation. Assumptions consistent with the Bernoulli-Euler theory of beam vibrations are as follows:

1. Guideways are stressed within elastic limits.
2. Materials are homogenous and isotropic.

3. Deflections are small as compared to the overall dimensions of the guideway.
4. Plane surfaces which are plane before deformations are plane after deformations.
5. The effects neglected in this analysis are:
   a) Rotary inertia,
   b) Longitudinal vibrations,
   c) Shear deformations,
   d) Viscous material damping,
   e) External fluid damping,
   f) Surface effects of local stresses

PART ONE

Moving Pressure Loads

One dynamic model of the guideway is represented in Figure 1. Herein p(x,t) is a known pressure distribution which moves along the guideway. This case is discussed in Reference (2), and those results are summarized.

The governing equation is most easily obtained by isolating a small segment of length "dx" along the beam, as shown in Figure 2. Application of Newton's Second Law in the y-direction gives the governing differential equation for constant EI as

$$EI \frac{\partial^4 y}{\partial x^4} + ky + \rho A \frac{\partial^2 y}{\partial t^2} = p(x,t) \qquad (1)$$

subjected to the following initial and boundary conditions:

a) Initial Conditions

$$y(x,t_o) = y_o(x)$$

$$\frac{\partial y}{\partial t}(x,t_o) = v_o(x)$$

b) Boundary Conditions

$$y(o,t) = y(L,t) = 0$$

$$\frac{\partial^2 y(o,t)}{\partial x^2} = \frac{\partial^2 y(L,t)}{\partial x^2} = 0$$

The boundary conditions (b) correspond to a simply supported beam, where

K = elastic constant of the foundation

EI = stiffness of the guideway

ρ = mass density of the guideway

A = cross sectional area of the guideway

p(x,t) = traversing pressure

The approaches to the problem are quite different when the pressure segment is traversing the span length and while it is off the span. These two cases, in other words, are the forced and free vibration cases, respectively.

A. Free Vibration Case

In this case, p(x,t) which corresponds to the forcing function is zero. Assuming a function of the type:

$$y_n(x,t) = Y_n(x)\sin \omega_n t$$

and substituting into equation (1) one obtains

$$Y_n'''' - \frac{(\rho A \omega_n^2 - K)}{EI} Y_n = 0$$

Solutions to the above differential equation are of the form

$$y_n(x,t) = \sin \frac{n\pi x}{L} \sin \omega_n t \qquad (n = 1,2...)$$

when ω_n is the guideway frequency.

B. Forced Vibration Case:

Assuming a solution of the form:

$$y(x,t) = \sum_{n=1}^{\infty} q_n(t) Y_n(x)$$

where $q_n(t)$ is a time varying coefficient, and substituting into equation (1) one obtains,

$$\sum_{n=1}^{\infty} \ddot{q}_n + \omega_n^2 q_n) Y_n = \frac{p(x,t)}{\rho A}$$

After mathematical manipulations, there results [2]

$$\ddot{q}_n + \omega_n^2 q_n = F_n(t) \qquad (2)$$

where,

$$F_n(t) = \frac{2}{L\rho A} \int_o^L p(x,t) \sin \frac{n\pi x}{L} \, dx$$

The solution to Eq. (2) is best obtained by Laplace transforms, and the result is:

$$q_{ni}(t) = \frac{1}{\omega_n} \dot{q}_{nj}(t_j) \sin \omega_n(t-t_j) + Q_{nj}(T_j) \cos \omega_n(t-t_j)$$

$$+ \frac{1}{\omega_n} \int_{t_j}^{t} F_{ni}(\tau) \sin \omega_n(t-\tau) d \qquad (3)$$

where $j = i = 1$

and knowing $q_{ni}(t)$ we obtain the final solution,

$$y(x,t) = \sum_{n=1}^{\infty} q_{ni}(t) \sin \frac{n\pi x}{L}$$

The values of $q_{ni}(t)$ could be calculated explicitly from equation (3) by the Leibnitz rule, which is formulated below for the sake of completeness.

$$\varphi(x) = \int_{U_o(\alpha)}^{U_1(\alpha)} f(x,\alpha) dx$$

$$\frac{d\varphi}{\partial\alpha} + f(U_1\alpha)\frac{dU_1}{\partial\alpha} - f(U_o,\alpha)\frac{dU_o}{\partial\alpha} = \int_{U_o(\alpha)}^{U_1(\alpha)} \frac{\partial f(x,\alpha)}{\partial\alpha}\, dx$$

Thus

$$\dot{q}_{ni}(t) = \dot{q}_{nj}(t_j)\cos\ \omega_n(t-t_j) - \omega_n q_{nj}(t_j)\sin\ \omega_n(t-t_j)$$

$$+ \int_{t_j}^{t} F_{ni}(\tau)\cos\ \omega_n(t-\tau)\,d\tau$$

A single moving patch of uniform pressure representing an air cushion vehicle can be divided into three loading intervals as it traverses the span. These intervals are illustrated in Figure 3. In a similar way, a double patch of pressure loading can be represented in seven loading intervals, as illustrated in Figure 4.

For single pressure loading, computation of the last term involving an integration of equation (3) is fairly short and straight-forward. The double pressure loading case, however, is lengthy. The integrations for this case have been performed but will not be presented here. The results will be used in the future to study guideway dynamics and heave accelerations on air cushion vehicles which can be represented by double pressure segments.

C. Numerical Results for the Single Pressure Case:

A computer program, which was originally written by J. F. Wilson [2] at the NASA Langley Research Center, has been adapted to the IBM 360/75 system. It was also modified to include the free vibrations case after vehicle passage. Using this computer program, along with an integration subroutine* the effects horizontal vehicle accelerations were studied.

---

*From the Langley Research Center, Computer Library

One important conclusion reached is the negligible effect of horizontal vehicle acceleration on the deflection ratio R.** This is illustrated in Figure 5 and Figure 6. In these figures the effects of an increasing vehicle speed, or horizontal accelerations of 0g and 1g are studied. The relative difference in the deflection ratio (R) is plotted against the ratio of passage frequency to 1st beam frequency, (ω/p_1), based on v_o, the initial vehicle speed.

The range of ω/p_1 is taken from 0.5 to 1.5. The passage frequency ω and the 1st beam frequency p_1, are defined as

$$\omega = \pi v/L$$

$$p_1 = \frac{\pi^2\sqrt{EI}}{L^2\sqrt{\rho A}}$$

where L is the span length and the pressure to span length ratio is (384/900).

Figures 5 and 6 show that the percentage difference in the deflection ratios are of the order of a few percent and reach a maximum of 6.5% for $\omega/p_1 = 0.95$, after the vehicle has left the span.

One very important question that comes to mind is how fast one could accelerate these vehicles without surrendering the ride comfort. Test results show that the maximum horizontal acceleration within the human comfort range is 0.1g., [7]. In this study accelerations of the range of 1.0g. have been considered and might very easily be applicable to high speed ground vehicles which carry freight. For vehicles carrying passengers the horizontal accelerations never exceed 0.1g.

**The ratio of maximum dynamic to static deflection at mid-span.

PART TWO

Moving Mass Loads

There is a considerable difference in the results of the problem involving moving loads with and without inertias. This very important distinction is sometimes overlooked. Timoshenko [4] solved the problem of an inertialess moving force on a simply supported span and obtained R = 1.71. Panovko and Gubanova [5] studied the same geometry, but with infinitely long loading involving inertia. They concluded that there is a critical velocity (V_{cr}) such that R approaches infinity. The expression for V_{cr} is

$$V_{cr} = \frac{\pi}{L}\sqrt{mEI}$$

where m is the mass to length ratio.

Timoshenko [4] has also given the result for a moving point mass (M) on a simple span. For this case R is given by

$$R = 1 + \frac{V^2ML}{3EI}$$

Here we address ourselves to the problem of a moving point mass and constant point force for infinitely long beams on elastic foundations. In a review of the literature it was found that some authors did not include all convective terms in the heave acceleration expression [6]. Their results, while approximately valid for present day vehicle speeds, would not be applicable at proposed high speed ground transportation speeds.

The analysis which includes all convective terms for the verticle heave acceleration were developed but are not presented here. The analysis revealed that the same critical velocity is obtained for both the point mass and the point force moving at constant velocity. That is, there is no contribution of the

heave acceleration term for these cases, contrary to the results found in the elevated span of finite length. This is also an expected steady state result and can be visualized as the mass "plowing" along the beam of infinite length with no obstacle to induce any heave accelerations. To get a physical understanding of the problem one can substitute reasonable values for the variables appearing in the critical velocity expression,

$$V_{cr}^2 = \frac{2\sqrt{EIK}}{\rho A}$$

Values chosen were:

$$EI = 2.52 \times 10^{11} \text{ lb-in}^2$$

$$\rho A = 0.188 \text{ lb-sec}^2/\text{in}^2$$

$$k = 5000 \text{ lb/in}^2$$

With these values one obtains a critical velocity of 350 mph. Such an analysis is of vital importance when the guideways are at grade and the length between rigid footings are long compared to the vehicle length. A plot illustrating the results of the analysis are shown in Figure 7, where deflection ratio R is plotted against vehicle velocity.

Conclusions

Explicit results for the double pressure segment case were derived. These results will be used in the future to study guideway dynamics and heave accelerations on air cushion vehicles which can be represented with a double pressure segment. The boundedness of guideway deflections to both traveling pressures and traveling masses were compared. Horizontal accelerations within the range of 0 to 1 g have been considered which might very easily be applicable to high speed ground vehicles that will

carry freight. The existence of the same critical velocity was obtained for both the moving mass and the point force moving at constant velocity.

Further studies are needed to generate meaningful design charts to aid engineers in the design of guideways for high speed ground transportation systems.

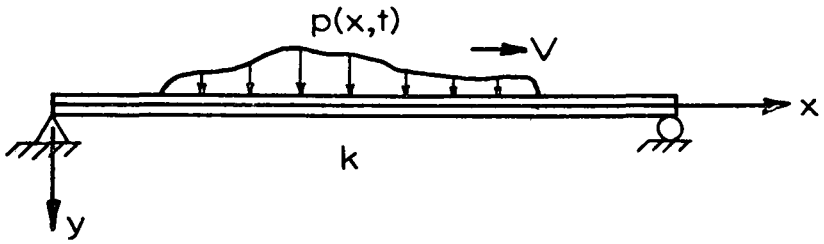

Figure 1

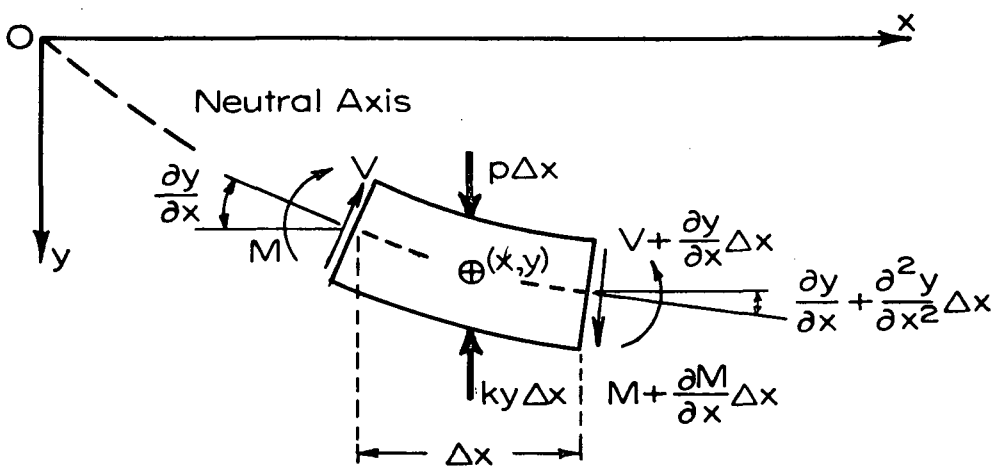

Figure 2

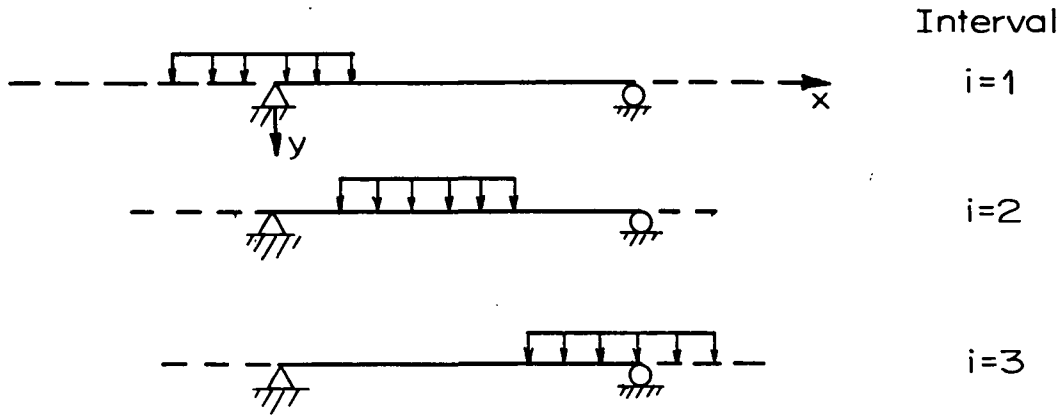

Figure 3. Single Pressure Loading Traversing a Span.

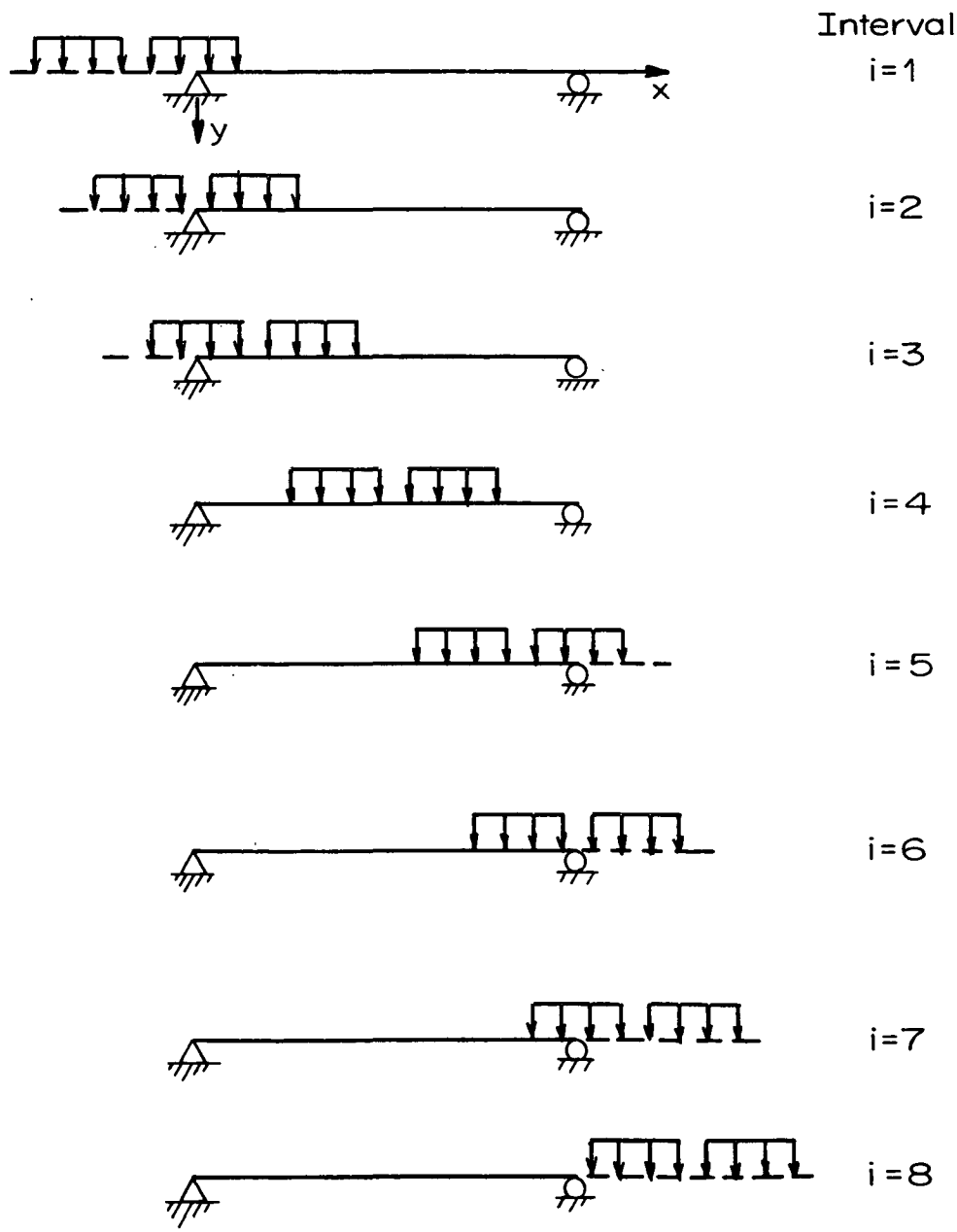

Figure 4. Double Pressure Loading Traversing a Span.

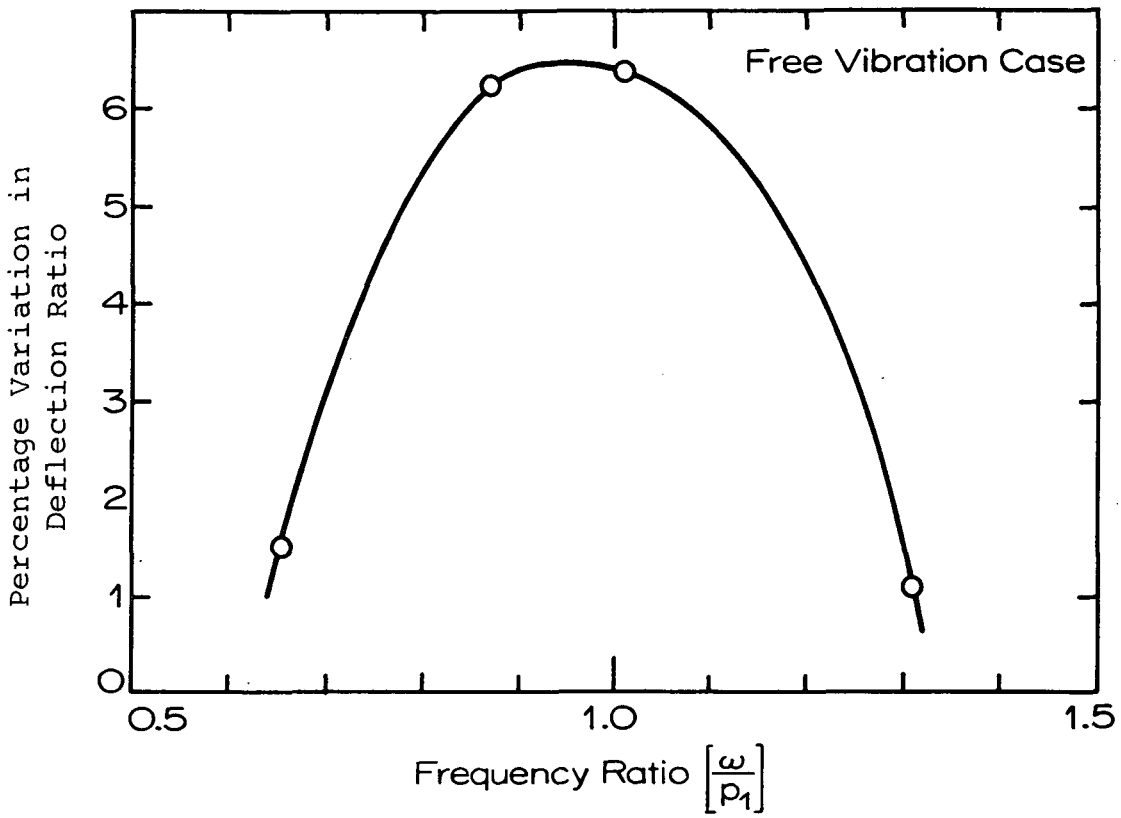

Figure 5. After Passage of Pressure.

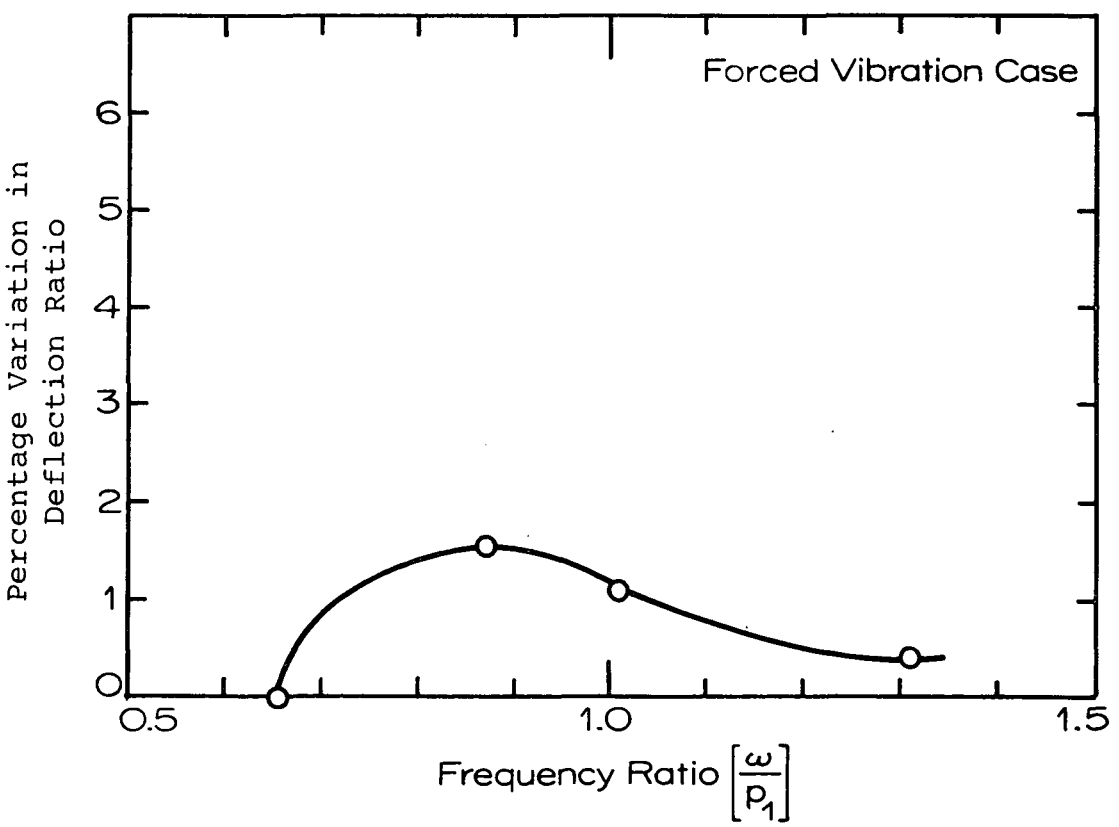

Figure 6. During Passage of Pressure.

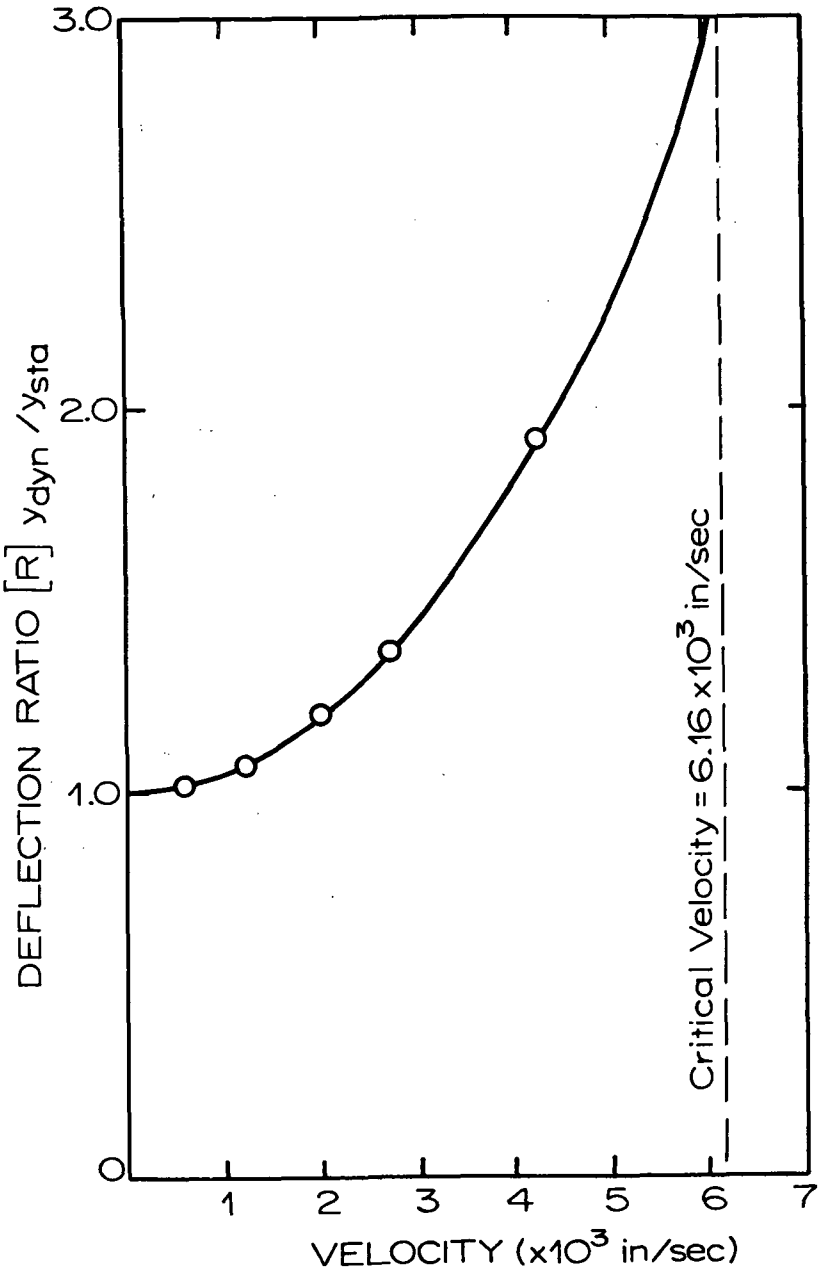

Figure 7. Deflection Ratio vs. Vehicle Velocity Curve for Moving Mass and Pressure Loading for a Beam on an Elastic Foundation

$k = 5000$ lb/in^2 $\rho A = 0.188$ lb-sec^2/in^2 $EI = 2.52 \times 10^{11}$ lb-in^2

References

1. I.S. and E.S. Sokolnikoff, Higher Mathematics for Engineers and Physicists, McGraw-Hill, N.Y.

2. J.F. Wilson, "Dynamic Response of Beams to Moving Pressure Loads as Related to Tracked Air Cushion Vehicles," The Shock and Vibration Bulletin, Volume 40, Part 4, pg 47, Naval Research Laboratory, Washington, D.C., Dec. 1969.

3. R.S. Burington, Handbook of Mathematical Constants and Formulas, McGraw-Hill, N.Y.

4. S. Timoshenko, Vibration Problems in Engineering, D. Van Nostrand Comp., Inc., Princeton, N.J.

5. Y.G. Panovko and I.I. Gubanova, "Stability and Oscillations of Elastic Systems." Consultants Bureau Enterprises, Inc., New York, N.Y.

6. M.M. Stanisic and J.C. Hardin, "On the Response of Beams to an Arbitrary Number of Concentrated Moving Masses," Journal of Franklin Institute, Vol. 287, No. 2, Feb. 1969.

7. Quarterly Report of the Railway Technical Research Institute, Japanese National Railways, August, 1964.

DESIGN OPTIMIZATION OF PRESTRESSED CONCRETE SPANS FOR HIGH SPEED GROUND TRANSPORTATION

Andre' Touma and James F. Wilson
Department of Civil Engineering, Duke University

The problem of designing stiff, lightweight, and least expensive elevated spans to support ground vehicles is investigated. A computer program using the direct search method was developed to calculate optimum geometric configurations of prestressed concrete girders with nonlinear constraint conditions involving stresses and deflections; with specified inputs on loading, unit costs and overall size; and with checks on buckling, shear, and ultimate section strength. Parameters allow for choices between stiff, expensive configurations or flexible, less expensive designs. Several numerical results for simple spans are included.

Introduction

Cost economy is one of the most important considerations in the design of elevated spans covering long distances, especially for guideway spans which can accommodate ground vehicles with speeds up to 300 mph. Preliminary studies have shown that certain box-type prestressed concrete spans are more economical than several all-steel spans with the same load-carrying capacity [1]. The present work offers a computer-aided approach for calculating the "best" geometric configuration for the prestressed concrete span, where the weight of the span and its piers is minimized, but span frequency is kept high enough for suitable dynamic design.

A simply supported box girder (Fig. 1) of uniform thickness along the span length, prestressed to prevent tensile stresses in

the outer fibers at working load conditions and to keep the span relatively flat under its own weight, was chosen as the basic span configuration for several reasons. First, design and fabrication techniques are currently available. Second, large numbers of such prefabricated spans, about 75 ft. long, can be transported and erected on piers with minimum difficulty, as recently accomplished by the British [2]. Third, uniform rather than longitudinally tapered spans were chosen mainly for simplicity. Although peak static bending moments occurring near the midspan might indicate the possibility of heavier cross sections in that region, dynamic moment distributions due to the passage of high speed air cushion vehicles are very complex indeed, depending on vehicle load distribution, suspension systems and speed [3,4]. Fourth, a box section symmetrical with respect to its horizontal centroidal axis was chosen because recent calculations show that the negative or dynamic heave deflections which occur in free vibration after vehicle passage are nearly equal to the positive deflections occurring during vehicle passage [4,5]. Thus, symmetrical deflections suggest symmetrical geometrical configurations. Although the ideas presented here can be employed to calculate the "best" configurations for unsymmetric composite cross sections (the inverted "T" shape, for instance) it is now felt that the symmetrical box, with or without the central web section of Fig. 1, represents the most economical or least weight design, and has a high enough natural frequency to accommodate high speed vehicles and their passengers with safety and comfort.

System Variables

Before formulating the approach used to calculate the span configurations, it is necessary to define the guideway system and to enumerate its many variables. The system is composed of identical, simple spans, each of length ℓ, placed end to end, together with its supporting piers. These piers are made up of caps across the tops of columns, which in turn rest on footings and also possibly on piles.

Fig. 1 defines the geometry of the box girder, including triangular fillets, and the location of the prestressing steel strands. The steel web reinforcements or stirrups, are attached to the steel strands and are spaced at longitudinal distances ℓ_s. The cross sectional area of each strand and stirrup is S and S' respectively. In all, there are thirteen geometric variables, or

geometric variables: A, B, C, D, E, F, G, H,
R, S, S', ℓ_s, ℓ (1)

There are a total of ten material variables. For concrete and steel, subscripted c and s respectively, these are: Young's moduli E_c and E_s; densities γ_c, γ_s; the compressive strength σ_c of concrete and the ultimate strength σ_s of the steel strands; the fatigue strengths σ_{fc} of concrete and σ_{fs} of the steel strands. In addition, the yield stress of the stirrups is σ_{ys} and the fractional losses in strand load (after preloading) due to creep and shrinkage of the concrete, to relaxation of the steel, and to elastic shortening of concrete just after transfer, is f_ℓ. Thus,

material variables: E_c, E_s, γ_c, γ_s, σ_c, σ_s,
σ_{fc}, σ_{fs}, σ_{ys}, f_ℓ (2)

There are a total of twelve variables associated with the span loading conditions. The load classifications are two: the "dead load" which includes all span loads except the vehicle weight; and the "live load", or the total apparent load due to the moving vehicle. The loading variables are: The "load factors" F_d and F_ℓ for moments at midspan due to dead and live loads, respectively; the midspan ratios of maximum dynamic response (vehicle at the design speed) to maximum static response (vehicle at zero speed): for deflection r_d and for bending moment r_m; the ratio of the dead load to the weight of the box girder alone u; the minimum allowable ratio of span length to midspan deflection v; the vehicle length ℓ_v; the maximum portion of the vehicle weight which acts on one girder W_v; the initial prestressing force in the top strands P^0; the additional prestressing force in the bottom strands, P_1^0, necessary to keep the midspan at zero deflection under dead load; and the final values of P^0 and P_1^0 after all preloading losses occur, or P and P_1 respectively. Thus,

$$\underline{\text{span loading variables}}: \quad F_d,\ F_\ell,\ r_d,\ r_m,\ u,\ v,\ \ell_v,\ W_v,\ P^0,\ P_1^0,\ P,\ P_1. \tag{3}$$

There are six cost variables, including the unit costs of the concrete x_1; of the reinforcing steel x_2; of the caps and columns x_3; of the footings x_4; and of the piles x_5. In addition, the fractional amount of the total number of piers supported on piles, x_6, is an important cost factor. The total cost per unit span length of the guideway system, including the cost of one pier for each span, is X, where

$$\underline{\text{cost variables}}: \quad X = X(x_1, x_2, x_3, x_4, x_5, x_6) \quad . \tag{4}$$

In this analysis, since linear relations between each unit cost item and material weight are assumed the span system of least weight implies the one of least cost. Typical expressions for the cost variables are listed in Appendix A.

In designing a span for distributed, high speed moving loads, an important design variable is Ω, the fundamental span frequency for flexural vibration [5]. With units consistent with Appendices, Ω is

frequency variable:
$$\Omega = \pi^2 \left(\frac{E_c I g}{(12\ell)^3 W_d} \right)^{\frac{1}{2}} \tag{5}$$

where I, calculated by elementary methods and given explicitly in Appendix B, is the second moment of area of the cross section, where the area of steel strands have been "converted" to an equivalent area of concrete by the multiplicative factor (E_s/E_c); W_d is the dead load given by (20), Appendix A; and g=386 in/sec^2, the gravitational constant. Although the variables comprising Ω are implied in the variables listed in (1) and (2), Ω is nevertheless significant enough to be listed as a separate item.

It is seen, then, that Ω and the six cost variables which comprise X may depend on a total of 35 separate quantities enumerated by (1), (2) and (3). The task now is to define precisely the meaning of system optimization and to write down the interrelations among the variables which define the system constraints.

Optimization Function and Constraint Inequalities

The optimization function Φ is defined by

$$\Phi = zX - (1-z)\Omega \tag{6}$$

where z, the cost-frequency judgement factor, is arbitrarily chosen in the range $0 \leq z \leq 1$. The minimum of Φ, when subjected to the fourteen constraint conditions below, gives the optimum system configuration. Eq. (6) allows the option of choosing $z = 1$, for which only total costs will be minimized. However, such a choice may lead to span configurations which are very flexible, with values of Ω below 15 or 20 radians per second, and such spans could overtax vehicle suspension systems designed for comfortable rides. In such cases, choosing a smaller value for z (0.8 for instance) would lead to stiffer, more costly spans, but ones with higher and more tolerable values of Ω.

Of the fourteen constraints, nine are defined as the major constraints and five as the minor ones. In many practical cases, if the following major constraint inequalities are satisfied, the minor ones are too. Thus, the minor ones are simply checked for validity, while the major ones are incorporated as a part of the optimization scheme for minimizing Φ.

The first major constraint is on span deflection, or

$$\frac{\ell}{y_{max}} \geq v \qquad (7)$$

where y_{max} is the maximum absolute value of midspan deflection, calculated from elementary beam theory, and based on live (moving) loads only. The minimum allowable value of v is often in the range of 1000 to 1500.

The second and third major constraints involve the prestressing loads. The most obvious one is that each final strand

load should be non-negative, or

$$P \geq 0 \quad . \tag{8}$$

The other condition is that the maximum prestress in any bottom strand should not exceed a fraction (say 0.7) of its ultimate stress, or

$$\frac{(P^0 + P_1^0)}{S} \leq 0.7\ \sigma_s \quad . \tag{9a}$$

Due to losses, P^0 and P_1^0 are both reduced by a factor of $(1 + f_\ell)$ where f_ℓ is the loss factor, about 0.14. Thus, in terms of final loads, the third major constraint inequality becomes

$$(1+f_\ell)(P+P_1)/S \leq 0.7\ \sigma_s \quad . \tag{9b}$$

If (9b) is satisfied, then the steel strands will generally be safe from fatigue failure, since $\sigma_{fs} \geq 0.7\ \sigma_s/(1+f_\ell)$ for high strength steels. An explicit expression for P_1 in terms of geometric and material variables is given in Appendix C.

The remaining six major constraints are on the normal stresses in the concrete. These stresses are defined in Fig. 2 as positive numbers σ_1, σ_2, σ_3 and σ_4 for the three possible critical loading conditions. Stresses are based on strand loads P and P_1, after all losses have occurred. The first two of these constraints are based on loading condition I which exists near the supports, where all bending moments are negligible. Here, the stresses at the top of the section must never be in tension, or

$$\sigma_1 - \sigma_2 \geq 0 \tag{10}$$

and at the bottom of the section the net compressive stresses should

not exceed a certain fraction (say 0.45) of the compressive fatigue strength of concrete, or

$$\sigma_1 + \sigma_2 \leq 0.45\ \sigma_{fc} \tag{11}$$

The second two major stress constraints involve loading condition II, occurring at midspan. Here, in addition to prestressing, flexure stresses from positive moments due to both dead and live loads can occur during the downward vibration cycle. For stresses in the top of the section

$$\sigma_1 + \sigma_3 + \sigma_4 - \sigma_2 \leq 0.45\ \sigma_{fc} \tag{12}$$

and for stresses in the bottom of the section

$$\sigma_1 + \sigma_2 - \sigma_3 - \sigma_4 \geq 0 \quad . \tag{13}$$

The final two major stress constraints correspond to loading condition III, which also exists at midspan. The only difference from loading condition II is the reversal of the sign of the bending moment due to live loads, or the condition of reversed bending in free vibration discussed previously [4]. For the top of the section

$$\sigma_1 + \sigma_3 - \sigma_2 - \sigma_4 \geq 0 \tag{14}$$

and for the bottom of the section

$$\sigma_1 + \sigma_2 - \sigma_3 + \sigma_4 \leq 0.45\ \sigma_{fc} \tag{15}$$

Explicit expressions for each stress in these inequalities (10)-(15) are summarized in Appendix D in terms of geometric, material, and span loading variables. Stirrup reinforcement variables ℓ_s, S' and σ_{ys} were excluded from these inequalities and

from the optimization procedure since they have a minor effect on unit costs and span frequency. Stirrups should be included if codes are to be followed, however [6], during span fabrication.

The five minor constraints are summarized. Detailed formulations are available elsewhere [7].

(1). The web sections must be thick enough to resist buckling, to provide sufficient cover for the strands, and to facilitate fabrication.

(2). The largest principal tensile stress in the concrete should not exceed the maximum allowable value. Both the addition of stirrups and an increase in web thicknesses B and C increase the capacity of the span to resist principal tensile stresses.

(3). The span frequency Ω should be above a minimum value consistent with the ride quality for a particular vehicle and its suspension system. As will be demonstrated, span configurations at increasing Ω can be calculated by revising z downward, resulting in cost increases.

(4) and (5). The maximum bending moments from external loads, positive and negative, should never exceed the span's moment carrying capacity at ultimate, as determined by methods of limit analysis [6,8].

System Optimization Algorithm

A computer program was written to minimize Φ of (6), subject to the major constraint inequalities (7)-(15). The span with the

dimensions and preloading forces so obtained which also satisfies all of the five minor constraints, is an optimum span.

Up to now, 42 variables were enumerated, including those in (1)-(4) and z. For optimization calculations, these are reduced to 34 variables as follows: web reinforcement is omitted, eliminating ℓ_s, S' and σ_{ys}; fatigue failure for concrete and steel, respectively, are assumed to obey the relations $\sigma_{fc} = 0.59\ \sigma_c$ and $\sigma_{fs} = 0.75\ \sigma_s$, eliminating σ_{fc} and σ_{fs}; initial strand loads are assumed to be related to P and P_1 by (9b) and (9a) through the factor $(1+f_\ell)$, eliminating P^0 and P_1^0; and the incremental strand load P_1 depends on geometric and material variables only (Appendix C), eliminating the need to choose P_1 independently. Of the remaining 34 possible independent variables, the following 27 are chosen as fixed input constants:

6 geometric quantities: B, C, D, E, F, H

7 material quantities: E_c, E_s, γ_c, γ_s, σ_c, σ_s, f_ℓ

8 loading quantities: F_d, F_ℓ, r_d, r_m, u, v, ℓ_v, W_v

6 cost quantities: x_1, x_2, x_3, x_4, x_5, x_6

Optimization is performed based on the remaining variables:

7 optimization variables: P, G, S , R, A, ℓ, z.

A configuration composed of a set of the above 33 variables exclusive of P is defined as admissible if there corresponds an allowable range of P which satisfies all major constraints (7)-(15). Here, calculations are based on the maximum allowable value of P in this range, although any value of P in this admissible range could have been used. The optimum span is the least cost admissible configuration based on fixed values for the 27 fixed input constants and is calculated

as follows.

1. Specify a lower bound, an upper bound and the increment used to determine intermediate values, for each optimization variable: G, S , R, A, ℓ, z.

2. Assign the lower bound values to: R, A, ℓ, z.

3. Including all discrete values, for all combinations of G and S , calculate P, I, X, Ω and Φ. From the admissible configurations so obtained, select the (G, S) combination for which Φ is minimum.

4. Keep ℓ and z fixed. For all combinations of R and A, repeat step 3. From the admissible configurations so obtained, select the (G, S , R, A) combination for which Φ is minimum.

5. Keep z fixed. For each successive value of ℓ, repeat step 4. From the admissible configurations so obtained, select the (G, S , R, A, ℓ) combination for which Φ is minimum.

6. For each successive value of z, repeat step 5. Obtain sets of results (P, G, S , R, A, ℓ, z), if they exist.

7. Check each set of step 6. to see if all of the minor constraints are satisfied. For those sets satisfying all constraints, choose the most inexpensive one as the optimum span.

8. If there is difficulty in obtaining admissible solutions or in satisfying the five minor constraints, then some of the fixed input quantities could be increased (web thicknesses B and C, for instance). Also, ranges on (G, S , R, A, ℓ) might be modified so that shorter span lengths and heavier sections could be investigated.

In numerical examples such as the ones which follow, all constraints are satisfied for some range of z. For other values of z, however, calculated positive ultimate moments of resistance are too low. The latter results are accomplished by trial and error calculations in subroutine CALC. The entire program of about 1000 statements, including this subroutine, is listed elsewhere [7].

Typical Numerical Results

Of the many optimum span configurations calculated [7], three classes of span systems (I, II, and III) are presented here. Most of them are capable of supporting an air cushion vehicle weighing 50,000 lbs, with a uniform pressure loading length of 50 ft., traveling at constant speeds up to 300 mph. Realistic values of the fixed input constants for all three span systems are listed in Table 1 and are based on the references cited there. The ranges of the optimization variables are given in Table 2.

Results of Configurations I, II and III are listed in Table 3 for several values of z. The optimum solution for I is for $z = 0.9$, corresponding to $\Omega = 36.8$ rad/sec, a span length $\ell = 60$ ft. and a total cost $X = 127.1$ dollars per ft. For $z = 1.0$, this span length is 70 ft. and the cost is slightly less - but the constraint on the positive ultimate moment of resistance is not satisfied. For values of z decreasing below 0.9, a desirable increase in frequency occurs, but the costs likewise increase for Configuration I.

Table 1 - Summary of the 27 fixed input variables with typical numerical values.

SYMBOLS		MEANING	VALUES* FOR CASES I,II,III
Text	Program		
		Geometric Variables (Fig. 1)	
B	B	outer web thickness	3.5 in
C	C	middle web thickness	6 in(I,II)
			5 in(III)
D	D	strand spacing in slabs	3 in(I,II)
			5 in(III)
E	E	strand spacing in webs	3 in
F	F	fillet dimension	3.5 in
H	H	strand spacing from slab edge	1.75in
		Material Variables	
E_c	EC	Young's modulus for concrete	3.44×10^6 psi
E_s	ES	Young's modulus for steel strands	28×10^6 psi
γ_c	WC	density of concrete	145 lb/ft^3
γ_s	WS	density of steel	490 lb/ft^3
σ_c	FC1	compressive strength of concrete	6000 psi
σ_s	FS	ultimate strength of steel strands	270,000 psi
f_ℓ	(0.14)	fractional losses in strand load	0.14

* These values are common to all configurations I, II and III, except as noted in parentheses.

Table 1 - (Continued)

SYMBOLS		MEANING	VALUES* FOR CASES I,II,III
Text	Program		
		Loading Variables	
F_d	ALFDL	load factor (dead load), [8]	1.5
F_ℓ	ALFLL	load factor (live load), [8]	1.8
r_d	ALPHA	at midspan: max. dynamic deflection/ max static deflection [3]	1.64
r_m	DYN	at midspan: max. dynamic moment/max. static moment [3]	1.75
u	RATIO	span dead weight/box section dead weight [9]	1.35
v	TERM	span length/max. midspan deflection [8]	1600
ℓ_v	AL2	max length of vehicle pressure on span	50 ft.
W_v	W71	max. portion of vehicle weight on span	50,000(I,II) 25,000 (III)
		Cost Variables [9]	
x_1	COSTC	cost of concrete	\$ 105. /yd^3
x_2	COSTS	cost of steel strands	\$ 0.58/lb
x_3	(122)	cost of caps and columns	\$ 122. /yd^3
x_4	(58)	cost of pier footings	\$ 58. /yd^3
x_5	(22)	cost of piles per sq. ft. of footing	\$ 22. /ft^2
x_6	XAA	no. of piers on piles/no. piers	0.3

* These values are common to all configurations I, II and III, except as noted in parentheses.

Table 2 - Typical ranges of values for the optimization variables

SYMBOLS		MEANING AND UNITS	CONFIGURATION I			CONFIGURATION II			CONFIGURATION III		
Text	Program		lower bound	upper bound	increment	lower bound	upper bound	increment	lower bound	upper bound	increment
ℓ	AL	span length,ft.	40	90	10	40	90	10	40	90	10
A	A	span width,in.	147.5	153.5	6	143.5	153.5	10	75.5	81.5	6
R	R	span height,in.	43.5	83.5	5	43.5	83.5	5	38.5	83.5	5
G	G	slab thickness,in.	3.5	7.5	0.5	3.5	7.5	0.5	3.5	7.5	0.5
S	S	single strand area,in^2	0.085	0.149	0.032	0.085	0.149	0.032	0.085	0.149	0.032
z	GJ	judgement factor	0.5	1.0	0.1	0.5	1.0	0.1	0.5	1.0	0.1

Table 3 - Typical numerical results for optimum span configurations

SYMBOLS		MEANING AND UNITS	CONFIGURATION I			CONFIGURATION II			CONFIGURATION III		
Text	Program		z = 1.0	z = 0.9	z = 0.8	z = 1.0	z = 0.9	z = 0.8	z = 1.0	z = 0.9	z = 0.8
ℓ	AL	span length,ft.	70	60	40	60	50	40	60	60	40
A	A	span width,in.	147.5	147.5	147.5	143.5	143.5	143.5	81.5	81.5	75.5
R	R	span height,in.	48.5	43.5	43.5	43.5	43.5	43.5	38.5	38.5	38.5
G	G	slab thickness,in.	3.5	3.5	3.5	3.5	3.5	3.5	3.5	3.5	3.5
S	S	single strand area,in.^{2}	0.085	0.085	0.085	0.117	0.085	0.085	0.085	0.085	0.085
P^0	PIN	initial strand load,lb.	3,012	5,693	11,455	5,153	4,194	8,467	2,527	2,527	9,893
P_1^0	P1IN	initial load increment,lb.	13,053	10,372	4,610	16,960	11,871	7,598	13,538	13,538	6,202
X	COST	system cost, $ per ft.	126.4	127.1	137.2	123.8	124.1	128.1	165.8	165.8	177.0
Ω	OMEGA	span frequency, rad/sec.	30.1	36.8	82.8	36.6	52.5	82.0	30.8	30.8	68.7
COMMENTS All values of X exclude stirrup costs; for case III, X is the total cost of both girders			minor constraint (4) not satisfied	most satisfactory solution	satisfactory but costly	most satisfactory solution	satisfactory but costly	satisfactory but costly	satisfactory but costly	satisfactory but costly	satisfactory but costly

For Configuration II, the horizontal spacing D of the strands is increased from the 3 inches of the previous case to 5 inches. Here, the optimum span occurs for z = 1.0. In comparison to the previous Configuration I, the span lengths and frequencies are essentially the same - but the widths A are smaller by a few inches and the total cost is less by about 3.3 dollars per ft.

In Configuration III, the optimum spans correspond to two narrower box sections, side by side, which share the vehicle load equally (W_v = 25,000 lb). Such sections may be easier to fabricate and erect than the integrate box of Configurations I and II. In comparison to Configuration I for z = 0.9, where the middle web was reduced from 6 to 5 in., the span length is the same, or 60 ft. However, the total cost of this two-girder system is much higher, exceeding the single one by 42.0 dollars per ft., even though Ω for the two-girder system has a reasonable value of 30 rad/sec. The costs of the optimum two-girder spans can be reduced, however, by decreasing the range of overall width A and perhaps by eliminating the center web in each case.

Concluding Remarks

The algorithm involving a direct search technique was found quite feasible for solving the present class of structural optimization problems involving a large number of variables and nonlinear constraint inequalities. Conclusions about optimum reinforced concrete box girder systems, designed for a 50,000 lb air cushion vehicle traveling at speeds up to 300 mph, are summarized.

1. Fillets, necessary to reduce stress concentrations, should be as small as possible to minimize costs; they have negligible effect on span frequency, other variables remaining the same.

2. Stirrups, when designed after the codes [8] and added to the optimum spans, increase unit costs by about 2 or 3% at the most.

3. For the single box section and for the two parallel box sections, natural frequencies of the optimum spans are in the range $30 \leq \Omega \leq 40$ rad/sec, which is satisfactory for passenger comfort with presently contemplated vehicle suspension systems.

4. The optimum, single box spans presently cost about 124 dollars per ft. including all pier costs, assuming pilings are under every third pier. Costs are considerably reduced as the number of pilings per pier are reduced.

5. From the practical standpoint of fabrication and erection, the system involving two parallel box girders, which divide the moving load between them, may be more attractive than the single girder system. Further studies are needed to see whether the high unit costs of the double system can be reduced to be competitive with the single one.

Acknowledgments

This research was sponsored by NASA grant NGL-34-001-005 and by the Department of Civil Engineering at Duke University. The authors thank Earl I. Brown,II, for helpful discussions.

Appendix A - Cost Composition

The unit cost of the guideway system is assumed in the form

$$X = 1.15 \left[12h_1 + h_2/\ell \right] \quad \text{(dollars/ft)} \tag{16}$$

where h_1 is the cost in dollars per inch of length of the box section; h_2 is the total cost (dollars) of one pier; and ℓ is the span length (ft.). The arbitrary multiplicative factor of 1.15 accounts for miscellaneous costs. Since 1 yd^3 = 4.65×10^4 in^3, the unit span cost is

$$h = \frac{S_c \cdot x_1}{4.65 \times 10^4} + \frac{N \cdot S \cdot x_2}{12^3} \gamma_s \tag{17}$$

where the cross sectional area (in^2) of the concrete is

$$S_c = 2A \cdot G + (2B+C)(R-2G) + 4F^2 - N \cdot S \quad ; \tag{18}$$

the number of strands, each of area S (in^2), is

$$N = \frac{2}{D}(A-B) + \frac{3}{E}(R-2H) - 1 \quad , \tag{19}$$

where dimensions (A, B, D, E, R, H) are chosen so that N is an integer. The units of material and cost variables are consistent with the definitions in Table 1. Following the ideas in [9], the cost of a pier depends on the maximum load p (in thousands of lbs) which it supports. This load is the sum of the span's dead weight (lbs) given by

$$W_d = \frac{u\,\ell}{12^2} \left(S_c \gamma_c + N \cdot S \cdot \gamma_s \right) \tag{20}$$

and the live load $r_m W_v$, so that

$$p = \frac{W_d + r_m W_v}{1000} \tag{21}$$

A typical pier is composed of a cap and column of volume (0.0186 p + 3) yd^3; of a footing of volume 0.065 p yd^3, with a required area for each footing of (p + 75)/1.55 ft^2; and piles (when necessary) costing x_5 dollars per ft^2 of footing. In terms of unit costs x_3, x_4 and x_5 of these pier components, the cost of one pier is

$$h_2 = x_3(0.0186p+3) + 0.065p\ x_4 + x_6\left(\frac{p+75}{1.55}\right)\ x_5 \qquad (22)$$

where x_6 is the fractional number of piers on piles. By substituting (17) and (22) into (16), using (17)-(21), X is expressed as a linear function of the steel and concrete densities and of live load, for a specified set of span and strand dimensions.

Appendix B - Section Property

From elementary theory, using the symbols of Fig 1 and Tables 1 and 2, the equivalent second moment of area for the girder cross section can be written in terms of just two of the geometric optimization variables, G and S. That is

$$I = A_4G^3 + A_5G^2 + A_6G + A_7 + A_8S \tag{23}$$

where the coefficients are given in terms of the remaining section dimensions and the ratio of moduli, E_s/E_c, or

$$\begin{aligned}
A_4 &= \frac{2}{3}(A - 2B - C) \\
A_5 &= 4F^2 + C\cdot R + 2B\cdot R - A\cdot R \\
A_6 &= \frac{8}{3}F^3 - 4R\cdot F^2 - B\cdot R^2 - \frac{1}{2}C\cdot R^2 + \frac{1}{2}A\cdot R^2 \\
A_7 &= \frac{1}{12}C\cdot R^3 + \frac{1}{6}B\cdot R^3 + \frac{2}{3}F^4 + F^2\cdot R^2 - \frac{4}{3}F^3\cdot R \\
A_8 &= \frac{A\cdot R^2}{2D}\left(\frac{E_s}{E_c} - 1\right) + \frac{2}{D}A\cdot H^2 - \frac{2}{D}R\cdot H\cdot A - \frac{B\cdot R^2}{2D} \\
&\quad - \frac{2H^2\cdot B}{D} - \frac{2\ R\cdot H\cdot B}{D} - R^2 - 4H^2 + 4R\cdot H + A_9\cdot E^2
\end{aligned} \tag{24}$$

The constant A_9, necessary to determine A_8, has two possible values. Let

$$I_5 = (R - 2H)/E \tag{25}$$

where dimensions R, H and E are always chosen so that I_5 is either an even integer or an odd integer to assure evenly-spaced strands in the webs. If I_5 is an <u>even</u> integer,

$$A_9 = 6\ [1^2 + 2^2 + 3^2 + \ldots.(I_5/2)^2] \tag{26a}$$

If, however, I_5 is an <u>odd</u> integer, then

$$A_9 = 1.5\ [1^2 + 3^2 + 5^2 + \ldots I_5^2] \tag{26b}$$

Appendix C - Incremental Load

For a simply supported span under uniform prestressing ($P \geq 0$, $P_1 = 0$), subjected to a uniform transverse dead load, the downward midspan deflection is

$$y_1 = \frac{5W_d\,(12\ell)^3}{384\,E_cI} \tag{27}$$

where W_d and I are given by (20) and (23) respectively. For zero dead load, but for non-zero incremental forces P_1, $P_1/2$ and $P_1/4$ in the bottom part of the section, the upward midspan deflection due to the resultant moment $P_1 \cdot C_2$ is

$$y_2 = \frac{(12\ell)^2\,P_1 \cdot C_2}{8\;E_c \cdot I_c} \tag{28}$$

where

$$C_2 = \frac{1}{2D}\,(A-B)(R-2H) + 1.625\,R - 3E - 3.25\,H \tag{29}$$

and the gross moment of inertia is

$$I_c = I - A_s \cdot S \tag{30}$$

and is defined by (23) and (24). For zero net deflection at midspan, $y_1 - y_2 = 0$, which, from (27) and (28), corresponds to an incremental load of

$$P_1 = \frac{40\,W_d \cdot I_c \cdot (12\ell)}{384\,C_2I} \tag{31}$$

where W_d, I_c, C_2 and I are given by (20), (30), (29) and (23), respectively.

Appendix D - Concrete Stresses

The normal stresses σ_1, σ_2, σ_3 and σ_4 shown in Fig 2 are based on the strand load distribution of Fig 1. The direct compressive stress σ_1, acting throughout the span (except close to the ends) is

$$\sigma_1 = \frac{\text{total strand load}}{\text{total section area}} = \frac{N \cdot P + P_1 \cdot (A-B)/D + 3.25\ P_1}{S_c + N \cdot S} \qquad (32)$$

where S_c and N are given by (18) and (19). From beam theory, the maximum bending stress arising from incremental strand loads, or the equivalent bending moment $P_1 \cdot C_2$ is

$$\sigma_2 = \frac{P_1 \cdot C_2 \cdot R}{2\ I_c} \qquad (33)$$

where C_2 and I_c are given by (29) and (30). At midspan, the bending moment due to dead loads (a uniform span load of intensity W_d/ℓ lbs/ft) is

$$M_d = \frac{W_d(12\ell)}{8} = \frac{3}{2} W_d \cdot \ell \text{ (in-lbs)}$$

which gives rise to the bending stress

$$\sigma_3 = \frac{M_d R}{2\ I} = \frac{3 W_d \ell}{4\ I} \quad \text{(psi)} \qquad (34)$$

where W_d and I are given by (20) and (23). Finally, the maximum bending moment due to live loads, M_ℓ, occurs approximately at midspan [3] and is found by increasing the maximum static moment (at midspan) due to vehicle pressure by the factor r_m. Assuming that the vehicle weight W_v is uniformly distributed over length $\ell_v < \ell$, the live load moment is

$$M_{\ell} = r_m \frac{W_v}{8} (2\ell - \ell_v)(12) \quad \text{(in lbs)}$$

which gives the bending stress

$$\sigma_4 = \frac{M_{\ell} R}{2\ I} = \frac{3\ r_m W_v}{4\ I} (2\ell - \ell_v) \quad \text{(psi)} \ . \tag{35}$$

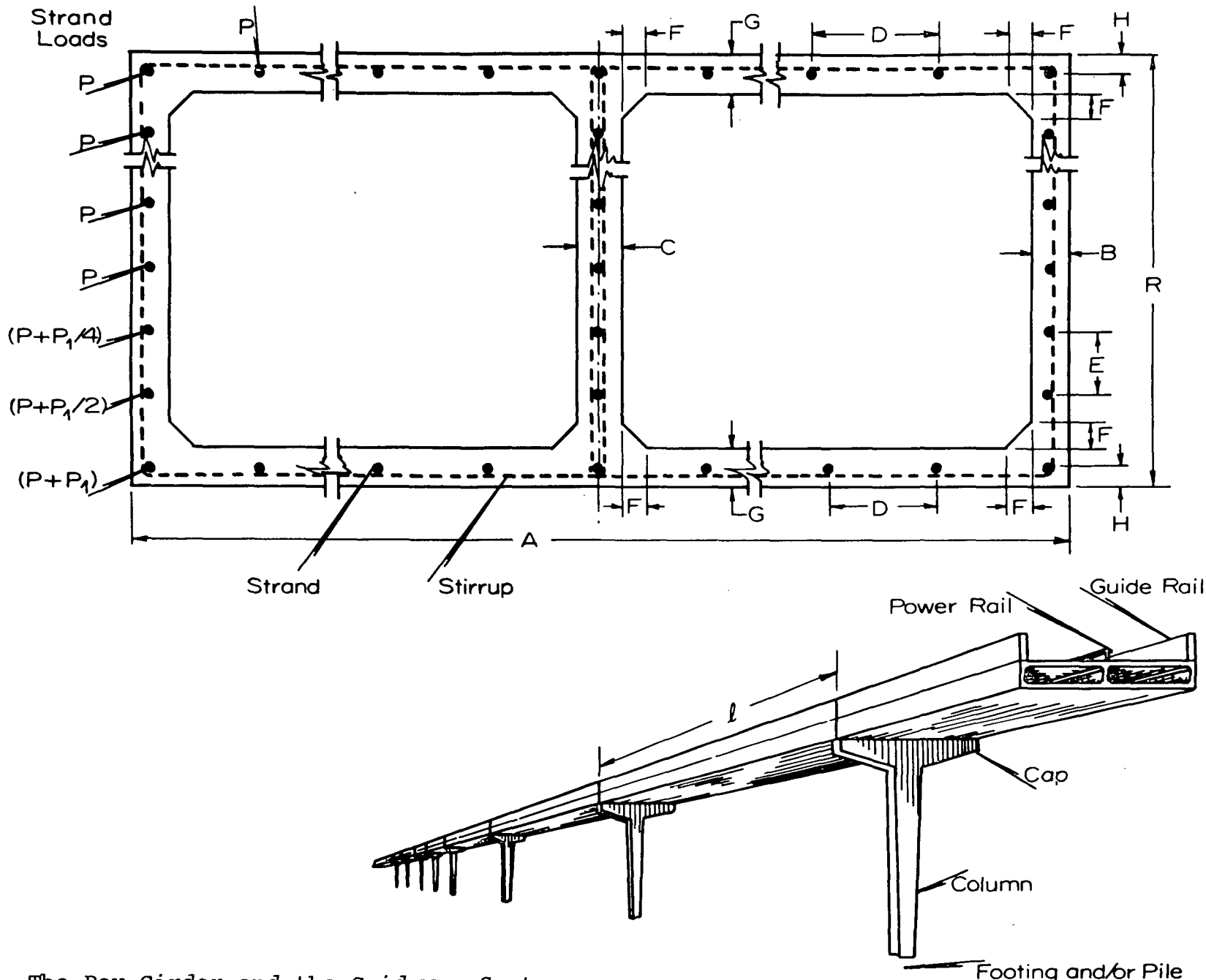

Fig. 1. The Box Girder and the Guideway System

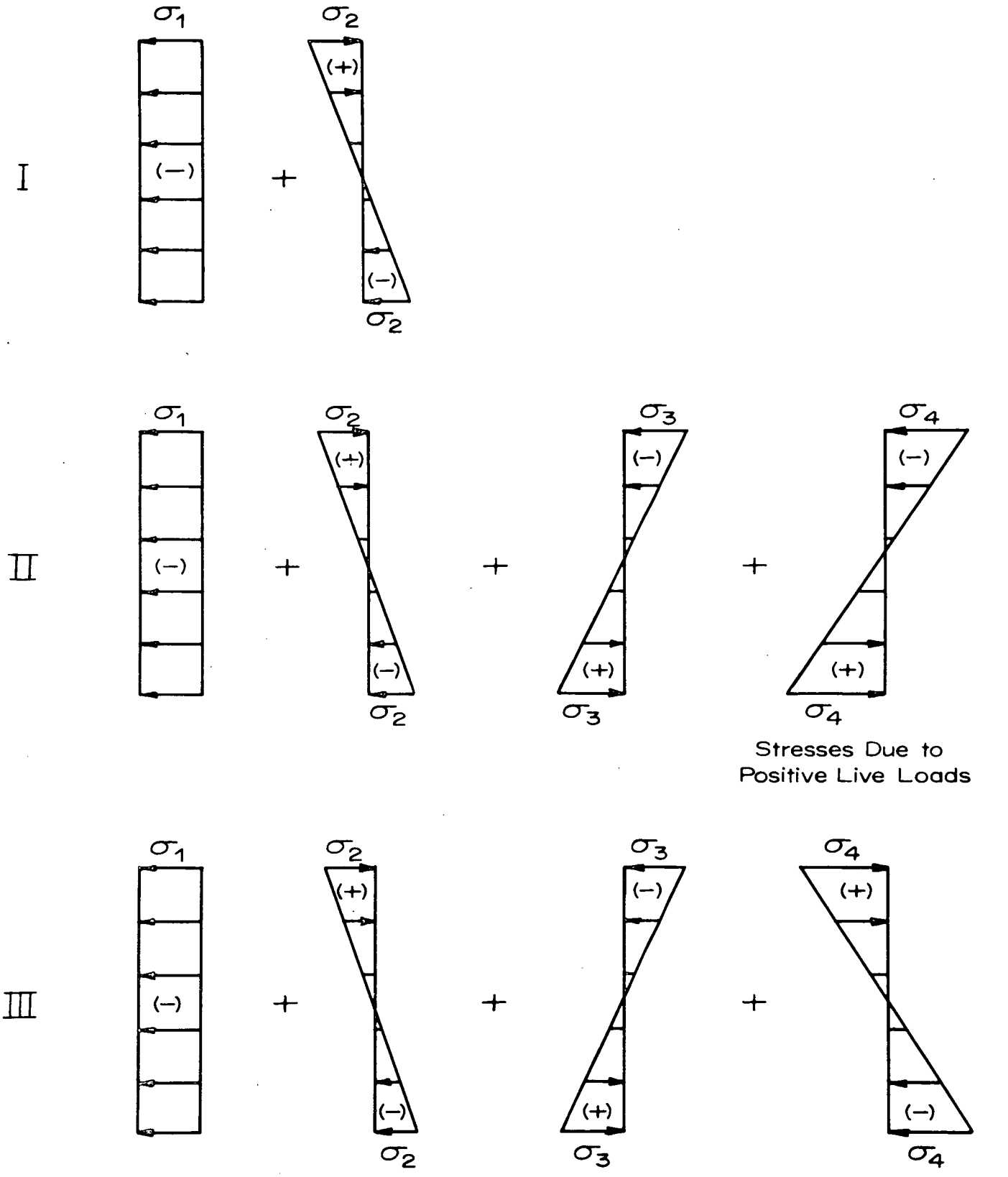

Fig. 2. Stress Distributions in Concrete

References

[1] J. Birchill, TACV Guideway Considerations, (draft report), TRW Systems Group, Calif. (1968)

[2] G.J. Easton, C.G. Swanson, and A.F. Lampros, British and American TACV System Developments: Technical and Environmental Factors, Am. Soc. of Mech. Engr. preprint 70-Tran-50, (1970)

[3] S.B. Biggers and J.F. Wilson, Dynamic Interactions of High Speed Tracked Air Cushion Vehicles with their Guideways, a Parametric Study, Proc. of 12th AIAA/ASME Structures, Structural Dynamics and Materials, No. 71-386,(1971)

[4] J.F. Wilson, Dynamic Interactions between Moving Loads and their Supporting Structures, with Applications to Air Cushion Vehicle-Guideway Design, Report No. FRA-RT- 72-27, Clearinghouse for Federal Scientific and Technical Information, 197 pages (1971)

[5] J.F. Wilson and S.B. Biggers, Dynamic Interactions between Long Trains of Air Cushion Vehicles and their Guideways, J. of Dynamic Systems: Measurement and Control, Trans. ASME, 1, 16-24 (1971)

[6] P.W. Abeles. Introduction to Prestressed Concrete, Vols 1, 2, Concrete Publications Limited, London (1964)

[7] A. Touma, Design Optimization of Guideways and Dynamic Analysis of Rail Plates for High Speed Transportation, Ph.D. dissertation, Dept. of Civil Engineering, Duke University, Durham, N.C. (1972)

[8] American Concrete Institute, Building Code Requirements for Reinforced Concrete, (1963)

[9] TRW Systems Group, High Speed Rail Systems, Report No. FRA-RT-70-36, Clearinghouse for Federal Scientific and Technical Information, 605 pages (1970)

ACTIVE SUSPENSION SYSTEMS: EXPERIMENTATION AND SIMULATION STUDIES

John Beattie and Donald Wright
Department of Mechanical Engineering, Duke University

The design of suspension systems for high speed ground transportation vehicles will probably require active elements to achieve a required standard of passenger comfort. Active elements in parallel with passive suspensions provide a flexibility and low frequency isolation capability unavailable in conventional passive systems. The active system consists of a hydraulic actuator, electrohydraulic servovalve, and electronic relative displacement and acceleration feedback circuits. An experimental active suspension system was constructed and a mathematical model developed. Close agreement between frequency response data from the experimental system and an analog computer simulation validate the analytic model. The conditions for dominance of system control dynamics and system stability are determined through application of root locus and Routh-Hurwitz techniques to the analytic model. Parameter plane analysis is used to determine system response over a wide range of feedback gains and time constants. Future work is needed to compensate or eliminate a mechanical resonance in the experimental system, and to develop a multi degree of freedom experimental system.

Introduction

The primary purpose of a vehicle suspension system is to isolate the vehicle from roadway disturbances. In designing suspensions for high speed ground transportation (HSGT) vehicles,

special problems arise because of the need to provide an acceptable standard of passenger comfort while travelling at high speeds over reasonably smooth guideways. The need for further research in suspension system technology, to meet the requirements of HSGT systems, has been well documented [1]*.

The use of active elements in conjunction with conventional passive springs and shock absorbers showed promise for improving vehicle isolation. Cooperrider [2] showed that conventional passive suspensions on HSGT vehicles would not be able to satisfy passenger comfort requirements without guideways significantly smoother than the Japanese New Tokaido Line. By analog computer simulation he showed that active elements in parallel with the passive suspension could satisfy comfort criteria. Osbon and Putman [3] studied methods of adding active suspension components to high speed rail cars. Their design was also based on analog computer studies. Calcaterra [4] made an extensive study of several active suspension configurations by analog computer simulation. These and other research efforts have culminated in the use of active suspension components in the Tracked Air Cushion Research Vehicle being developed for the DOT by Grumman [5].

Some research on active suspension technology has been carried on at Duke University since 1970. Belani [6], in a detailed review of recent literature on active suspensions, noted that most studies had used only simulation analyses. DiRienzo [7] and Southerland [8] conducted tests on an experimental model of an active suspension system, with one degree of freedom. This project has the objectives:

---

*Numbers in brackets refer to List of References.

(1) To design and develop a one degree of freedom experimental model of an active suspension system.

(2) To devise a mathematical model of the system which accurately predicts its response.

(3) To investigate the effect of design parameters on the system response.

Guideway disturbances are usually considered to be a superposition of random broad-band guideway roughness and discrete frequency disturbances caused by dynamic guideway deflection as the vehicle passes between guideway support structures. These disturbances can be modelled by sine waves of appropriate amplitude and frequency [4]. Secondary effects, such as wind gusts, are not considered in this work.

Vehicle ride comfort specifications have been developed which specify maximum levels of acceleration considered comfortable by human passengers [6]. These specifications indicate that the range of critical frequencies from the standpoint of human comfort is from 1.0 to 15.0 Hz. For given guideway characteristics and human comfort requirements, a suspension system natural frequency and damping ratio can be determined such that comfort requirements are satisfied while travelling at the vehicle design speed over the guideway.

Active suspension systems create a low natural frequency by increasing, artifically, the vehicle mass through acceleration feedback. Passive suspension systems cannot provide natural frequencies less than about 0.8 Hz because of spring design constraints [2].

Experimental System Design

Active Suspension Components:

The major components of an active suspension system are

as follows:

1. Hydraulic Actuator

   The actuator converts pressure or flow signals from the servovalve to force or displacement. The size of the actuator is governed by two considerations. The first is that the piston area must be large enough to handle maximum loads. The second is that the hydraulic resonant frequency associated with the actuator and its load must provide acceptable servobandwidth. The servobandwidth should be high enough to cover the 1 to 15 Hz range of maximum human sensitivity to vibration.

2. Electrohydraulic Servovalve

   This is the primary control element. It converts a low power electric signal into a hydraulic press or flow output to drive the actuator. Frequency bandwidth of the servovalve should be higher than the hydraulic resonant frequency. Linearity is highly desirable and should cover such things as flow gain, allowable friction.

3. Hydraulic Power Supply

   This device provides the flow and pressure needed to operate the servovalve and actuator. The components include the pump, pressure filter, relief valve, accumulator and reservoir. The power supply is usually assumed to be a constant pressure source. The supply operating pressure is an important design factor. Higher pressures have smaller flow requirements resulting in system weight savings. However, leakage increases and life decreases with higher pressures.

4. Vehicle model

   The experimental model of an active suspension system consists of a rigid mass connected to the actuator by a flexible coupling and constrained by ball bushings to one degree of freedom motion. The flexible coupling provides added isolation at frequencies near and above the hydraulic resonant frequency, and corrects misalignment between the actuator and vehicle model.

5. Electronic Feedback and Amplifying Components

   The electronic components generate and control the feedback acceleration and relative displacement signals which set up the artificial suspension natural frequency. Included are an accelerometer, a linear variable differential transformer (LVDT), an LVDT modulator, control amplifiers, and a power amplifier.

A complete pictorial schematic diagram of the experimental system is presented in Figure 1. Voltage supply was by DC batteries, and the output was recorded on a two-channel Sanborn strip chart recorder.

Experimental Results

Transfer Functions

In deriving analytic transfer functions for electrohydraulic system components, a number of assumptions must often be made to linearize the equations [11, 17]. These assumptions limit the usefulness of theoretical analysis. An alternate approach is to approximate the experimental response of components with linear transfer functions accurate over the de-

sired frequency bandwidth. The transfer functions selected or derived for the various components of the model system are presented below.

1. Hydraulic Actuator

$$\frac{y_1}{Q_L} = \frac{1}{A_p s}$$

where

y_1 = piston position, A_p = piston area (.086 in^2)

Q_L = load flow, s = Laplace operator

2. Electrohydraulic Servovalve

$$\frac{Q_L}{i_o}(s) = K_s \left(\frac{1}{1 + \tau_v s}\right)$$

where

i_o = input current to torque motor

K_s = servovalve static flow gain

τ_v = apparent servovalve time constant

3. Hydraulic Power Supply

$$f_{max} = \frac{Q_{L\,max}}{A_p 2\pi A}$$

for

Q_{Lmax} = 4 cu.in.sec., A_p = .086 in^2, and A = 0.40 in, f_{max} is 18.5 Hz. This is double the maximum exciter frequency of 9 Hz thus validating the assumption of a constant pressure source.

4. Power Amplifier Circuit (PAC)

$$\frac{i_o}{e_i}(s) = \frac{K_{PAC}}{1 + \tau_{PAC} s}$$

where

K_{PAC} = PAC gain constant (0.95 ma/volt)

e_i = input error signal

τ_{PAC} = Apparent PAC time constant (.000352 sec.)

5. LVDT and Demodulator Circuit

$$\frac{e_d}{y_1}(s) = \frac{K_{LVDT}}{1 + RC\,s}$$

where

e_d = voltage output of LVDT

K_{LVDT} = LVDT gain in volts/in

R = Resistance of filter circuit ($5 \times 10^4 \Omega$)

C = Capacitance of filter circuit (1×10^{-8} farads)

6. Accelerometer

$$\frac{e_{acc}}{y_3}(s) = \frac{K_a s^2}{s^2 + 2\xi_a \omega_a s + \omega_a^2}$$

where

e_{acc} = accelerometer output voltage

y_3 = displacement of vehicle mass

K_a = accelerometer gain constant (.01295 v/in/sec^2)

ξ_a = damping factor (0.61 of critical)

ω_a = natural frequency (622 rad/sec)

7. Vehicle Mass and Flexible Coupling

$$\frac{y_3}{y_o + y_1}(s) = \frac{K_2 + C_2 s}{M_L s^2 + C_2 s + K_2}$$

where

$y_o + y_1$ = input displacement and actuator position

K_2 = flexible coupling spring constant

C_2 = flexible coupling damping

M_L = vehicle mass

8. Feedback Amplifiers

$$e_i = C_a \frac{1}{1 + R_1 C_1 s} e_{acc} + C_d e_d + \frac{100}{s} C_{Id} e_d$$

The circuit represented by this equation provides acceleration, relative displacement and integral relative displacement feedbacks with adjustable gain constants.

The complete analytic model as represented by the above component relationships in combination is illustrated in Figure 2. The input, y, shown is not used in this study but may represent some type of control input, e.g., a guideway preview control signal.

Analog Computer Modeling

Analog computer modelling has been widely used in the analysis of hydraulic control systems and active suspensions [2, 3, 4, 10, 16]. In developing the analog computer model it is assumed that dynamic effects with natural frequencies more than 100 Hz or time constants less than .0016 sec. may be neglected when compared with the suspension natural frequency range of 1 to 5 Hz and the flexible coupling-vehicle mass natural frequency of 17.25 Hz. This assumption allows modelling without the need for large time scaling factors, which would greatly lengthen the time required for a simulation run, probably without producing significant additional data on the system response. The assumption results in the removal of the servovalve (time constant = .0015 sec), PAC (time constant - .000352 sec), LVDT demodulator (time constant = .0005 sec) and accelerometer

(natural frequency = 100 Hz, damping ratio = 0.61) dynamics from the simulation. The resulting simplified block diagram is shown in Figure 3. The block diagram notation is given in Table 1.

The analog computer results serve two purposes. The first is to provide a comparison between the response of the analytic model and the experimental system. A good comparison shows the validity of the model. The second purpose is to show the effect on system response (characterized by natural frequency and damping ratio) of variations in system design parameters.

The first purpose is accomplished with a frequency response test of the analog model. System parameters are set equal to those of the experimental system and output magnitudes are recorded for various disturbance input frequencies from 1 to 20 Hz. These results are shown below in conjunction with the experimental results. In general, excellent agreement exists between the analog computer and experimental results.

Five sets of computer runs were made to determine the effect on system response of variations in:

(1) Acceleration feedback gain (K_{acc})

(2) Relative Displacement feedback gain (K_d)

(3) Supply pressure (K_v)

(4) Acceleration feedback time constant (τ_N)

(5) Integral Relative displacement feedback (K_{Id})

The results consist of an effective natural frequency and damping ratio for each value of each parameter. These values were computed from an analysis of the response of the system to a sudden release of the vehicle mass from a fixed displacement, essentially a step input to the system.

Table 1. Simplified Block Diagram Parameters

Symbol	Meaning	Value
A_p	Actuator area	.086 in^2
a	Displacement circuit feedback signal	-
b	Acceleration circuit feedback signal	-
C_2	Flexible Coupling damping	1.06 lbs.sec/in
K_2	Flexible coupling spring constant	608 lbs/in
K_v	Combined servovalve & PAC gain $K_v = K_s K_{PAC}$	1.53 in^3/sec/volt
K_{acc}	Acceleration feedback gain $K_{acc} = C_{acc} K_a$	Variable
K_d	Relative displacement feedback gain $K_d = C_d K_{LVDT}$	Variable
K_{Id}	Integral Relative displacement feedback gain $K_{Id} = 100 C_{Id} K_{LVDT}$	Variable
M_L	Vehicle Mass	0.0518 lb.sec^2/in
τ_N	Acceleration feedback time constant	Variable
s	Laplace operator	-
y	Control input	0.0
y_o	Guideway displacement	-
y_1	Actuator piston displacement	-
y_2	$y_o + y_1$	-
y_3	Vehicle mass displacement	-

Experimental Results

Experimental data was taken on the system illustrated in Figure 1. A frequency response test is used to provide data for comparison with analog computer results. In this test the input to the system is a sinusoidal oscillation of 0.30 inch amplitude and variable frequency from 1.4 to 9.0 Hertz. The vehicle mass acceleration was recorded for several values of acceleration feedback gain and supply pressure. From peak values of acceleration the amplitude of vibration of the vehicle mass can be computed. For sinusoidal oscillations:

$$\ddot{y}_3 = \omega_g^2 \, y_3$$

Dividing peak acceleration values by frequency squared yields peak displacements. Figure 4 presents the results of a typical experimental frequency response test, and compares them with the results of frequency response tests of the analog computer model. The excellent agreement shown here was also found in other tests where the system parameter K_{acc} had values of 0.00259 and 0.00518 and 0.01036 volts/in/sec^2. One exception was at low frequencies (1.5 Hz) at low values of acceleration feedback gain ($K_{acc} = 0.01036$).

Conclusions

It has been shown experimentally that a wide range in system natural frequency and damping ratio can be achieved by varying relative displacement and acceleration feedback gains, and the acceleration feedback lag circuit time constant. This indicates the flexibility in suspension operation afforded by the use of such electronic feedbacks. Given this flexibility

a computer-controlled system, which would adjust its natural frequency and damping ratio to maximize passenger comfort and minimize power usage for particular guideway conditions, can be envisioned. This type of system should prove to be economically feasible in an HSGT vehicle where good passenger comfort criteria are to be met and operating costs must be minimized. Passive suspensions do not have the flexibility necessary to meet such comfort criteria.

In the one-dimensional experimental model tested it was not possible to attain system natural frequencies less than about 1.5 Hz because of a high frequency oscillation occurring for large acceleration feedback gains. This oscillation, however, was believed to be caused by interaction of the model with its support table and could be eliminated by providing a more rigid mounting for the experimental model. The analytic study shows that natural frequencies in the 0.2 Hz range should be within the capability of the experimental system. This is the range proposed by Calcaterra [4] to provide adequate isolation of the broadband excitations caused by guideway irregularities.

The close comparison of analytic and experimental response curves for the system indicate that the fourth or fifth order linear equations adequately describe the system response and can be used for design purposes. It is important to note that the dynamics of the hydraulic and electronic components have almost no effect on the system dynamics since their natural frequencies and time constants are negligible compared to those of the control and flexible coupling dynamics. Providing nonlinearities (rate-limiting, backlash, etc.) are negligible, only the gain constants of the hydraulic and electronic elements are important in system dynamic response analysis.

A parameter plane analysis was developed and appears to

be an excellent means of determining the effect of variations in system parameters on the response. This method is only accurate when system control poles dominate the response. However this requirement will automatically be met under most operating conditions. The type of information provided by parameter plane analysis can be effectively used for the design of a guideway-adaptive control system. It has been confirmed that active systems provide a flexibility and low natural frequency capability which is unavailable in passive suspensions.

Analytic and experimental studies of a model provides useful knowledge in the design of a real active suspension system. Before a multi degree of freedom system is built, further useful testing could be conducted with the one degree of freedom system.

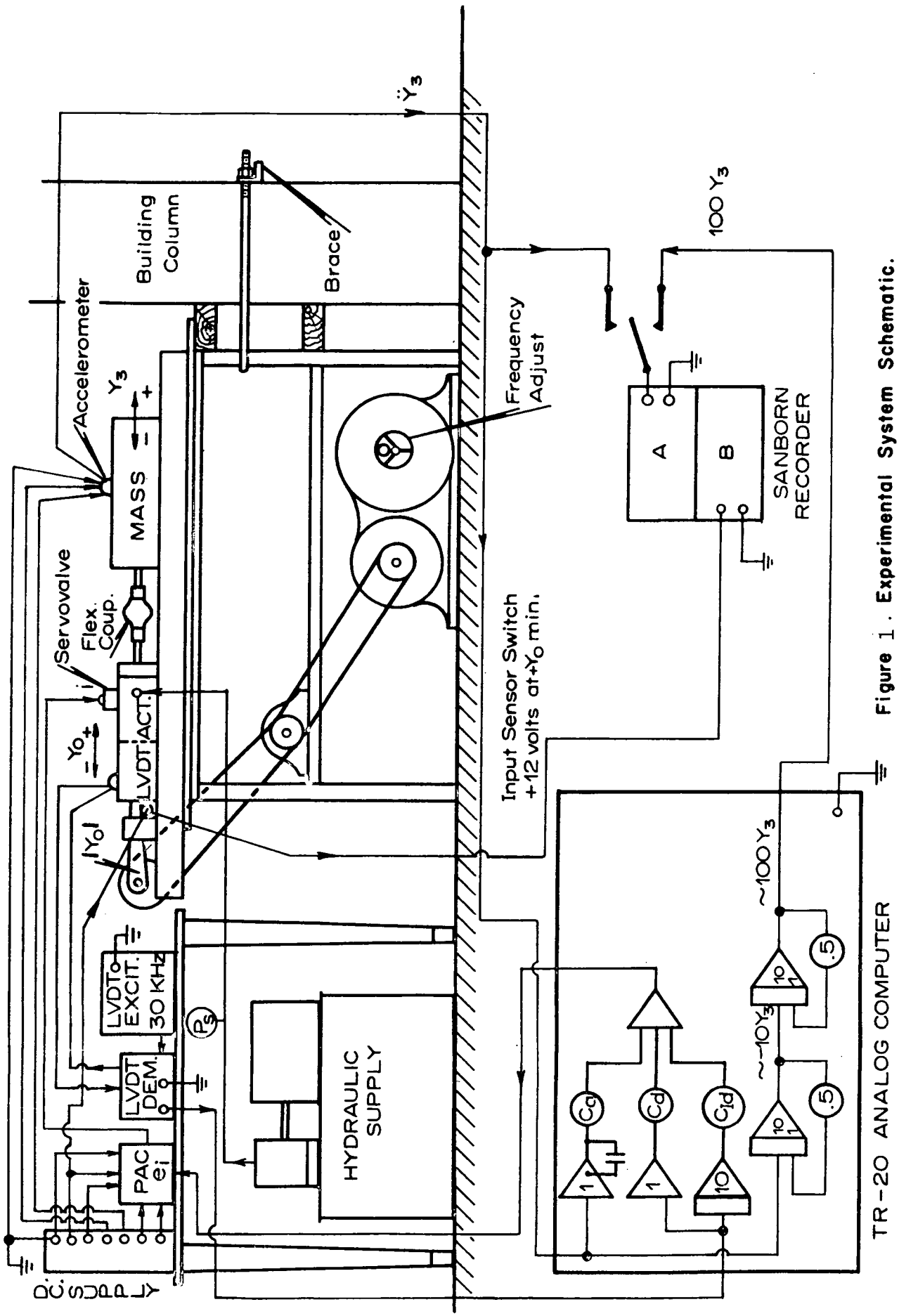

Figure 1. Experimental System Schematic.

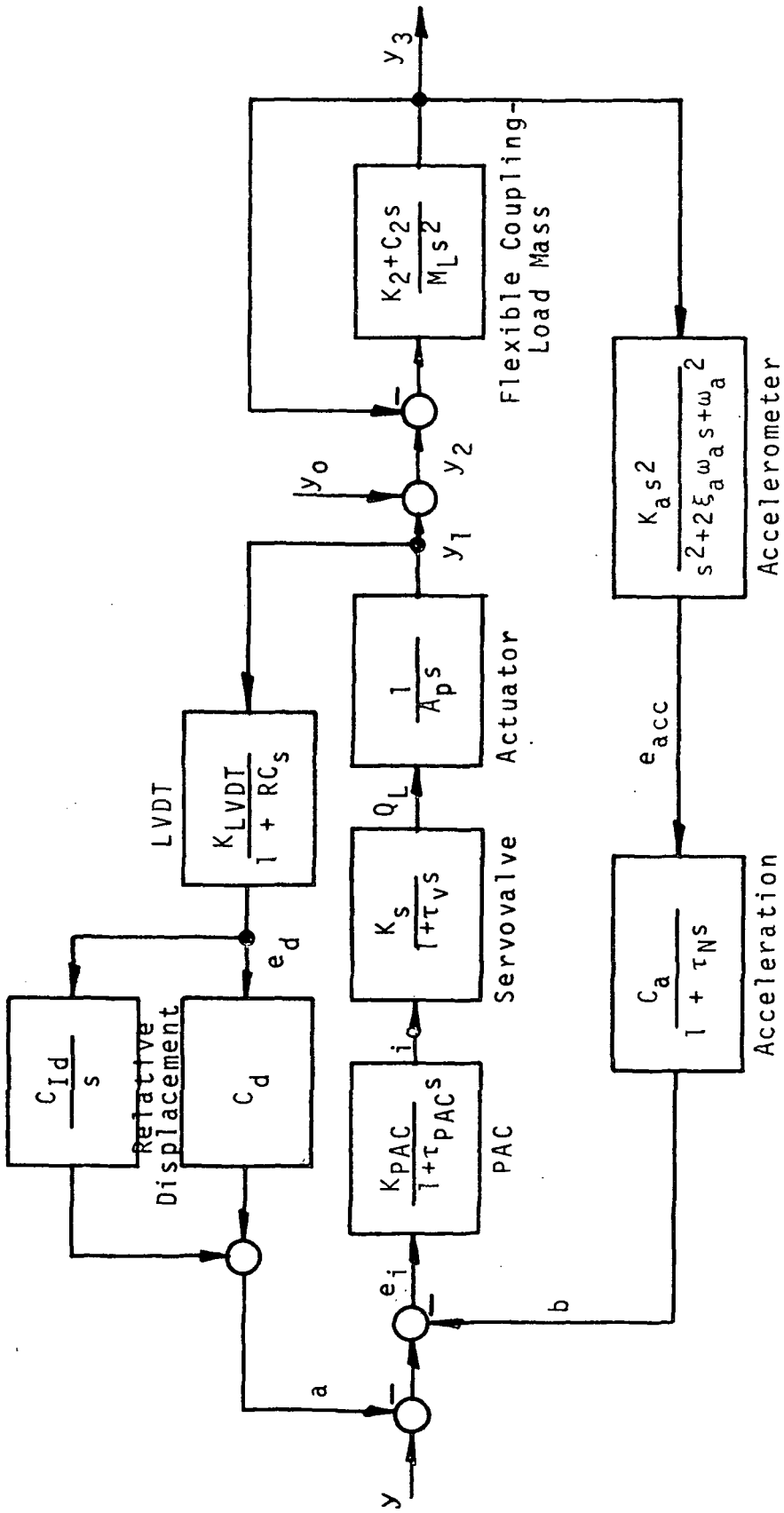

Figure 2 . Active Suspension System Comprehensive Block Diagram.

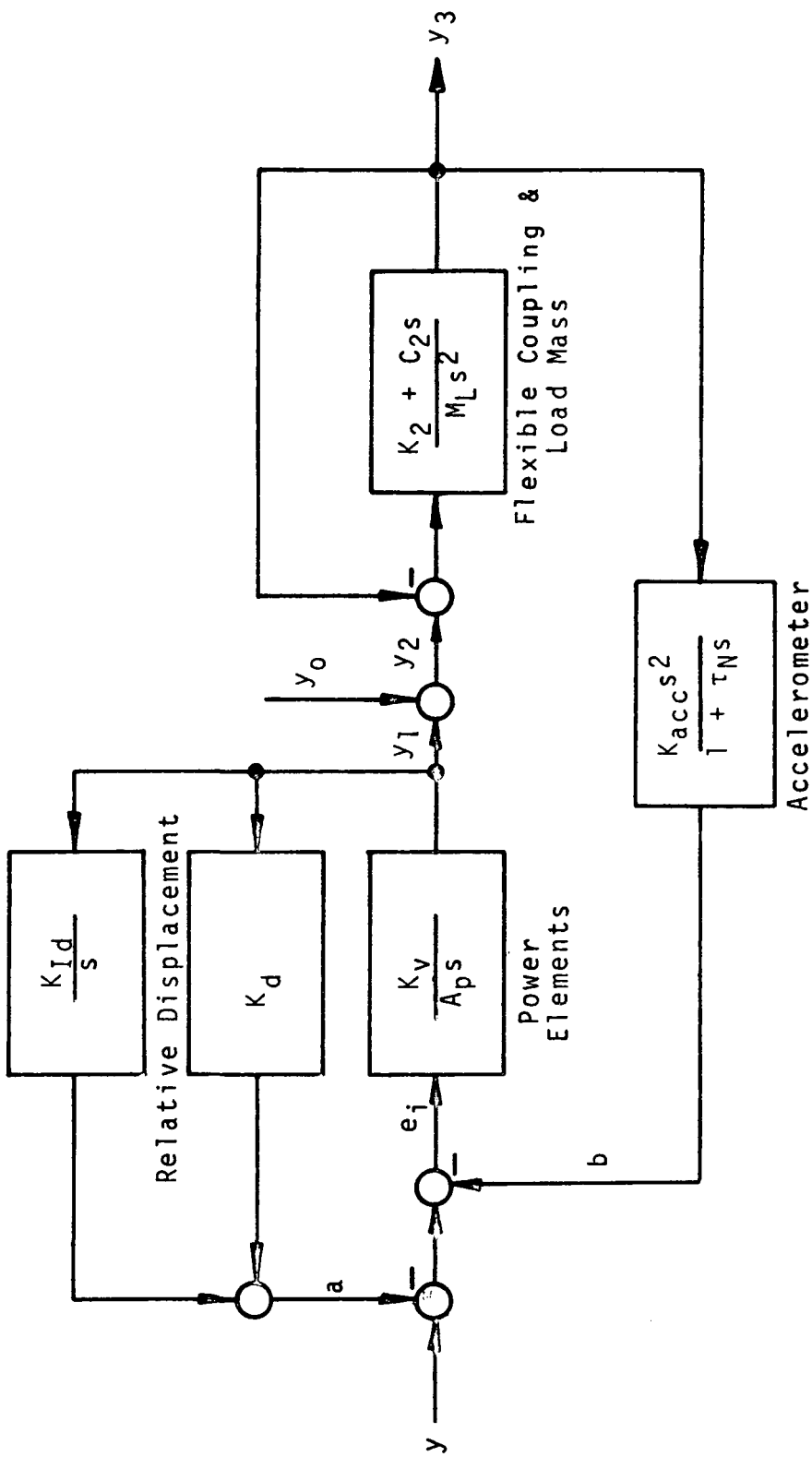

Figure 3. Active Suspension System Simplified Block Diagram.

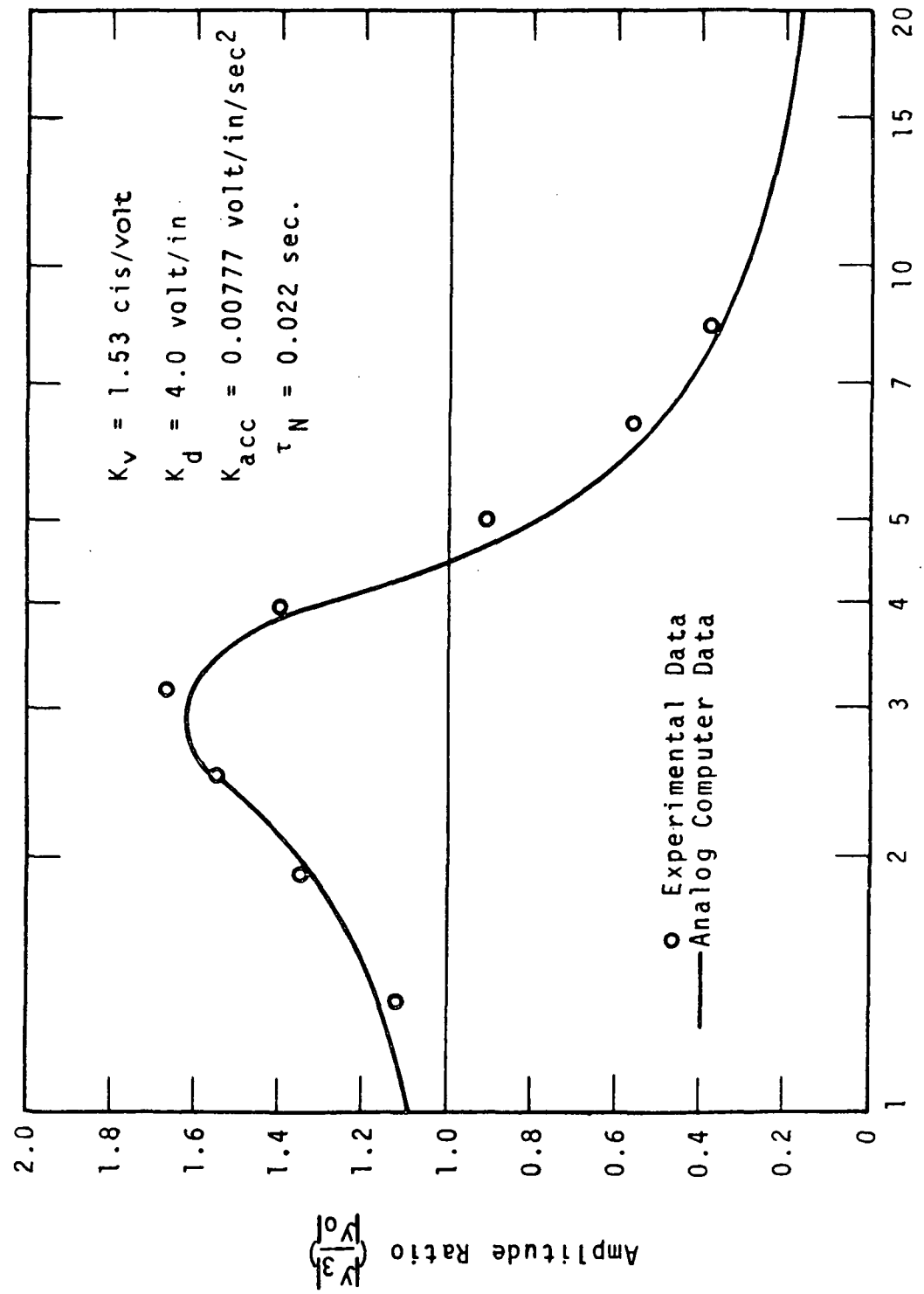

Figure 4. Experimental vs. Analog Frequency Response.

List of References

1. "Survey of Technology for High Speed Ground Transport, Part I." Prepared for U.S. Department of Commerce by MIT, Cambridge, Massachusetts, June 15, 1965, PB 168 648.

2. Cooperrider, N.K., "Suspension Systems for Tracked Air Cushion Vehicles," Report No. 0 9-C-014, Mechanical Engineering Laboratory, General Electric Research and Development Center, Schenectady, New York, December, 1968.

3. Osbon, W.O., and Putman, T.H., "Engineering Design Study of Active Ride Stabilizer for the Department of Transportation's High Speed Test Cars," Westinghouse Electric Corporation, Research Laboratories, Contract No. 3-0267, PB 185 008.

4. Calcaterra, Peter C., et al., "Study of Active Vibration Isolation Systems for Severe Ground Transportation Environments," Barry Wright Corporation, Watertown, Massachusetts, NASA Contract No. NAS1-8611, Nov., 1969.

5. Grumman Aircraft Engineering Corporation, "Tracked Air Cushion Research Vehicle, Volume I Research Vehicle Preliminary Design," Bethpage, New York, March, 1969, PB 183 172.

6. Belani, S. G., Active Vehicle Suspensions: A Preliminary Study, M.S. Thesis, Dept. of Mechanical Engineering, Duke University, May, 1970.

7. DiRienzo, F.H., "Hardware Design of an Active Suspension System for a High Speed Transport Vehicle," Project Report, Dept. of Mechanical Engineering, Duke University, May, 1970.

8. Southerland, S.D., "High Speed Ground Transportation Suspension System Progress Report," Project Report, Dept. of Mechanical Engineering, Duke University, Sept. 1970.

9. Merritt, H.E., Hydraulic Control Systems, John Wiley & Sons, New York, N.Y., 1967.

10. Lewis, E. E. and Stern, H., Design of Hydraulic Control Systems, McGraw-Hill, New York, N.Y., 1962.

11. Thayer, W. J., "Transfer Functions for Moog Servovalves," Technical Bulletin #103, Moog Servocontrols Inc., East Aurora, N.Y., 1958.

12. Campbell, M. E., "Discussion on Dynamics of Hydraulic Servomotors," Trans. ASME, October, 1953, pp. 1390-1392.

13. Holman, J. P., Experimental Methods for Engineers, McGraw-Hill, New York, N.Y., 1966.

14. Schaevitz Engineering, "Linear and Angular Servo Accelerometers," Technical Bulletin B-9, Pennsauken, N.J., August 1969.

15. Schaevitz Engineering, "The LVDT vs. the Resistance Potentiometer," Technical Bulletin A-34, Pennsauken, N.J., December, 1968.

16. Crozier, J. R., Design and Development of a Hydraulic Control for an Instructional Laboratory, M.S. Thesis, Dept. of Mechanical Engineering, Duke University, October, 1969.

17. Shasha, N., Simulation of a Nonlinear Hydraulic System, A Dissertation in the Faculty of Engineering, Sir George Williams University, Montreal, Canada, Sept. 1970.

18. Vierck, Robert K., Vibration Analysis, International Textbook Company, Scranton, Pennsylvania, 1967.

19. Dorf, R. C., Modern Control Systems, Addison-Wesley, Reading, Massachusetts, 1967.

20. Siljak, D. D., Nonlinear Systems, John Wiley & Sons, New York, N.Y., 1969.

C. TUBE TRANSPORTATION

1. "Control Concepts for Pneumatic Tube Vehicles," Donald Wright and K. P. White, Jr., Mechanical Engineering Department, (Paper to be submitted to ASME Journal of Dynamic Systems and Controls).

2. "Energy Study of Underground Rapid Transit," Jack B. Chaddock and Ish Sud, Mechanical Engineering Department, (Accepted for publication in High Speed Ground Transportation Journal, Vol. 6, No. 3, Fall 1972).

3. "Experimental Investigation of Tubed Vehicle Aerodynamic Characteristics," Bruce R. Munson and Leslie D. Smith, Department of Mechanical Engineering, (Paper to be submitted for publication to AIAA Journal).

4. "A Dynamic Modeling Method of Unsteady Flows in Fluid Lines with Large Bias Velocities," Donald Wright and Omer Mercier, Department of Mechanical Engineering, (to be submitted for publication in Journal of Basic Engineering).

CONTROL CONCEPTS FOR PNEUMATIC-TUBE VEHICLES

Donald Wright and K. P. White, Jr.
Department of Mechanical Engineering, Duke University

I. Introduction

The use of totally enclosed guideways or "tubes" in high speed ground transportation (HSGT) systems has received considerable interest in the past decade. Because enclosed systems are isolated from their external environment, they are ecologically sound, aesthetically malleable, and safe from environmental intrusions. Enclosed systems are equally applicable to elevated, surface, and subway configurations and, in general, require minimum right-of-way. These attributes permit direct access to urban centers not readily afforded by conventional HSGT systems.

The physical characteristics of an enclosed guideway, principally the guideway's ability to hold a partial vacuum, allow radical conceptual departures from conventional HSGT modes. Among the most novel of these new concepts is the pneumatic-tube system, proposed initially by Kumar [1][1]. As shown in Figure 1, the essential elements of the system are (1) an enclosed, tubular guideway, (2) a sealed vehicle within and closely fitting the guideway, and (3) a compressor or other means of evacuating air from within the guideway. The principle of operation of the system is similar to that employed in an ordinary soda straw: air is withdrawn by the compressor from the guideway segment between the vehicle and the compressor outlet creating a region of low pressure ahead of the vehicle; air is admitted at the inlet creating a region of high pressure behind the vehicle; the pressure difference established across the vehicle propels the vehicle

[1] Numbers in brackets designate References at the end of the paper.

down the tube toward the outlet.

Although investigations into the dynamics of the pneumatic-tube system have been in progress since 1965, research largely has ignored considerations of vehicle control. Conventional HSGT systems generate propulsive forces directly at the vehicle, either through traction or by momentum transfer, and control is obtained directly at the vehicle by governing the magnitude and direction of these propulsive forces. The pneumatic-tube system departs from this convention both in the nature of the propulsive force and in the manner and location of its generation. The vehicle may be conceived of as a free piston in a column of air. The motive force, the pressure difference, is generated by expelling air from the column at a fixed position along the tube. In effect, the force propelling the vehicle is transmitted to the vehicle through and by a changing column of air. Control considerations are complicated by the desire to maintain the passivity of pneumatic-tube vehicles, by the nonlinearity of the fluid mechanics describing air flow within the tube, and by complexities resulting from the possible transmission of control signals through a fluid medium.

The complexity and nonlinearity of this propulsive scheme obscures the optimal means by which the propulsive force, and thus the motion of the vehicle, may be controlled. Two possibilities are:

(1) regulate the pressure ahead of the vehicle by adjusting the volume flow rate of the air expelled at the compressor (valve-control), and

(2) supplement the pressure-difference propulsive force with forces generated by a secondary, on-board propulsive system (force control).

The purpose of the research presented in this paper is to investigate by simulation the response of these control mechanisms.

Current theory [2] advances a mathematical model of the pneumatic-tube system predicated on the assumptions of Fanno flow[2] of the air between the tube inlet and the stern of the vehicle and Fanno flow with adiabatic compression of the air between the fore of the vehicle and the tube outlet. Application of this model requires the simultaneous solution of multiple, implicit, nonlinear equations by numerical techniques. Design procedures for control of pneumatic-tube vehicles based on this theory must allow for the numerical solution of the system model by digital computation.

The formulation of the numerical analog of the pneumatic-tube system [2] is reviewed in Section II. The analog simulates the dynamics of the uncontrolled system. In Section III, two schemes for vehicle control are advanced. Simulations of the system response employing each scheme are presented in Section IV. In Section V, results of the simulation are presented and discussed. Conclusions based on simulation results are discussed in Section VI.

[2] Fanno flow is the one dimensional, adiabatic, frictional, steady flow of a perfect gas in a duct of constant area. For a full development of the Fanno equations, see Shapiro [3].

II. The Pneumatic-tube Analog

The Fanno flow model[3] of the pneumatic-tube vehicle system developed by Cudlin and Harman [2] is employed extensively in the simulations to represent the uncontrolled motion of the vehicle and to determine the reaction of the vehicle to both valve-control and force-control mechanisms. By dividing the tube into small intervals, the analog permits an iterative, numerical solution of the system equations across each interval successively.

The motion of the vehicle within the tube is described by Newton's second law of motion:

$$\Sigma F = ma = m \frac{dV}{dt}$$

$$= m\ V \frac{dV}{dx}.$$

The forces acting on the vehicle are attributable to the pressure difference across the vehicle and to friction, i.e.,

$$\Sigma F = (P_b - P_a) - f_f$$

and thus, the equation of motion becomes

$$((P_b - P_a)A - f_f)\ dx = m\ v\ dv.$$

[3] Although the Fanno flow model is not entirely satisfactory as an explanation of the vehicle's motion, experimental work shows the model viable under the limited conditions for which it is developed [4]. Application of the Fanno theory in the simulation for conditions of variable outlet air-flow velocity is necessitated by lack of an improved theory.

Concurrent research into the control of pneumatic-tube vehicles may result in such an improved theory. This research is not based on assumptions of Fanno flow, but formulates a model of the system by linearization of the basic equations describing unsteady flow in the tube [5].

Attempts to simplify the Fanno flow model by direct linearization of the Fanno equations [6] have proven untenable.

Integrating this expression over a small interval Δx and assuming pressures and velocities vary linearly across this interval yields

$$\{[\tfrac{1}{2}(P_{b2}+P_{b1}) - \tfrac{1}{2}(P_{a2}+P_{a1})]A - f_f\}\Delta x = \tfrac{1}{2}m(V_2^2-V_1^2). \quad (1)$$

Unknown in this equation are the pressures behind, P_{b2}, and ahead, P_{a2}, of the vehicle and the terminal vehicle velocity, V_2. The numerical solution for these unknowns is initiated by assuming the pressures remain constant over the interval, i.e., $P_{b1} = P_{b2}$ and $P_{a1} = P_{a2}$, and solving the equation of motion (1) for V_2. This velocity value is used to solve for P_{b2} through the Fanno equations. Assuming the air-flow velocity (U_b) immediately behind the vehicle equals the vehicle velocity, the Fanno velocity relationship:

$$\frac{U_b}{V^*} = M_b \quad \frac{k+1}{2(1+\frac{k-1}{2})M_b^2} \quad (2)$$

and the relationships:

$$T^* = \frac{2}{k+1} T_s, \text{ and } V^* = \quad g\, kRT^*$$

can be solved for the flow Mach number at the vehicle, M_b. In the above equation, T_s is the known stagnation temperature of the air. The value of flow Mach number is used to solve the relationship for frictional adiabatic flow:

$$(4f \frac{L_{max}}{D})_b = \frac{1-M_b^2}{kM_b^2} + \frac{k+1}{2k} \ln \frac{(k+1)M_b^2}{2(1+\frac{k-1}{2}M_b^2} \quad (3)$$

for $(4f\ L_{max}/D)_b$. By applying the Fanno relationship:

$$(4f \frac{L_{max}}{D})_i = (4f \frac{L_{max}}{D})_b + 4f \frac{x}{D} \quad (4)$$

with knowledge of the vehicle's position in the tube, x, the value of $(4f\ L_{max}/D)_i$ is determined. The flow Mach number at the inlet, M_i,

is obtained by the solution of equation (3) rewritten for inlet conditions. Since this equation is implicit in M_i, a numerical technique, three-point Lagrangian interpolation upon the tabulated values of Mach number versus ($4f\ L_{max}/D$), is employed to affect its solution. The ratio's (P_{b2}/P^*) and (P_i/P^*) are obtained directly by substituting the values of M_b and M_i, respectively, into the Fanno pressure relation:

$$\frac{P}{P^*} = \frac{1}{M} \quad \frac{k+1}{2(1 + \frac{k-1}{2}M^2)}. \tag{5}$$

Since P_i is the known inlet pressure,

$$P_{b2} = \frac{(P_{b1}/P^*)}{(P_i/P^*)} P_i \tag{6}$$

yields a second estimate of the pressure behind the vehicle.

The value of P_{a2} is obtained somewhat differently. The Fanno equations (2) through (4) are applied to the column of air ahead of the vehicle beginning with the known, outlet air-flow velocity, U_o, and resulting in the flow Mach number immediately ahead of the vehicle, M_a. Solution of equation (2), rewritten for conditions ahead of the vehicle, then yields the air-flow velocity at this point, U_a. This value is substituted into the compression relation:

$$v = V_2 - U_a \tag{7}$$

to obtain v, the rate of compression per unit cross-sectional area ahead of the vehicle. Employing a linearized average of this quantity across an interval permits solution of the incremental adiabatic compression relation:

$$\frac{P_{a1}}{P_{a2}} = \left[\frac{(L-x) - vt}{L - x}\right]^k \tag{8}$$

for P_{a2}, the second estimate of the terminal air pressure ahead of the vehicle. The value of t in equation (7) is obtained by dividing the interval length by the average vehicle speed,

$$t = \frac{\Delta x}{\frac{1}{2}(V_1 + V_2)}.$$

These second estimates of terminal pressures can be used as above to generate third and subsequent estimates of the variables P_{b2}, P_{a2} and V_2. This iterative process is continued until the same values of these variables are obtained repeatedly.

Application of this scheme to successive intervals, beginning at the inlet, yields the values of output variables at a finite number of positions along the tube. Assuming pressures and velocities vary linearly across each interval results in a simulation of the uncontrolled motion of the pneumatic-tube vehicle.

III. Control Schemata

For the purposes of simulation, two tentative control schemata are proposed. The first schema applies valve control (Figure 2); the second applies force control (Figure 3). The function of each schema is to regulate the velocity of a single vehicle during one traverse of a single segment of the pneumatic-tube. The objectives of vehicle control are limited to:

(1) starting the vehicle from rest while avoiding sudden, forward jerk (change in acceleration),

(2) limiting the magnitude of vehicle accelerations and decelerations to humanly tolerable levels[4], and

[4] Values of maximum comfortable accelerations, decelerations, and jerk for various transportation systems reported by Gebhard [7] are presented in Section V.

(3) attaining and maintaining a constant, steady-state vehicle velocity.

Each schema divides the tube into intervals of equal length Δx. Transducers located along the tube and on-board the vehicle record the values of measured variables, $\underset{\sim}{m}(P_i, P_o, P_a, P_b, T_s, U_o, x, V)$, as the vehicle arrives at the beginning of an interval. The digital vector $\underset{\sim}{m}$ defining the present system state is supplemented by the vector $\underset{\sim}{q}(a_{max}, V_{ss})$ defining control criteria. From the information contained in $\underset{\sim}{m}$ and $\underset{\sim}{q}$, a computer control algorithm computes the vehicle velocity (V_2) desired at the end of the increment.

In the valve control schema, the algorithm then solves numerically the equations describing vehicle motion and predicts the new outlet air flow velocity (U_2) required to achieve V_2. A valve system adjusts the air flow rate at the outlet in accordance with the computer prediction. The change in flow rate causes a change in pressure ahead of the vehicle such that, at the end of the interval, the vehicle has attained the desired velocity.

In the force control schema, the algorithm solves the equations describing the motion of the vehicle, and predicts the magnitude of the supplementary force required to achieve V_2. Based on this prediction, a control signal is generated and transmitted to the on-board, supplementary propulsion system. The propulsion system applies the force as directed and the desired vehicle velocity is attained.

IV. Simulation

Figures 4 and 5 are simplified flow diagrams of the valve-controlled and force-controlled system simulations. Comparison of these diagrams with the schematics of Figures 2 and 3 shows that the flow of information through each scheme is reproduced in the corresponding

simulation. Implementation of the simulation, however, requires the explicit, mathematical development of system components otherwise defined only in terms of their input-output relationships. Since simulation results depend upon the manner in which the control system components are specified, the simulations are less general than the proposed control schemes. The possibility of developing improved components which might alter simulation results renders tentative the conclusions of this paper.

The Valve-Controlled Simulation

The nucleus of the valve-controlled simulation is the computer algorithm. For each interval Δx, the algorithm predicts both the desired terminal vehicle velocity (V_2) and the outlet air-flow velocity (U_{o2}) required to achieve this vehicle velocity. Predictions are made on the basis of information regarding the values of state and control variables supplied to the computer from measurement transducers and the input controller. In the simulation, these values for the first interval are obtained from initial conditions. Information for subsequent intervals is obtained from the terminal values of the variables during the previous interval as calculated by the pneumatic-tube analog.

The first operation of the algorithm is to determine V_2. It is desired that the vehicle attain the prescribed steady-state velocity (V_{ss}) as rapidly as is physically possible, subject to the condition that the vehicle acceleration never excede the threshold of human discomfort, the constant value a_{max}. Under these con-

ditions, only three values of V_2 are possible: V_{ss}[5], the steady-state velocity; V_{pmax}, the maximum physically realizable velocity; and V_{cmax}, the velocity when acceleration over the entire interval is a_{max}. The value of V_{ss} is specified in the input data. The value of V_{pmax} is computed from the equations describing vehicle motion (presented below) by setting the value of the outlet air-flow velocity (U_{o2}) equal to the maximum obtainable by the compressor (given in the input data). Assuming vehicle velocities vary linearly across an interval,

$$V_{cmax} = V_1^2 + 2\ \Delta x\ a_{max}.$$

The logic for assignment of the appropriate value to V_2 is straightforward and is eliminated from this discussion for the sake of brevity.

The next operation of the valve-control algorithm is to solve the equations of motion for U_{o2}. First, P_{b2} is determined from equations (2) through (6) describing Fanno flow: equation (2) is solved for M_{b2}, the local Mach number of the air flow behind the vehicle, assuming the air-flow velocity immediately behind the vehicle (U_{b2}) equals the terminal vehicle velocity (V_2); the value of M_{b2} is substituted into equation (3) to determine $(4f\ L_{max}/D)_{b2}$; this value then is substituted into equation (5), where x is the measured distance from the vehicle to the tube inlet, and equation (5) is solved for $(4f\ L_{max}/D)_{i2}$. Using this value, equation (3) can be solved for the value of the inlet Mach number (M_{i2}) by Lagrangian interpolation.

[5] In practice, a value somewhat different from V_{ss} is assigned to V_2, based on a percentage difference between V_{ss} and the initial vehicle velocity, V_1. By underestimating the required change in velocity, the magnitude of peak velocity overshoot is suppressed.

The values of M_{b2} and M_{i2} each are substituted in equation (5) yielding the ratios P_{i2}/P^* and P_{b2}/P^*. Since P_{i2} is the known, measured inlet pressure, these ratios can be solved via equation (6) for P_{b2}.

The equation of motion (1) now can be solved directly for P_{a2}. This value is then substituted into the incremental relationship for adiabatic compression (8) and the equation solved for v. From (7), the value of the air flow velocity immediately ahead of the vehicle (U_{a2}) is computed. The Fanno flow equations are reapplied to the system to determine the outlet air-flow velocity required to induce the desired vehicle velocity V_2.

For the purposes of simulation, attention is turned to the time required to transmit control signals from the computer to the vehicle. This time lapse has two components, the time-response of the valve system and the transportion lag a of pressure wave through a fluid medium. Since the actual contribution of time lag from the valve response is small compared to the transportation lag, the precise form of the valve time response is of minor importance. A useful approximation (after Gibson [8]) is

$$T(t) = 1.0 - 0.508e^{-2t} - 0.497e^{-9t}\sin(48.8t + 1.43) \quad t \geq 0 \quad (9)$$
$$= 0, \quad t < 0$$

The valve-induced change in outlet air-flow velocity causes a change in pressure at the outlet. The pressure change in turn is transmitted up the tube in the form of a pressure wave. Assuming the wave travels with the speed of sound in air (c) and that wave reflections have severely reduced amplitudes, the time elapsed between inlet changes and vehicle velocity changes can be modelled as a pure delay of duration

$$d = \frac{L - x}{c}.$$

The transmission lag is accounted for in the simulation by delaying actuation of the valve system until time d. Initializing time in this manner, the valve system transfer function is made to represent directly the time-response of the system between the computer and the vehicle.

The pneumatic-tube analog (Section II) is used to determine the effects on the vehicle of the changing air-outflow velocity. The interval Δx is divided into m equal subintervals of length Δy. Based on the known initial values of variables, the analog model solves the equations of motion for the terminal values of these variables at each subinterval. The output value of U_{o2} employed at the $\underline{i}$th subinterval is obtained from multiplying the terminal value of U_{o2} computed in the algorithm by $T(t_i)$ from equation (9) assuming

$$t_i = d + \frac{i}{m} \cdot \frac{2\Delta x}{V_1+V_2}, \qquad i = 1,2,3 \ldots , m.$$

The terminal values of the variables computed by the analog at the last subinterval Δy become the input values of these variables for the subsequent total interval Δx.

The Force-Controlled System

The primary component of the force-controlled system is the computer algorithm. For each interval Δx, the algorithm predicts both the desired terminal vehicle velocity (V_2) and the magnitude of the supplementary control force (S) required to attain this velocity. The prediction of V_2 is made in the same manner as in the valve-controlled simulation. The predicted value and the input values of state and control variables are then used to solve the equations of vehicle motion for S. The force-controlled simulation, it will

be noted, does not necessitate a model of either the valve-dynamics or the transportation lag.

The equation of motion for the force-controlled system obtained from Newton's second law can be solved for S_2, the terminal value of the control force, as:

$$S_2 = \frac{m(V_2^2-V_1^2)}{x} - A[(P_{b2}+P_{b1}) - (P_{a2}+P_{a1})] + f_f - S_1. \qquad (10)$$

The only unknown quantities in equation (10) are the air pressures at the end of the interval and the terminal value of the control force. As before, P_{b2} is obtained by solving the Fanno equations (2) through (6) between the inlet and the stern of the vehicle. Since U_{o2} is a constant input parameter in the force-controlled system, the Fanno equations can be solved between the fore of the vehicle and the tube outlet for U_{a2}. Substituting this value into equation (7) yields the quantity v. Then, equation (8) can be solved for P_{a2} and the result used in equation (10) to solve for S_2.

The pneumatic-tube analog, modified by using equation (10) as the equation of motion, is employed to determine the effects on the vehicle of applying the supplemental control force. The control force is assumed to act instantly and linearly over the interval Δx. For the $\underline{+}$ith subinterval Δy, the magnitude of this force used in the analog model is therefore:

$$S_2(i) = \frac{i}{m} S_2, \qquad i = 1,2,3, \ldots , m ,$$

where S_2 is the terminal force value computed in the algorithm. As before, the final values of variables computed by the analog model at the last interval Δy becomes the input values of these variables for the subsequent total interval Δx.

V. Results

Results of the computer simulations contrast the response of the uncontrolled, the valve-controlled, and the force-controlled systems and demonstrate the sensitivity of these systems to variations in initial conditions and control parameters. Each computer run represents a simulated traverse of one tube segment by a single vehicle. The aggregate of computer runs permits assessment of the relative ability of each system to achieve the stated control objectives. Specific numerical values assigned to simulation parameters refer to the model pneumatic-tube test facility at Duke University and were selected to allow comparison of the simulation results with published analytical data regarding the uncontrolled motion of the model vehicle. Representative simulation results are presented in the accompanying figures and are discussed in the subsections below.

Control of Start-up Jerk

Gebhard [7] has determined that a maximum constant change in acceleration of 6 ft/sec^3 to 7 ft/sec^3 is tolerable in public ground transportation systems and suggests that elimination of jerks entirely is desirable. Simulation results (see Table I) show:

(1) that maximum jerk increases with decreases in initial pre-evacuation pressures,

(2) that, under all conditions tested, values of maximum jerk for the uncontrolled system are between one and two orders of magnitude greater than those values considered tolerable, and

(3) that under all conditions tested, maximum values of jerk for both the valve-controlled and force-controlled systems remain within those considered

tolerable.

Start-up is accomplished by the following procedure: the vehicle is held in place at the tube inlet; the compressor is allowed to partially evacuate the air from the tube segment ahead of the vehicle; when the air pressure ahead of the vehicle has dropped to a predetermined value, the vehicle is released and begins moving forward. This start-up procedure imposes a sudden, initial pressure differential across the vehicle equivalent to a step-function force input. In the uncontrolled system, start-up causes extremely rapid change in acceleration which would result in severe passenger discomfort. The valve-controlled system deminishes jerk by drastically reducing the rate at which air is expelled from the tube prior to the initial release of the vehicle. The reduction, in turn, decreases the initial air flow velocity immediately ahead of the vehicle. As the vehicle accelerates under the impetus of the initial pressure difference, the vehicle acquires a velocity greater than that of the air flow. Continued forward motion compresses the air between the vehicle and the outlet and causes the air pressure ahead of the vehicle to rise. Rising air pressure ahead of the vehicle slows the rate of increase of the forward-acting force on the vehicle and forestalls rapid changes in acceleration.

The force-controlled system also regulates vehicle jerk and provides safe and comfortable starts. As the vehicle accelerates, a force resisting the forward motion is gradually applied to the vehicle. The applied force holding the vehicle within acceleration constraints is gradually released as the vehicle reaches the desired steady-state velocity.

Control of Acceleration

Gebhard reports longitudinal accelerations in the range of 0.11g to 0.15g are comfortable and acceptable to the users of existing public ground transportation systems. Accelerations 0.1g in excess of these values, however, are accepted readily by automobile riders and accelerations of 0.5g are tolerated without discomfort by passengers on commercial aircraft. Assuming passengers in pneumatic-tube vehicles are well seated and warned of accelerations, tolerance of maximum acceleration levels of 0.2g to 0.4g does not seem unreasonable. Simulation results (see Table I) show:

(1) that the values of maximum acceleration generally increase with decreased initial pre-evacuation pressures,

(2) that the accelerations attained by uncontrolled vehicles are consistently in excess of the tolerable limit and have maxima between one and two orders of magnitude greater than this limit,

(3) that both valve-controlled and force-controlled systems have maximum accelerations greater than the 0.15g maximum of extant public ground transportation systems and less than the median of about 0.3g acceptable to automobile passengers,

(4) that both the uncontrolled and valve-controlled vehicle accelerations exhibit oscillatory behavior (Figures 7 and 9), and

(5) that force-controlled vehicle accelerations are non-oscillatory and relatively constant over much of the traverse from tube inlet to outlet.

The valve-controlled system succeeds in limiting accelerations to tolerable levels by a mechanism similar to that described in the previous subsection. The valve control mechanism, however, induces oscillatory accelerations similar to those of the uncontrolled system but significantly smaller in magnitude. These oscillations indicate the constant presence of jerk which, though tolerable, is undesirable.

The force-controlled system successfully limits the maximum value of vehicle accelerations without inducing oscillations. The relatively constant values of acceleration over much of the traverse indicates a desirable reduction of jerk not provided by the valve-control mechanism. When the vehicle achieves steady-state velocity approximately midway during the traverse, a clearly defined decline in the magnitude of acceleration begins. This general pattern suggests greater control of the resultant force acting on the vehicle than afforded by valve-control and implies the operation of the vehicle under force control is somewhat more efficacious.

Control of Steady-State Velocity

The control objective considered finally is that of attaining and maintaining a constant, steady-state vehicle velocity. Results show (compare Figures 6 and 8):

(1) that the uncontrolled vehicle velocity overshoots the steady-state value early during the traverse (in violation of the maximum acceleration criterion) and then oscillates about this value with a large but diminishing amplitude of oscillation,

(2) that the valve-controlled vehicle velocity rises to the steady-state value in near minimum time

and then oscillates about this value, and

(3) that the force-controlled vehicle velocity rises to the steady-state value in near minimum time, peaks at a value slightly greater than steady-state, and then slowly decreases.

These results are inconclusive regarding achievement of the objective of maintaining a constant, steady-state velocity and suggest the need for further simulation. Additional runs were made where the vehicle enters the tube segment with initial velocities within ±20% of the steady-state value and where the initial pressure difference across the vehicle at the inlet is approximately that required to overcome the force of sliding friction. These runs roughly correspond to the conditions encountered when the vehicle enters the second segment or subsequent segments of the total tube-guideway length. Results show (see Figures 10 and 11):

(1) that the uncontrolled vehicle velocity oscillates about the steady-state value at a slow, relatively constant rate of approximately 0.3Hz. with a maximum amplitude of approximately 8% of the steady-state velocity,

(2) that the valve-controlled vehicle velocity oscillates about the steady-state value at a rate of approximately 1 Hz. with a maximum amplitude of approximately 25% of the steady-state value and that the frequency of oscillation generally increases during the traverse, and

(3) that the force-controlled system approaches a constant, steady-state vehicle velocity without

oscillation and with a maximum error of less than 2% of the steady-state value.

Although the uncontrolled system does not maintain a constant, steady-state vehicle velocity, the period of velocity oscillations about the steady-state value is large and the magnitude of such oscillations is small. Operation of the uncontrolled system at this low oscillatory level will not appreciably diminish passenger comfort or detract from the system's performance.

The valve-control mechanism aggravates the natural tendency of the vehicle velocity to oscillate about the steady-state value, increasing both the magnitude and frequency of oscillations. This phenomenon results, in part, from the time delay required to transmit mechanical control signals generated at the tube outlet through the air column in the tube to the vehicle.

Of the three systems, only the force controlled system fully satisfies the final control objective. The force-controlled vehicle attains steady-state velocity in near minimum permissible time, overshoots this velocity only slightly, and then approaches steady-state velocity asymptotically.

Sensitivity to System Parameters

The sensitivity of the uncontrolled, valve-controlled, and force-controlled systems to variations in pre-evacuation pressures has been noted in previous subsections. From the results we conclude that generally it is desirable to limit the initial pressure differential across the vehicle to a value approximately that required to overcome the force of sliding friction. Pre-evacuation pressures yielding such differentials reduce jerk, ease acceleration control, and enhance the steady-state performance of each system.

Simulation results further show that, over the range of values tested, reasonable variations in system parameters do not alter the conclusions of the previous subsections.

Power-Cost Considerations

The cost of operating the pneumatic-tube system is critical to the system's acceptance as a viable transportation alternative. Cudlin [1] has estimated the steady-state power cost of an uncontrolled, prototype system, based on the assumed maintenance of a constant steady-state velocity. Simulation results indicate that neither the uncontrolled or valve-controlled systems achieve such a velocity and suggest, therefore, that the power cost of these systems is greater than Cudlin's estimate. Since both systems are infeasible from a control perspective, however, the issue of their respective power costs is academic.

Cost estimates of the force-controlled system are considerably more meaningful. Simulation reveals that the magnitude of the supplementary control force is generally negative during ascent to steady-state velocity, i.e., that the force acts to restrain the vehicle's forward motion. Such a restraining force conceivably could be provided by mechanical braking mechanisms at little or no direct power cost. Results further show that the magnitudes of both positive and negative control forces decline as the vehicle approaches steady-state. When the vehicle attains steady-state, the cost of small positive corrective forces required for control are negligible in comparison with pumping costs. Thus, the steady-state power requirements of the force-controlled system are essentially those estimated by Cudlin. The cost of meeting these requirements may be greater than estimated, however, because vehicle design will necessi-

tate inclusion of a supplementary propulsive unit.

VI. Conclusions and Recommendations

Simulation of the pneumatic-tube vehicle system warrants several conclusions regarding vehicle control. First, simulation results clearly emphasize the need for effective vehicle control to limit the magnitudes of vehicle jerk and acceleration and to guarantee the maintenance of a constant, steady-state vehicle velocity. The uncontrolled motion of the vehicle is deficient with regard to these criteria. Second, control schemes regulating vehicle motion by valve modulation are shown to be plagued with difficulties attending the transmission of physical control signals through a fluid medium. Such schemes are probably inadequate to provide steady-state velocity control. Third, results indicate vehicle accelerations and jerk are controlled satisfactorily during all phases of vehicle operation provided the pneumatic-tube concept is revised to include supplementary, on-board vehicle propulsion.

The conclusions of this research must be tempered with several observations. First, the simulation is based on a specific and unproven model of the pneumatic-tube system. Experimental verification of this model is required to underwrite simulation results. Second, simulation necessitates the use of numerical data and simplified system components. The dependence of conclusions on these specifications is not fully understood and, within the context of this research, it is obviously impossible to test all combinations and permutations or components and data. Finally, the inclusion of propulsive power on-board the vehicle may alter the air flow in the tube and, thus, invalidate basic assumptions of the fluid mechanics model. The evaluation of the feasibility of the pneumatic-tube

system presented here, however, is believed to be at least qualitatively correct.

The valve-control algorithm employed in the simulation is crude and, conceivably, an improved algorithm could render the valve-modulation control scheme more alluring. Development of a significantly improved algorithm, however, probably will require a more thorough understanding of the dynamics of the tube system than is presently available. The difference in pressures fore and aft of the vehicle and the variation between vehicle velocity and the flow velocity of the air column ahead of the vehicle each contribute to the vehicle's motion. The nonlinear coupling of these effects muddles analytical investigation of their control. Compounding this difficulty is the complexity of the mechanism by which control signals are transmitted to and reflected from vehicles, the certainty of time delay in this mechanism, and the equal certainty that such delay is a function of both the position and velocity of the vehicle. Formulation of an improved valve-control algorithm must be combined with further research into the dynamics of the tube system.

The desirability of applying a supplementary control force at the vehicle will influence the ultimate design of the tube system. The concept of a totally passive vehicle must be abandoned and means of supplying power to the vehicle must be investigated.

Nomenclature

A	Cross-sectional tube area
a	Acceleration
a_{max}	Maximum comfortable acceleration
c	Speed of sound
D	Tube diameter
d	Time Delay
F	Force
f	Friction factor
f_f	Frictional force
g	Gravitational acceleration
k	Specific heat ratio
L	Tube length
L_{max}	Maximum length of unchoked flow
M	Mach number
m	Mass
m	Number of subincrements Δy
$\underset{\sim}{m}$	Vector of measured variables
n	Number of increments Δx
P	Pressure
$\underset{\sim}{q}$	Vector defining control criteria
R	Universal gas constant
S	Magnitude of supplementary control force
T	Temperature
t	Time
$T(t)$	Valve time response
U	Air flow velocity

V	Vehicle velocity
v	Rate of air compression
V_{cmax}	Maximum comfortable velocity
V_{pmax}	Maximum realizable velocity
V_{ss}	Steady-state velocity
x	Distance from tube inlet
Δx	Length of tube interval
Δy	Length of tube subinterval
$(\ )_a$	Signifies condition immediately ahead of vehicle (subscript)
$(\ )_b$	Signifies condition immediately behind vehicle (subscript)
$(\ )_i$	Signifies condition at inlet (subscript)
$(\ )_o$	Signifies condition at outlet (subscript)
$(\ )_s$	Signifies stagnation condition (subscript)
$(\ )_1$	Signifies condition at beginning of increment (subscript)
$(\ )_2$	Signifies condition at end of increment (subscript)
$(\ )^*$	Signifies condition at Mach one (superscript)

Initial Evacuation Pressure (psi)	System	Maximum Acceleration (g)	Maximum Jerk (ft/sec^3)
13.5 (see Figures 6 and 7)	Uncontrolled	13.9	99.
	Valve-controlled	0.193	0.472
	Force-controlled	0.220	0.890
10 (see Figures 8 and 9)	Uncontrolled	29.3	535.
	Valve-controlled	0.202	4.40
	Force-controlled	0.200	4.32
8	Uncontrolled	25.4	396.
	Valve-controlled	0.290	10.36
	Force-controlled	0.277	6.00

Table 1. Approximate Maximum Values of Vehicle Acceleration and Jerk for Different Initial Evacuation Pressures.

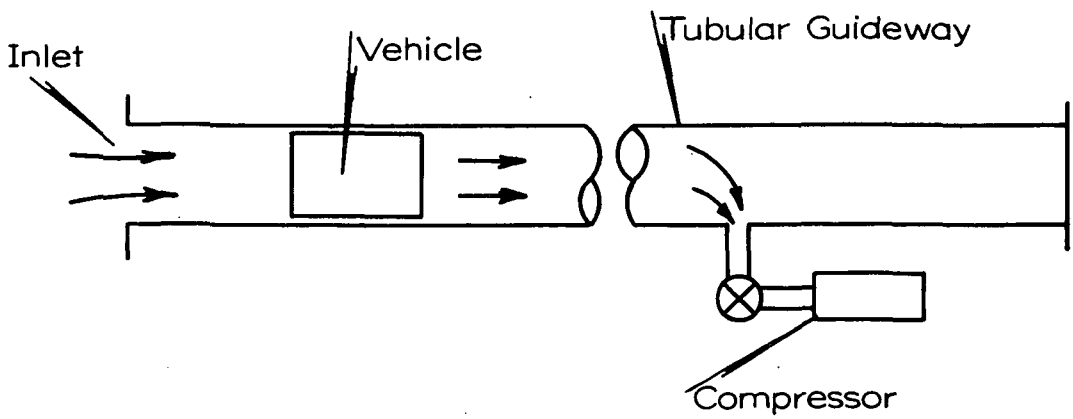

Figure 1. Essential Elements of the Pneumatic-Tube System.

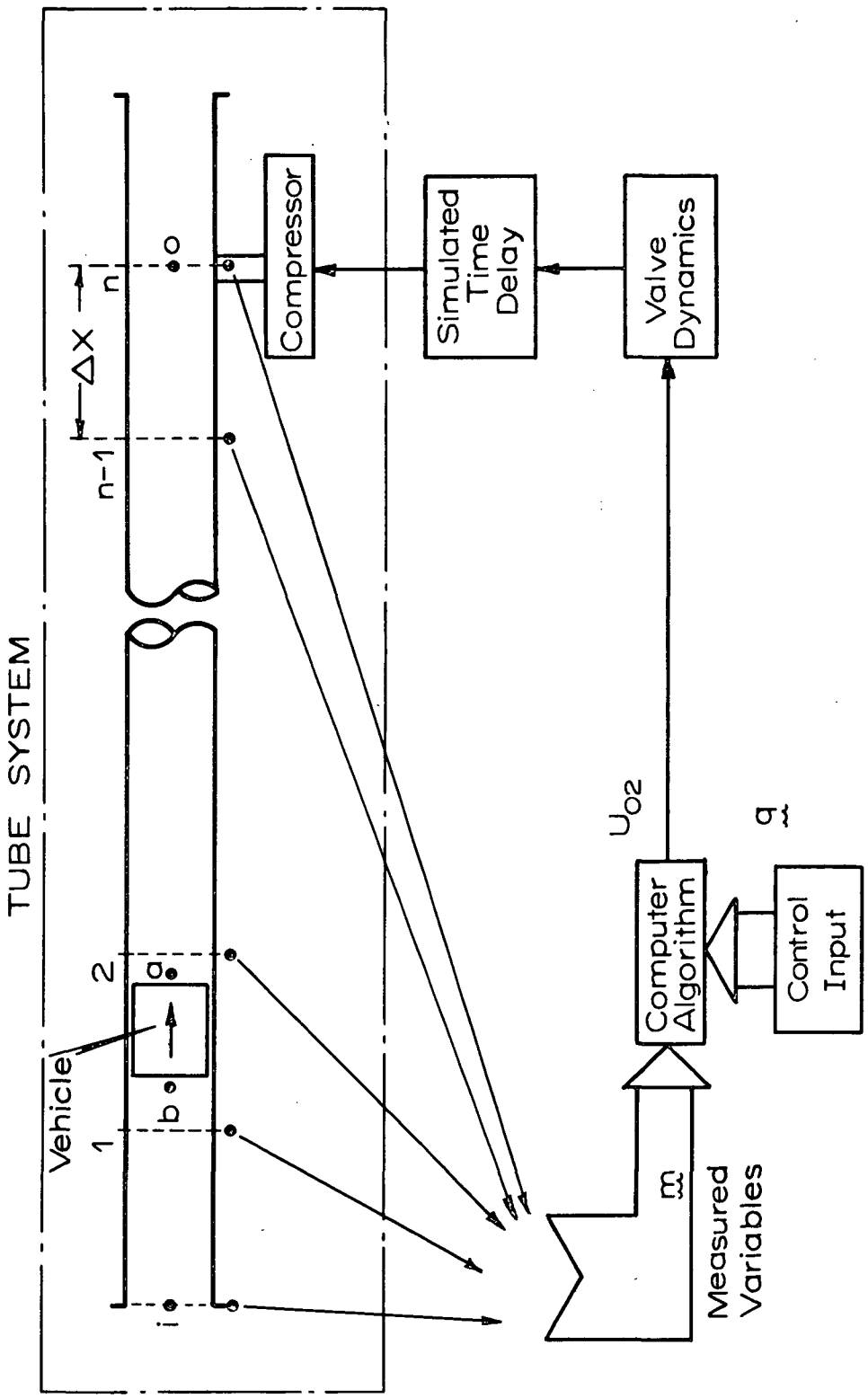

Figure 2. Schematic Diagram of Valve-Control Concept.

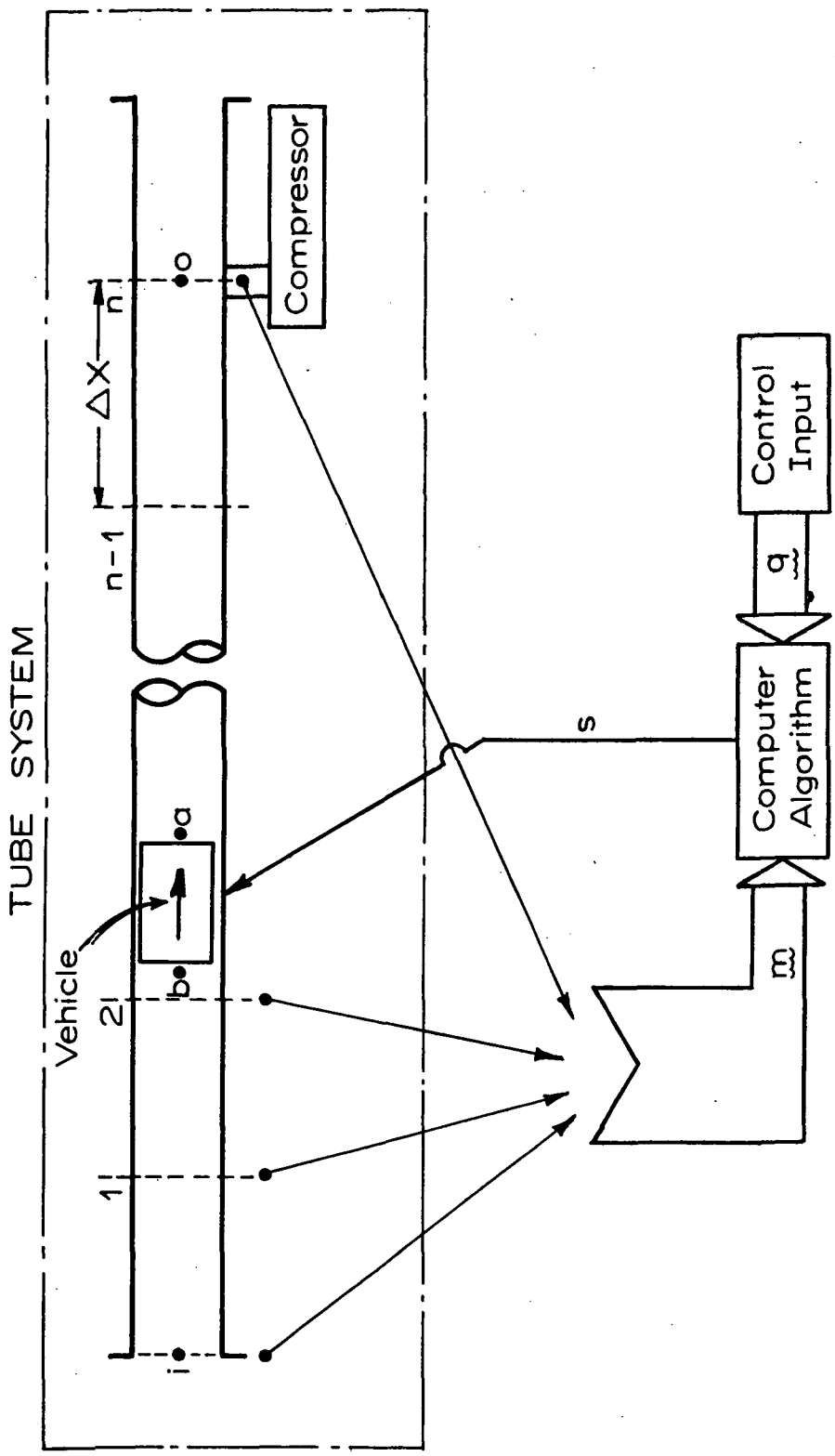

Figure 3. Schematic Diagram of Force-Control Concept.

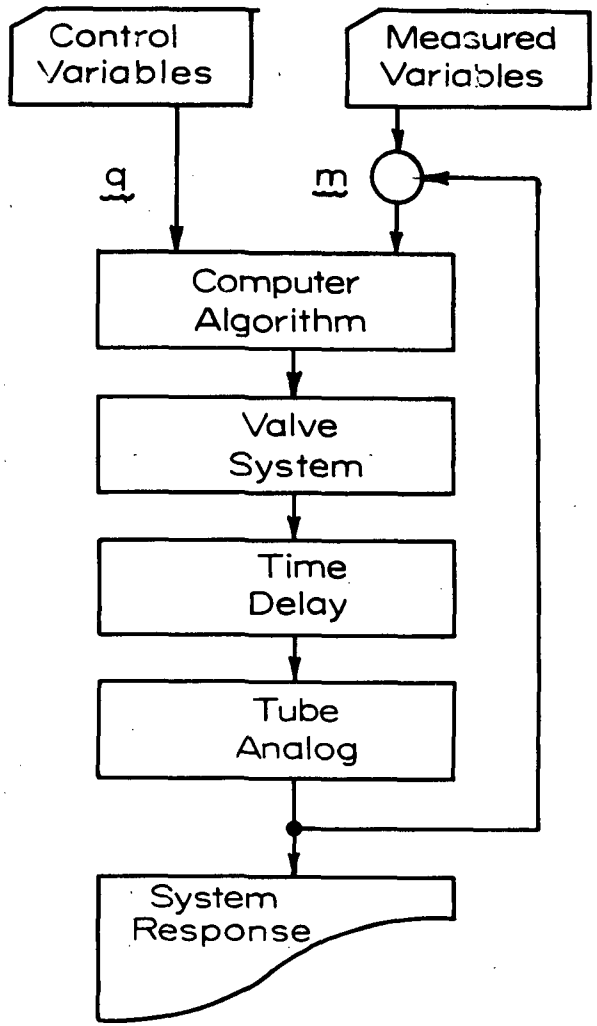

Figure 4. Simplified Flow Diagram of the Valve-Control Simulation.

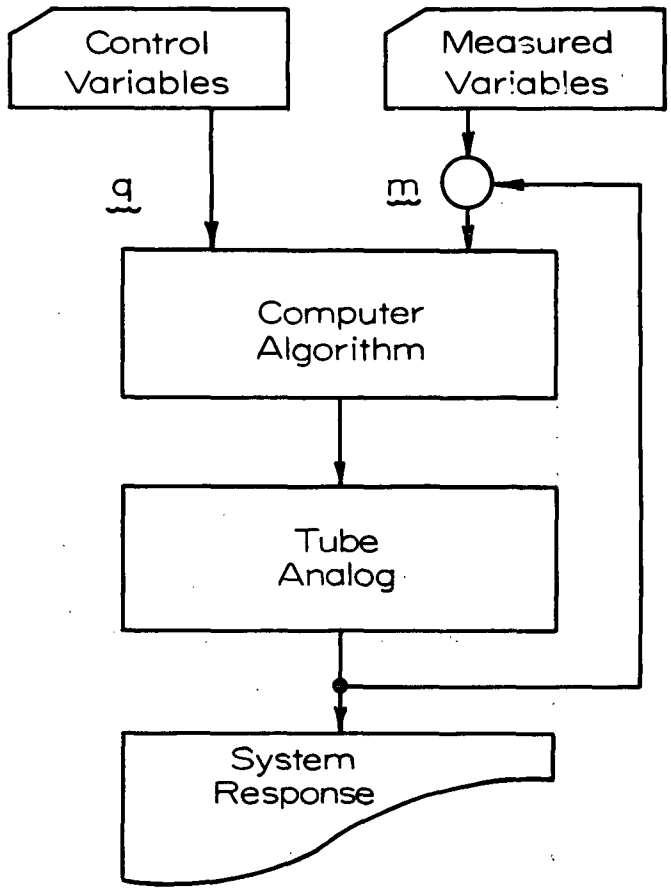

Figure 5. Simplified Flow Diagram of the Force-Control Simulation.

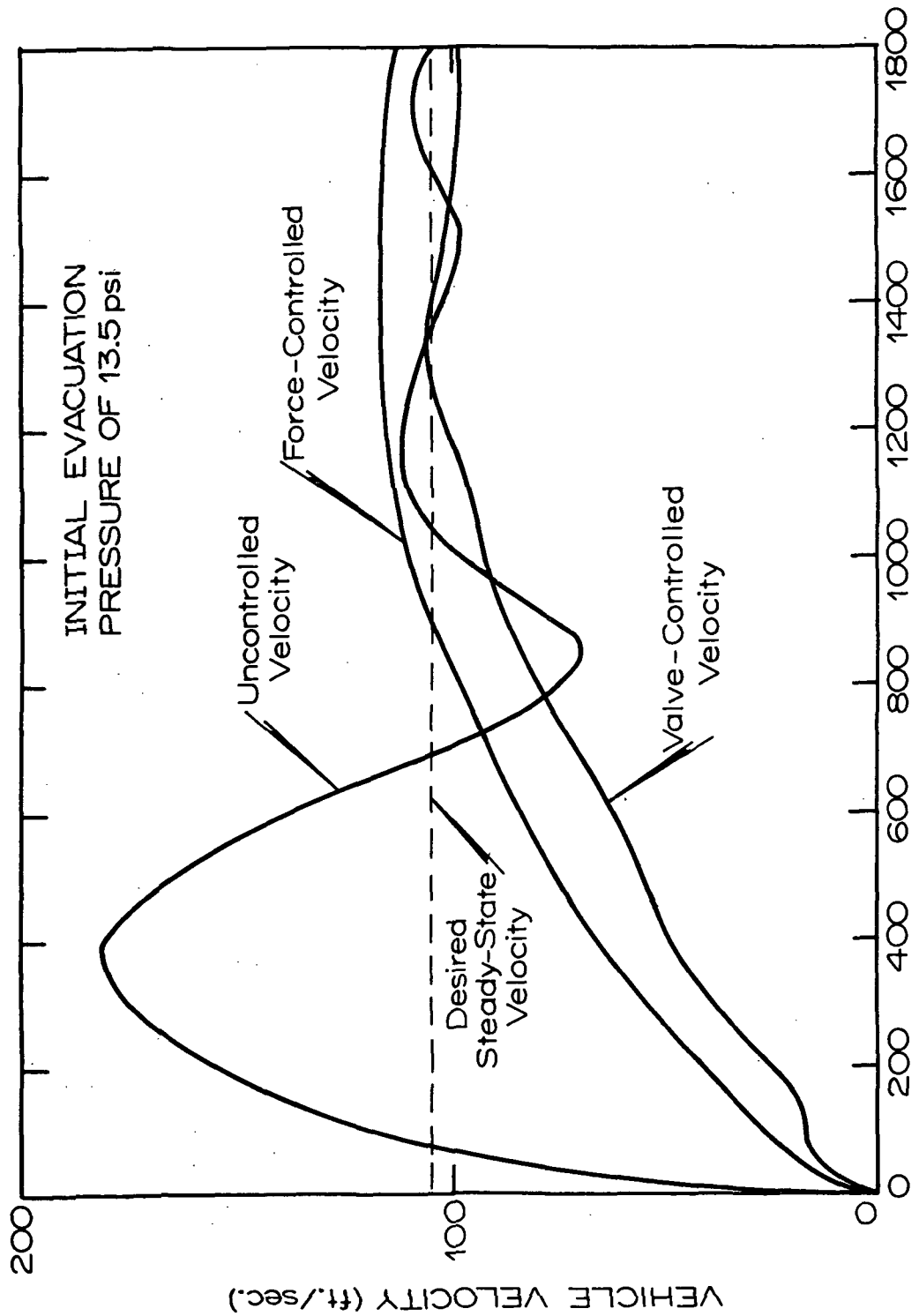

Figure 6. Velocity of Uncontrolled, Valve-Controlled, and Force-Controlled Vehicles at Initial Evacuation Pressure of 13.5 psi.

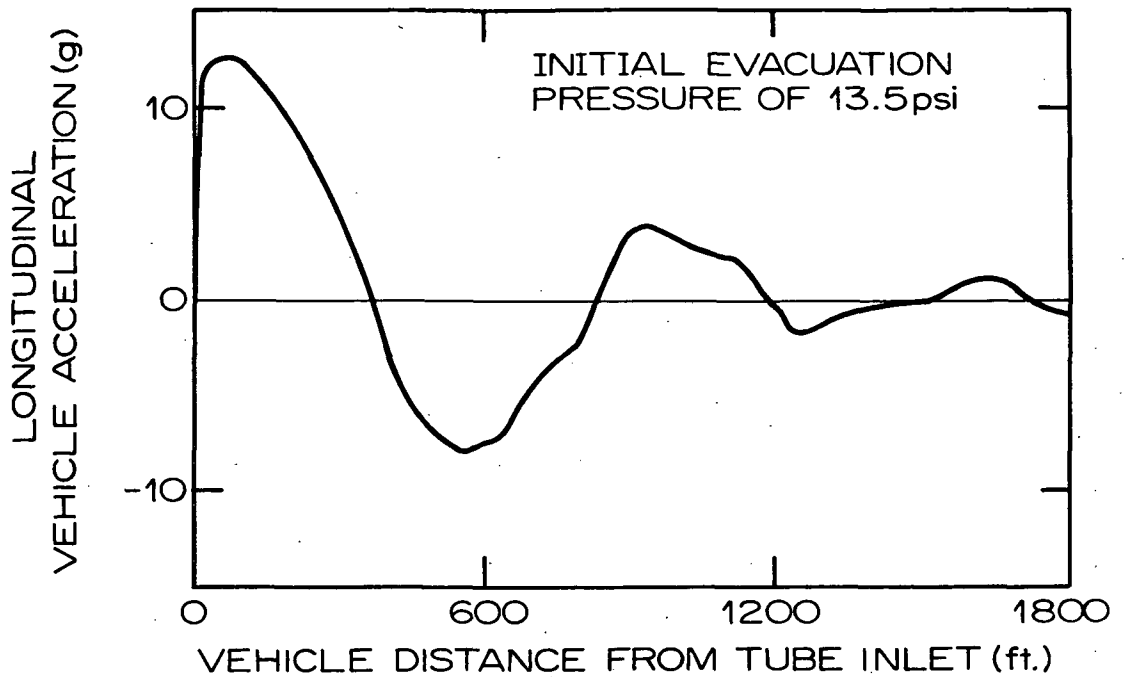

Figure 7a. Acceleration of Uncontrolled Vehicle with Initial Evacuation Pressure of 13.5 psi.

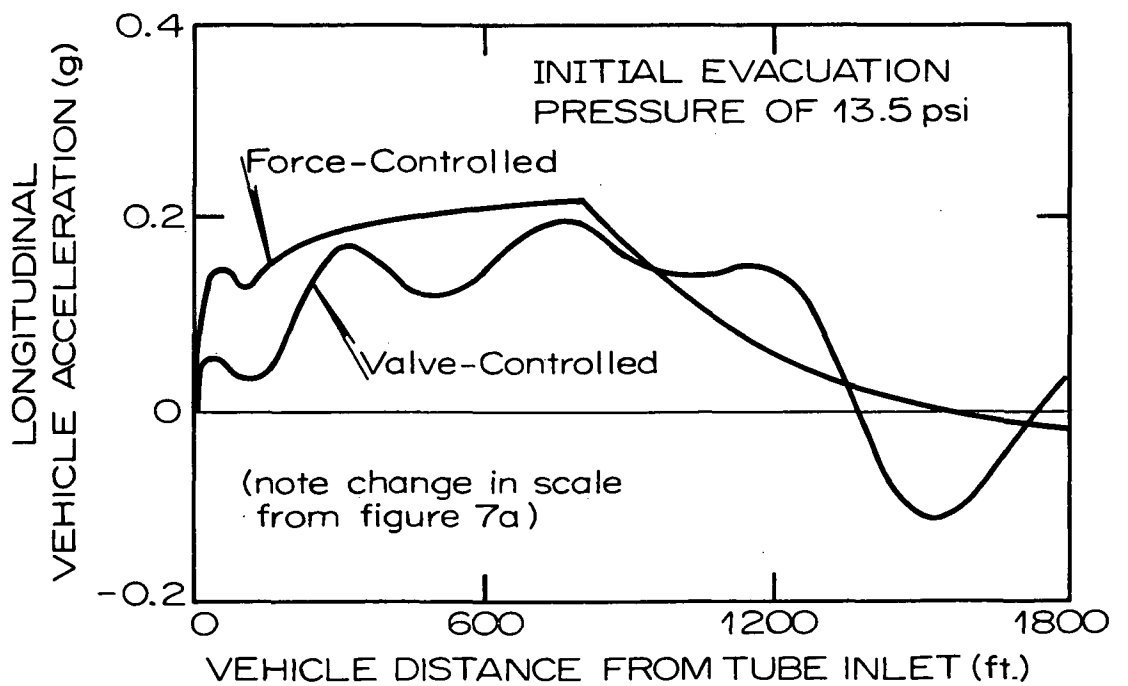

Figure 7b. Acceleration of Valve-Controlled and Force-Controlled Vehicles with Initial Evacuation Pressure of 13.5 psi.

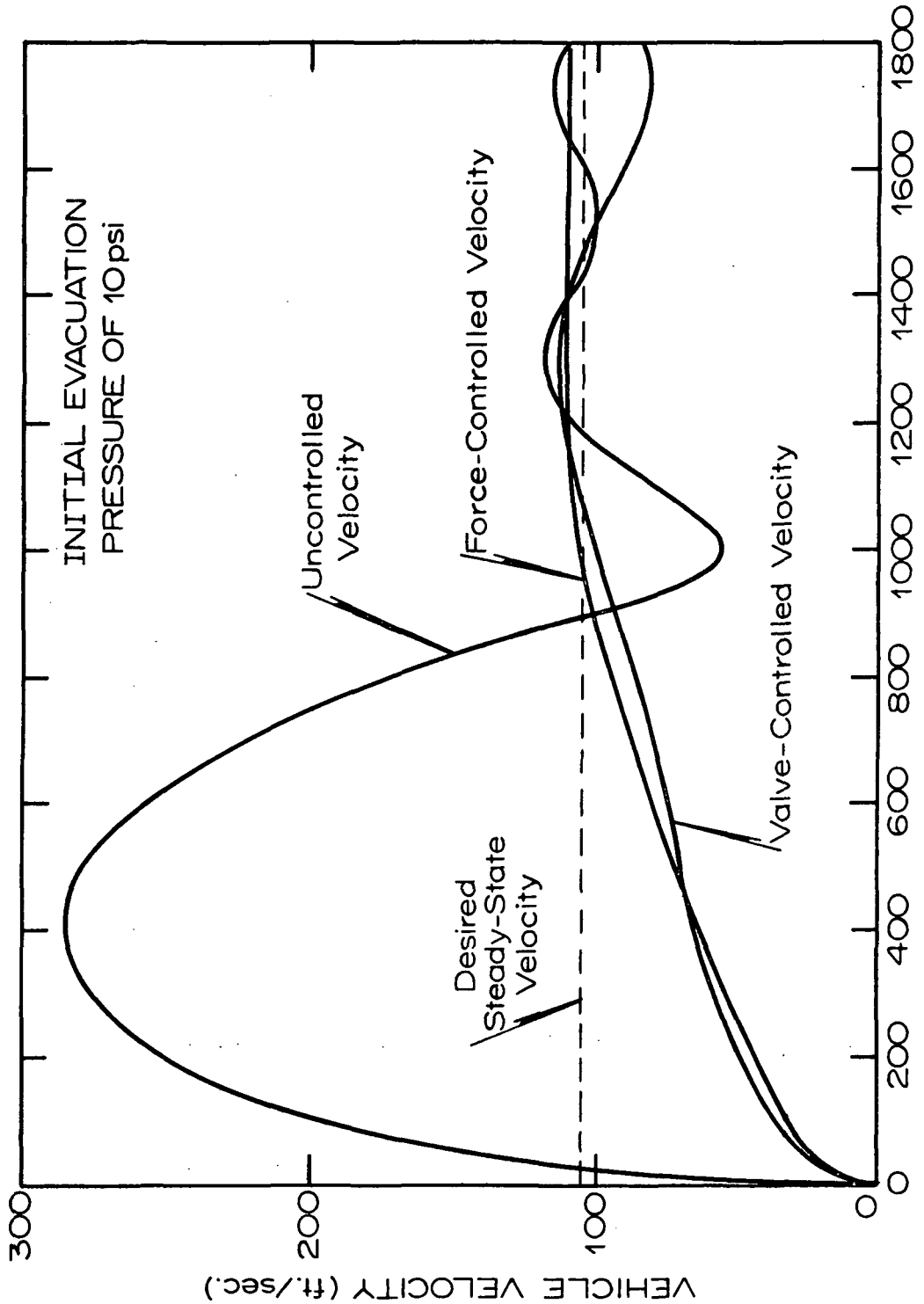

Figure 8. Velocity of Uncontrolled, Valve-Controlled, and Force-Controlled Vehicles at Initial Evacuation Pressure of 10 psi.

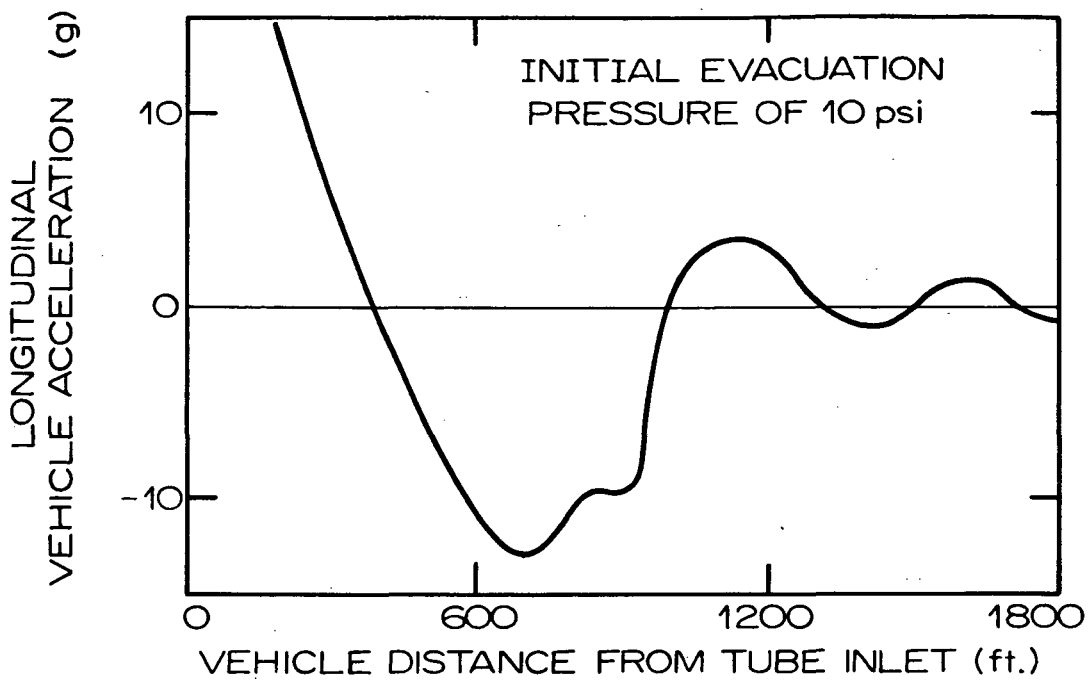

Figure 9a. Acceleration of Uncontrolled Vehicle with Initial Evacuation Pressure of 10 psi.

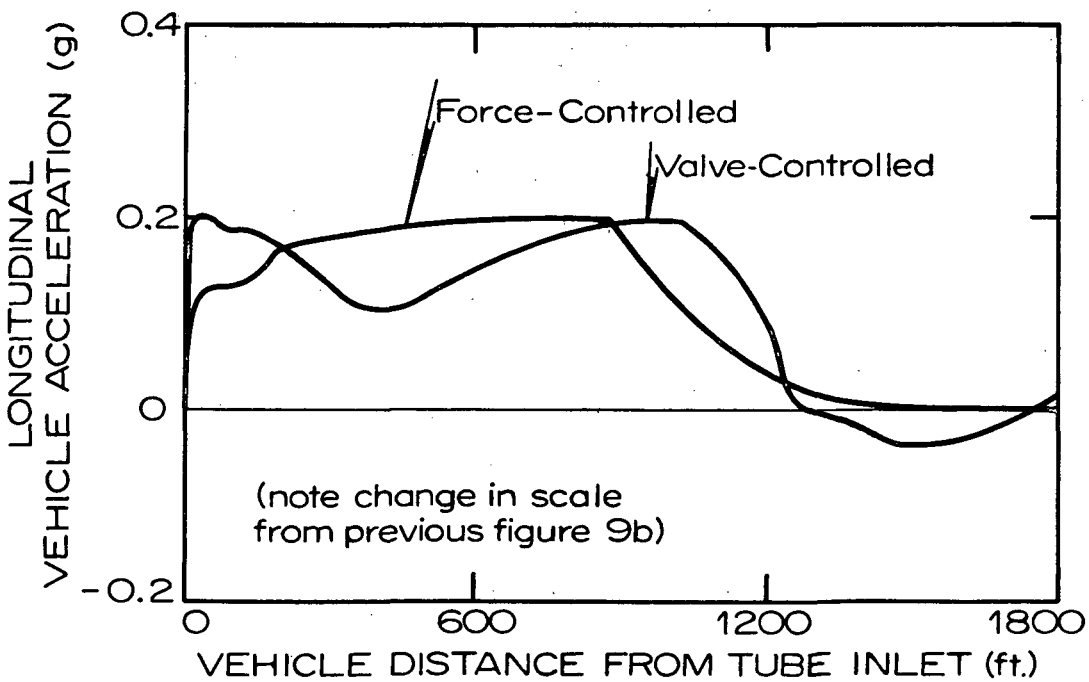

Figure 9b. Acceleration of Valve-Controlled and Force-Controlled Vehicle with Initial Evacuation Pressure of 10 psi.

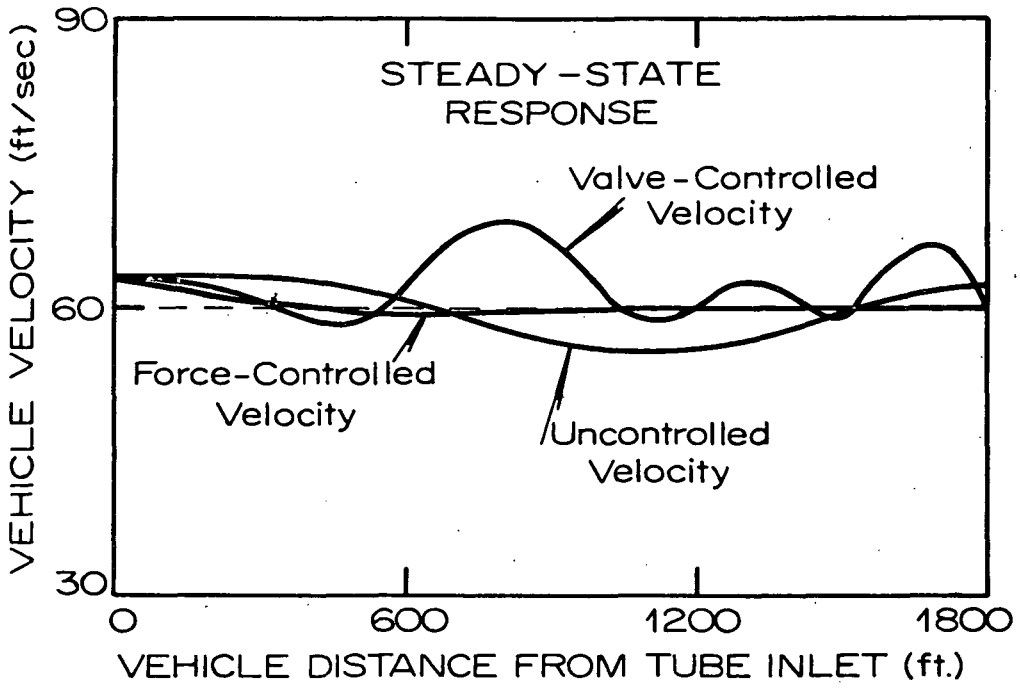

Figure 10. Approximate Steady-State Velocity with Initial Velocity of 63 fps.

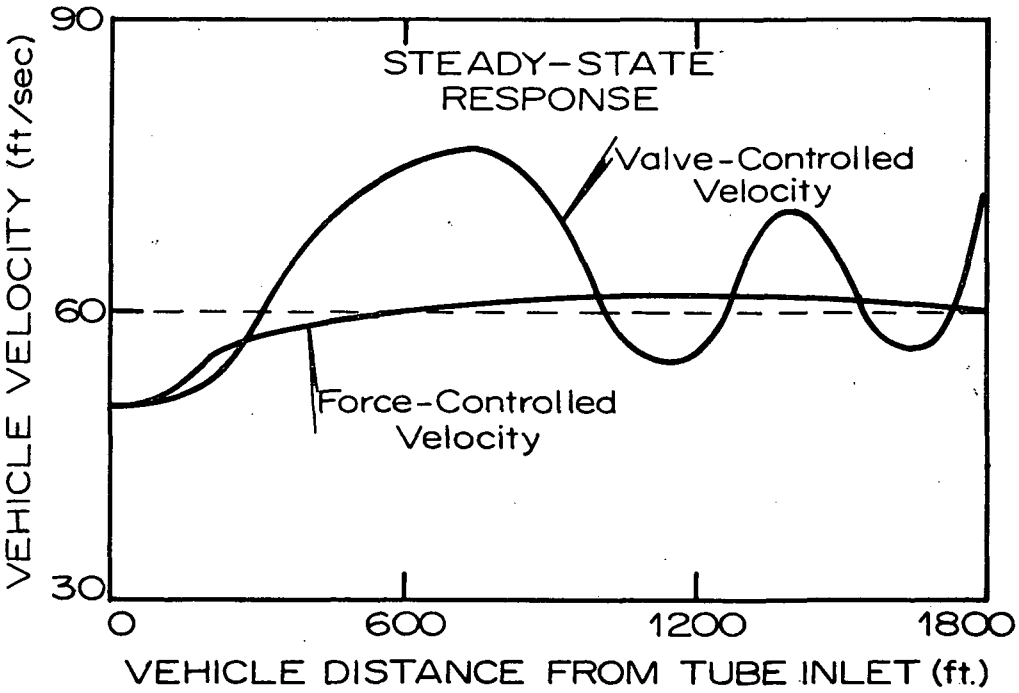

Figure 11. Approximate Steady-State Velocity with Initial Velocity of 50 fps.

References

1. Kumar, S., "Atmospheric Pressure Propelled Vehicle in an Evacuated Tube." Proceedings of the First High Speed Transportation Systems Committee Meeting, International Society for Terrain Vehicle Systems (December, 1965).

2. Cudlin, J. J., "Numerical Analog for a Model Vacuum-Air Transport System." Master's thesis, Dept. of Mechanical Engineering, Duke University, 1969.

   Substantially the same information may be found in the following papers:

   Harman, C. M., and Cudlin, J. J., "Mechanics of Vehicle Propulsion in a Pneumatic Tube," Proceedings of the First International Conference on Vehicle Mechanics (Wayne State University, Detroit, Mich., July, 1968), pp. 20-31.

   Harman, C. M., and Cudlin, J. J., "Pneumatic Tube Vehicle System Simulation." High Speed Ground Transportation Journal, III (September, 1969), 361-371.

3. Shapiro, A. H., The Dynamics and Thermodynamics of Compressible Fluid Flow. Vol. I. New York: The Ronald Press Co., 1953.

4. Cudlin, J. J., "Project Mountainwell: An Experimental Investigation of the Pneumatic Tube Transportation System." A lecture delivered at the Mechanical Engineering Seminar, Duke University, Durham, N. C., March 10, 1972.

5. Mercier, O. L., "Dynamic Modeling and Control of Pneumatic Tube-Vehicle Systems." Master's thesis, Dept. of Mechanical Engineering, Duke University, April, 1972.

6. Chen, D., "Vacuum-Air Propulsion with Supplemental Tube Inlet." Master's thesis, Department of Mechanical Engineering, Duke University, August, 1968.

7. Gebhard, J. W., "Acceleration and Comfort in Public Ground Transportation." Prepared for the U. S. Dept. of Commerce as TRP002, Johns Hopkin University Applied Physics Laboratory (Silver Spring, Md., Feb., 1970) PB 190-402.

8. Gibson, J. E., and Tuteur, Franz B., Control System Components. New York: McGraw-Hill Book Co., 1964.

ENERGY STUDY OF UNDERGROUND RAPID TRANSIT

Jack B. Chaddock and Ish Sud
Department of Mechanical Engineering, Duke University

INTRODUCTION

The Problem

Underground rapid transit systems can generate enough heat from their operations to raise tunnel and station temperatures as much as 15 or 20 degrees Fahrenheit above outdoor temperatures, the greatest differences being at night and in the early morning hours (1). Enclosed guideways for a high speed ground transportation system (HSGT) can have very severe heating problems. At a vehicle speed of 300 mph, and guideway depth of 500 feet, the temperature rise has been estimated at 1.44°F/vehicle transit per hour/ton of vehicle weight. For a vehicle weight of 50 tons and 10 transits per hour, this would give a 720°F temperature rise of the guideway contents (2). It is obvious that passenger discomfort will result in warm weather conditions for non-air conditioned rapid transit systems. Any human exposure to the HSGT environment would be fatal.

At the time this study was undertaken no detailed development of the energy transfers occurring in underground transportation systems had been made available in the open literature. Our purpose was to develop a preliminary analytical model for evaluating these energy transfers. The usefulness of such a development would be in its identification of major energy transfer problems and critical parameters for further engineering study.

No attempt was made to develop a model or to obtain input data for a real or proposed rapid transit system. Nevertheless, the data selected or posed was done under a strong influence of information available on the New York City subway system, and of the new Bay Area Rapid Transit System for the San Francisco Area.

Of particular significance in the study are its implications in the design of air conditioning for the transit cars and stations. It is likely that the most severe design conditions for air conditioning of rapid transit cars will be during underground operation. The complete air conditioning of stations is apt to be prohibitively expensive unless the station design permits routing away certain high energy sources.

Relevant Studies

The results of a study conducted by the General Electric Company for the New York City Transit Authority (1) on subway air conditioning showed that the thermal computer model developed was very useful in establishing air conditioning design loads. A primary finding of the study was that a vapor compression refrigeration system offered the best prospect for car cooling. Figure 1, as taken from the report, shows the predictions of the thermal model both with and without car cooling by vapor compression. The lower diagram in this figure shows how the station/tunnel air temperature exceeds the outdoor temperature. Note that adding vapor compression cooling increases the tunnel air temperature by about $3^{o}F$ over that without cooling.

Figure 2 is also reproduced from the G.E. Study (1), and shows the model predictions for the effect of nighttime ventilation. The results are for 1966 operating conditions with no air conditioning for cars or stations. The 1966 existing situation for the station is shown in the box labeled, "No Night Ventilation." A station ventilation rate of 200,000 cfm provides a reduction of about 25% in the number of uncomfortable hours for passengers. At 400,000 cfm the uncomfortable hours are reduced by 37.5%, any further increases in ventilation rate have diminishing effects. The study points up clearly the need for comfort cooling, and the benefits of analysis by a thermal model.

Figure 3 is taken from an M.I.T. report on the "Survey of Technology for HSGT" (2). It presents the long term steady state temperature increase of the guideway as a function of vehicle speed with no ventilation. For an overall propulsion efficiency of 25% (η) and a speed of 300 mph, the temperature rise per vehicle transit per hour and ton of weight is 1.44^{o}F at 500 foot depth. As stated earlier, this leads to a 720^{o}F temperature rise for 50 ton vehicles passing at the rate of 10 per hour. To reduce this to a maximum allowable temperature rise of 20^{o}F through the use of ventilation would require a ventilation pumping power of approximately 800 hp per mile (2). It was noted in the report that this rather awesome power requirement might be reduced by a factor of 3 through use of evaporative cooling.

Approach

The model developed in this study has a simple physical description. The underground tunnels are assumed cylindrical, to ease the

calculation of energy transfer to and from the surrounding walls. Even so, the heat transfer problems are quite complex. There are energy transfers between the moving cars, the tunnel air, and the surrounding walls. Ventilation air temperatures change with outdoor conditions. Train schedules and passenger volumes vary with the time of day. The major sources of energy are the passengers, the propulsion energy to the trains, braking, car air conditioners, and auxiliary equipment. All of these have been brought into the analysis developed here.

A model was first developed with the tunnel and station as subsystems. The complexity of the resulting relationships dictated the selection of a simpler model with a single "tunnel temperature" extending through the station. The simpler model was suggested by a scheme proposed in the study for the New York Transit Authority (1). It isolates the station platform from the tracks by transparent partitions and air curtains. The simpler model could be quite realistic for an underground guideway of a high speed ground transportation system.

The simplified model was solved by numerical methods on a digital computer. Ventilation rates are varied to show the effect on tunnel temperatures. The effect of vehicle traffic density was also included.

THE MODELING PROBLEM

Physical Configuration

The somewhat idealized physical configuration for Underground Rapid Transit is illustrated in Figure 4. For ease in mathematical analysis, the tunnels are assumed to be cylindrical in cross section, having an internal diameter equal to 2R. A hollow concrete cylinder

of thickness (a-R) enclosed the tunnel. Thermal penetration into the surrounding earth is assumed to be negligible beyond a radius b (shown dashed in Fig. 4a). The separation distance of the two tunnels is sufficient to make negligible any thermal interaction. Figure 4a shows only one track in each tunnel.

In a subway system, a common configuration is two tracks in a single tunnel, one for local and one for express service. The tunnel might be divided into half-tunnels by a partition wall. This configuration would approximately double the tunnel diameter and increase the volume of traffic to include local and express trains. This case has been included in the analysis performed herein. The model includes a station and the half-tunnels to either side, as shown in Figure 4b.

Thermal Exchanges

Figures 5 and 6 illustrate the types of thermal energy exchanges taking place in an underground transit system. In Figure 5, the various thermal energy exchanges in the tunnel are identified, and in Figure 6 those in the station. A complete listing of heat exchanges occurring in the system are given in Table 1.

Formulation

The many difficulties involved in accurately evaluating the above energy exchanges require some comments. The energy exchange to the walls of the tunnel require a solution for the temperature distribution in both the wall structure and the nearby surrounding earth. The convective heat transfer coefficients at the surface of the car and the tunnel walls are strongly dependent upon the motion of air induced by

Table 1

Thermal Energy Exchanges in Underground Rapid Transit

A. Tunnel Exchanges

1) Dissipation of the propulsion energy of the train cars at tunning speed
2) Braking energy losses
3) Heat transfer to the car from the tunnel air
4) Heat transfer from the tunnel air to the tunnel walls
5) Work input to the coach air conditioners
6) Internal heat load of the cars (people, lights, etc.)
7) Energy exchange through the use of ventilation air
8) Propulsion energy losses during acceleration and deceleration
9) Energy exchange between the tunnel and station air by a piston effect of the trains

B. Station Exchanges

1) Propulsion energy losses
2) Braking energy losses
3) Heat transfer to car from station air
4) Heat transfer from station air to station walls
5) Work input to coach air conditioners
6) Internal heat load of the cars
7) Station ventilation air energy exchange
8) Energy exchange between station and tunnel air by piston effect of trains
9) Internal load of people, lights, etc. on the platform

the passage of trains. The net effect of the piston action of the trains in mixing the air through the tunnels and stations is very difficult to predict. Let us make the somewhat gross assumption that the system can be lumped in such a way as to establish four subsystem temperatures. These are: 1) a tunnel air temperature, 2) a station air temperature, 3) a tunnel wall surface temperature, and 4) a station wall surface temperature. All of these will be functions of time but not position. Even with this simplification, there are six differential equations which must be solved simultaneously for the subsystem temperatures, and four of these are partial differential equations. The difficulty of preparing a solution for six coupled differential equations is obvious. In this case, the level of difficulty in obtaining a theoretical solution is increased manifold due to the fact that all the quantities (except physical properties) are very strongly time dependent. The formulation of this problem was made (3), but will not be given here. Because of its complexity, obtaining a numerical solution was viewed as beyond the scope of this preliminary analysis. A simplified model was developed and a numerical solution obtained, as described below.

THE MODEL ANALYZED

Simplification

To gain wide public usage, the station platforms should also be air conditioned. In this case, it would be essential to physically

separate the platform air conditioned space from the track region. This may be done by use of transparent partition extending the full length of each platform. Such an arrangement is shown in Figure 7. The piston effect of the trains would tend to cause thorough mixing of the air in the region where trains are running. It should be possible therefore, to lump the isolated track region in the station with the tunnel and treat this entire area as a lumped tunnel air region. The tunnel cross sections are again assumed to be circular. As before, they can also contain either one or two sets of tracks.

Thermal exchanges

By incorporating the station track region with the tunnel to give a single "tunnel" air temperature, the thermal exchanges to be included are as given in part A of Table 1, with the following changes or interpretations:

> Items 2), 5), 6), 7), and 8) include the total energy exchanges in both the tunnel proper and station.
>
> Item 9) is changed to read, "Energy exchange at the station platform during station stops."

If item 9) is assumed to be only a minor part of the total thermal exchange, and item 4) is exchange with the tunnel walls proper (not including the transparent partitions in the station), the station will be effectively eliminated as having an influence on the "tunnel" air temperature. In the case of Underground Rapid Transit this assumption approaches reality when the platforms of the stations are air conditioned. The above model and assumption should be quite accurate for enclosed high speed ground transportation systems since the stations

have great separation distance. The differential equation expressing the thermal exchanges with the tunnel air temperature is,

$$(1)\quad C_v M_T (dT_T/dt) = N_R Q_R = nMV^2/2 + N_{AV}\{\eta[U_v A_v (T_T - T_c) + Q_I] + Q_I\} + h_w A_w (T_w - T_T) + C_p E_T \rho (T_v - T_T)$$

The differential equations for the retaining wall and earth temperatures surrounding the tunnel are,

$$(2)\quad \frac{\partial \theta_1}{\partial t} = \frac{\alpha_1}{r} \frac{\partial}{\partial r}\left(r \frac{\partial \theta_1}{\partial r}\right)$$

$$(3)\quad \frac{\partial \theta_2}{\partial t} = \frac{\alpha_2}{r} \frac{\partial}{\partial r}\left(r \frac{\partial \theta_2}{\partial r}\right)$$

The initial and boundary conditions on these differential equations are,

$$(4)\quad \theta_1(r,o) = \theta_2(r,o) = 0$$

$$(5)\quad -K_1 (\partial \theta_1/\partial r)_R = h_w (\theta_T - \theta_1)_R$$

$$(6)\quad \theta_1(a,t) = \theta_2(a,t)$$

$$(7)\quad K_1 (\partial \theta_1/\partial r)_a = K_2 (\partial \theta_2/\partial r)_a$$

$$(8)\quad \theta_2(b,t) = 0$$

The above equations represent a considerable simplification over the formulation which treats independently the tunnel and station air temperatures. Nevertheless the task of solving the above three coupled differential equations is by no means a simple one. A theoretical solution was attempted (3). By making the assumption of a constant tunnel air temperature (as during a steady state operating period) a solution can be formulated by the LaPlace transform method. The task

of obtaining the inverse transform is so formidable as to have discouraged our attempting it. A numerical formulation offered a more promising method of solution and was adopted.

Numerical Solution

The partial differential equations (2) and (3) for the retaining wall and earth temperatures surrounding the tunnel are parabolic in nature. To set these equations in finite difference form, either an explicit or implicit formulation can be used. For a radial grid spacing of 0.1 feet, the explicit form is restricted to a maximum time step of a few seconds to have convergence. The implicit form, while somewhat more complicated, does not have this restriction and was, therefore, chosen.

Figure 8 illustrates the grid pattern selected for the numerical solution of the tunnel wall temperature. As it was desired to carry out the simulation over a period of several days, a time step of one hour was judged as ideal for calculations. To assure this would give accurate results preliminary computer runs were made with time steps of one-half hour, one hour, and two hours. The results were in close agreement.

An additional item to select was the thermal penetration depth into the surrounding earth. The concrete retaining wall was assumed to have a two foot thickness. Solutions were initially made for earth penetration depths of three and five feet. The calculated tunnel air temperatures and wall surface temperatures over a 24 hour period showed a maximum difference of $0.09^{\circ}F$, and $0.12^{\circ}F$, respectively, for these two

depth selections. A thermal penetration depth of three feet was, therefore, used in all subsequent computer runs.

With a grid spacing of 0.1 feet the numerical formulation gave a set of fifty-two simultaneous algebraic equations. Each of the equations contains only two or three variables, and the system is known as a tridiagonal set of equations. The equations were solved by the Gauss-Siedel iteration method with due considerations to convergence (7), (8), (9).

DATA AND PARAMETER SELECTIONS

Heat Transfer Coefficients

The values of the convective heat transfer coefficients at the wall and the train depend on the train velocity, tunnel and train diameter, and the tunnel and train lengths. A survey of available literature failed to provide information directly applicable to a calculation or estimation of these coefficients. Studies have been made on the hydrodynamic drag of vehicles in tunnels (10). An attempt was made to make use of the analogy between momentum transfer and convective heat transfer, to estimate the heat transfer coefficients from the results of these drag studies (3). The Reynolds Analogy gave values of approximately 1 (Btu)hr-ft^{2}^{o}F) for the heat transfer coefficients. Considering the value of a calculated free convection coefficient for the tunnel this analogy determined value was judged to be too low. The heat transfer coefficient at the tunnel wall was estimated at 2.5, and at the vehicle, 5.0 (Btu/hr-ft^{2}^{o}F). Subsequent calculations showed that the overall results for energy exchange were not sensitive to these values.

Tunnel and Station Characteristics

In a publication on the Bay Area Rapid Transit System (BART) (5), the body envelope of the train is shown to fit well into a circle with a diameter of 16'6". On this basis, the tunnel radius for our models were set at 8 feet for a single track and 26 feet for a double track. The average distance between subway stations in central Manhattan is about half a mile. This was taken as the tunnel length in the model.

Vehicle Characteristics and Operating Schedule

The vehicle characteristics were taken from BART (5), (6) as follows:

Vehicle weight (unloaded)	= 56,000 lbs
Vehicle dimensions - width	= 10'6"
- height	= 6'9"
Propulsion system capacity per coach	= 600 hp
Vehicle cruising speed (40 mph)	= 58 ft/sec
Propulsion energy at speed per coach	= 88 kw
Vehicle air temperature (air conditioned)	= 75^{o}F
Average propulsion energy during acceleration period	= 44 kw

A hypothetical schedule was drawn up for a tunnel serving inbound trains. This is shown in Table 2. The schedule was intended as a simulation for very large cities, like New York. Over 800,000 people enter the Central Business District (CBD) of New York and about the same number leave the CBD every day (12). The peak rush for the incoming trains was estimated to be between 7 and 8 a.m. In Table 2, the total number of passengers going in through one of the subway routes is 154,000. Using a multiplication factor of six, to account for other commuter routes (roads and other subway lines) gives a capacity of 924,000 people, per day, entering the CBD.

Table 2

Hypothetical Schedule for Tunnels Serving Incoming Trains

Time	Cars/Tr.	Total Trains/hr.	Locals	Inbound Passengers	Pass/Car	Headway (Min.)
12-1	5	3	1.5	500	33	20
1-2	5	3	1.5	500	33	20
2-3	5	3	1.5	500	33	20
3-4	5	3	1.5	500	33	20
4-5	5	4	2	1000	33	15
5-6	7	10	5	4900	70	6
6-7	10	20	10	15000	75	3
7-8	10	20	10	30000	150	3
8-9	10	20	10	20000	100	3
9-10	10	10	5	10000	100	6
10-11	10	10	5	8000	80	6
11-12	7	10	5	4900	70	6
12-1p	7	10	5	4900	70	6
1-2	8	10	5	7000	87	6
2-3	7	10	5	4900	70	6
3-4	5	7½	3.75	3000	80	8
4-5	5	7½	3.75	3000	80	8
5-6	7	10	5	4900	70	6
6-7	10	10	5	8000	80	6
7-8	7	10	5	4900	70	6
8-9	5	7½	3.75	3000	80	8
9-10	5	6	3	2000	67	10
10-11	5	4	2	1000	50	15
11-12	5	4	2	1000	50	15
Total		222½		154000		
Av./hr.		9.25		6430		

Weather Data

The week long periodic cycle was assumed to have a maximum temperature of 95°F, with a maximum fluctuation of 20°F over the day. The Carrier Handbook (11) was used to establish the hourly variation of outdoor temperature.

Parameter Selections

Solutions were obtained for three ventilation rates, namely, zero, 10,000 cfm, and a daily cycle rate of 60,000 cfm (14 hrs) plus 20,000 cfm (10 hrs). Both single and double track tunnels were included in the solutions generated. Two passenger traffic densities were used, a "normal" density as given by Table 2, and a "heavy" density at 1 1/2 times the values of Table 2.

HSGT Simulation

The conditions outlined above all related to an urban underground rapid transit system. A rough approximation to a High Speed Ground Transportation (HSGT) system was also included in our study. The parameter selections for this simulation were as follows:

Vehicle cruising speed	=	200 mph
Propulsion energy at speed*	=	9680 kw
Average propulsion energy during acceleration period	=	4840 kw
Distance between stations	=	20 miles

*The propulsion energy is approximately proportional to the cube of the vehicle speed. In this simulation the HSGT vehicle speed is 200 mph vs a rapid transit system speed of 40 mph. The propulsion energy at 200 mph was therefore taken as 110 times that for 40 mph or 110 x 88 kw = 9680 kw.

The train schedule was taken as one-half of the total in Table 2, i.e., corresponding to the express trains only. All other conditions were as described above, e.g., vehicle size, air temperature, tunnel temperature, tunnel size, etc.

RESULTS AND CONCLUSIONS

Cases Studied

From among the above parameter choices of ventilation rate, single or double track tunnel and traffic density, six cases were selected for numerical solution. These were as follows:

A. Single track tunnel

1. Normal Traffic Density (Table 2 values)

   a. No ventilation

   b. Ventilation at 10,000 cfm

   c. Ventilation at 60,000 cfm (14 hrs) and 20,000 cfm (10 hrs)

2. Heavy Traffic Density (1.5 times Table 2 values)

   Ventilation at 60,000 cfm (14 hrs) and 20,000 cfm (10 hrs)

B. Double Track Tunnel

   Ventilation at 60,000 cfm (14 hrs) and 20,000 cfm (10 hrs)

C. HSGT Simulation

   No ventilation, vehicle speed of 200 mph and station separation distances of 20 miles.

Temperature Plots

To build up an appropriate starting temperature profile in the tunnel wall, the ambient air temperature was cycled through a $75^{o}F$

to 95°F temperature range for 8 days, while starting from a uniform ground temperature of 55°F. It was found that after 3 days, the tunnel wall had very nearly achieved a steady state profile. For each of the above cases, then, the program was run over a period of thirteen days. The first 3 days for wall profile development and the next 10 days as a summer weather simulation. In Figures 9, 10, 11, and 12, the assumed ambient air temperature, and the resulting calculated tunnel air and surface temperatures, are plotted for the 10 day simulation, day 4 through 13.

Figure 9 demonstrates the effect of ventilation rate in a single track tunnel at normal traffic density. With no ventilation, Case A1(2), the ambient air temperature has no effect on the tunnel temperatures. The energy from the trains is conducted away by the surrounding earth at a far-field temperature of 55°F. The daily course of the tunnel air temperature follows the variation of the energy inputs due to the train schedules and passenger loads. Note that at days 10 and 11, following a drop of about 15°F in the daily air temperature cycle, the tunnel air temperature cycle is unaffected. In case A1(c), where the ventilation rate is large, however, the tunnel air temperature on days 10 and 11 shows a marked departure from the prior days.

Figure 10 shows the temperatures for case A2, a single track tunnel at heavy traffic density and high ventilation rate. A comparison should be made to case A1(c) which has the same conditions except for the change in traffic density. At the early morning peak traffic period (about 8 a.m.) the tunnel air temperature is from 3°F to 5°F higher with the

heavy traffic schedule of case 2. Near midnight, when the traffic volume is low, this difference in the two cases reduces to $1^{o}F$ to $2^{o}F$.

To give some insight to the heat problems in High Speed Ground Transportation Tunnels case C was included. The propulsion energy input is 110 times greater for this case. The effect of this kind of high energy release is illustrated in Figure 11. The tunnel air temperature has reached a peak value of $171^{o}F$ after 13 days from a cold start, and is rising at the rate of $3^{o}F$ per day. No ventilation is provided here, so this compares with case A1(c) for an urban rapid transit system, where the maximum tunnel air temperature has stabilized at about $88^{o}F$.

The final temperature plot is Figure 12, which is case B, the double track tunnel with local and express train service. It should be compared with case A1(c) and case A2, which have the same high ventilation rates. The comparison will show that the tunnel temperatures for the double tunnel are intermediate between these two single tunnel cases for normal and heavy traffic volumes. This result is consistent with the fact that, the double tunnel has, by virtue of local and express trains, a traffic density intermediate between cases A1(c) and A2.

Energy Transfers

Energy transfers during each hour of the day for the various energy sources or sinks, as obtained from the computer program, have been presented in a detailed report of this study (3). The results for two of the cases are presented here in Figures 13 and 14. The figures are for Day 7, i.e., a day for which a steady periodic tunnel temperature has been established.

Figure 13 shows clearly there are five major energy transfer classifications in subways, namely; running energy, braking losses, tunnel wall conduction, ventilation air and air conditioning. Coach air conditioning results in an energy transfer of about one-half that of the tunning energy. These results are generally in agreement with the results of the G.E. study for the N.Y.C. Transit Authority (1) except for the tunnel wall conduction and ventilation air. The disagreement in the relative magnitude of wall conduction is, no doubt, due to the difference in the thermal models used. G.E. modeled the N.Y.C. subway, laid below a city street; whereas our model simulates a deep-ground tunnel. The choice of a ground temperature at $55^{o}F$, further changes the role of ventilation air from a sink to a source.

The energy simulation for a High Speed Ground Transportation System is shown in Figure 14. In this case the high propulsion power requirement results in the running and braking energy transfers as the predominant sources and the tunnel wall transfer again as the predominant sink.

The assumption that the earth thermal penetration distance is 3 feet was retained for the HSGT simulation. Undoubtedly the fact that the propulsion energy is 110 times higher for this case makes that assumption questionable. Increasing the thermal penetration depth would result in increased tunnel wall and air temperatures. Hence the temperatures plotted in Figure 11 should be viewed as minimum values for high earth thermal conductivity.

Significant Factors in Energy Transfers

The simplified analysis of energy transfers on underground rapid

transit, presented here, suggests that the factors which will have major influence are as follows:

1. Ground Sink-Temperature and Geometry.

For a tunnel well below grade, the surrounding earth can act as a heat sink for large amounts of energy transfer. The tunnel temperature will be a function of the energy release in the tunnel, the ground temperature and the ventilation. This situation may apply to new concepts in high speed ground transportation, where tunneling is used.

In a city subway the underground geometry will be vastly different. The ground sink will have little influence here (1). Rather, the tunnel temperature will be a function of the energy release in the tunnel, the ventilation and the ambient temperature as influenced by the neighboring construction.

2. Vehicle Propulsion and Braking

The energy to overcome aerodynamic drag and surface friction, and the braking of the train approaching stations, constitute the major energy release in the tunnel. Running speeds such as those proposed for new types of high speed ground transportation systems can result in severely elevated tunnel temperatures. The simulation here for a 135 mph rapid transit system resulted in raising the tunnel temperature from an initial $55^{o}F$ to a mean daily temperature of approximately $130^{o}F$ in four days and $160^{o}F$ in thirteen days (Figure 11).

3. Ventilation

The influence of ventilating air on the tunnel temperature and energy transfer can vary from almost no effect to a significant one. In the thermal model developed here, ventilation usually added heat to the tunnel, because of the ground acting as an effective low temperature ($55^{\circ}F$) sink. For a city subway, ventilating air becomes the primary means of heat removal. The use of high nighttime ventilation rates have been recommended (1) for significantly increasing the number of hours when the tunnel temperature will be in the comfort range (Figure 2).

4. Passenger Density

Passenger demand determines the train scheduling and consequently the rate of propulsion energy release. The number of passengers per coach also is the major factor in determining air conditioning loads.

5. Air Conditioning

The installation of coach air conditioning adds another major energy release source in the tunnel. For our model, during periods of p eak passenger density at 8 a.m., the energy rejection from air conditioning equipment was approximately equal to the propulsion energy release. For a 24-hour period the air conditioning equipment contributed about 50 percent as much energy release as the propulsion system.

Insignificant Factors

1. Vehicle Thermal Insulation - Heat Transfer Coefficient

   With any reasonable thermal insulation in the vehicle body, the energy transfer between the vehicle and tunnel is negligible. The value of the vehicle surface heat transfer coefficient is, therefore, insignificant.

2. Tunnel Wall Heat Transfer Coefficient

   In the tunnel walls, the relatively low thermal conductivity of concrete or earth is such as to make this controlling in the rate of energy transfer to the ground. Again, then, an accurate determination of the tunnel wall surface heat transfer coefficient is unnecessary.

Conclusions

The results obtained for the simplified thermal model of an underground rapid transit system permits drawing three major conclusions.

1. The proper design of the ventilating and air conditioning systems for underground rapid transit will require a detailed energy budget study. Rough calculations cannot give reliable results because of the complexity of the energy transfer processes occurring and the sensitivity to particular parameters. For example, an error of $3^{o}F$ in the difference between tunnel air and wall temperatures could cause a 100 percent error in the energy transfer to the ground as a heat sink.

2. The thermal modeling of the underground system must be true to the physical conditions imposed. The simplified model used

here for a tunnel well below grade gave very different results for energy transfer to the ground and to ventilation air as compared with the predictions of a thermal model developed for the New York City Transit Authority (1).

3. The importance of ventilation as a means of heat removal is strongly a function of the tunnel air to ambient air temperature difference. The tunnel air temperature is a complex function of all the factors influencing the energy release and energy transfer mechanisms in the tunnel. Tunnels with high rates of energy release, such as high traffic density and high speed systems will require large ventilation pumping rates to avoid excess buildup of temperature.

As a final note it should be added that the Urban Mass Transportation Administration has placed a contract (DC-MTD-7) with the Institute of Rapid Transit in Washington, D.C., for a comprehensive three year study to develop a Subway Environmental Design Handbook. The study began in October 1970 and several reports on preliminary work have recently become available (13, 14, 15, 16).

Acknowledgement

The work presented in this paper was supported under the NASA Sustaining University Grant to Duke University (NGL-34-001-005).

NOMENCLATURE

a = Outside radius of tunnel retaining wall

A_c = Area of car walls

a_w = h_w/L_1

A_w = Area of tunnel walls

b = Radius to which thermal energy penetrates in the earth

C_v = Specific heat at constant volume (of air).

C_p = Specific heat at constant pressure (of air).

E_T = Tunnel ventilation rate

g = $T_T\ (h_w/K_1)$

h_w = Average convective coefficient of heat transfer at tunnel wall

K = Thermal conductivity of wall material

M = Mass of a car (normalized to give kinetic energy in Btu)

M_T = Mass of air in the tunnel

n = No. of cars stopping at the station per hour

N_{AV} = Average no. of cars present in the system at time t

N_R = Average no. of cars running at speed in the system

Q_I = Internal heat load of a car (lights, people, etc.)

Q_R = Propulsion energy per car

R = Inside radius of tunnel wall

R_i = Radius of ith grid circle

$T_{i,k}$ = Temp. at ith grid circle at k time steps

T_c = Car inside air temperature

T_o = Initial uniform wall temperature at t = 0

T_T = Tunnel air temperature

T_v = Inlet ventilation air temperature

T_w = Tunnel wall temperature

U_o = Average wall conductance for a stationary car

U_v = Average heat conductance of the train car walls (including convective heat transfer coefficients based on motion of the car at cruise speed).

V = Cruise velocity

α = Thermal diffusivity of wall material

Δr = Grid spacing

Δt = Magnitude of time step

ζ = Air density of ventilation air

η = Reciprocal value of the average coefficient of performance of the car air conditioner

θ_e = $T_e - T_o$

Subscripts

e = 1 (for concrete tunnel wall) or 2 (for earth)

i = Radial position on grid circle

k = No. of time steps passed

m = k + 1 (time step under consideration)

Superscript

n = Number of time steps

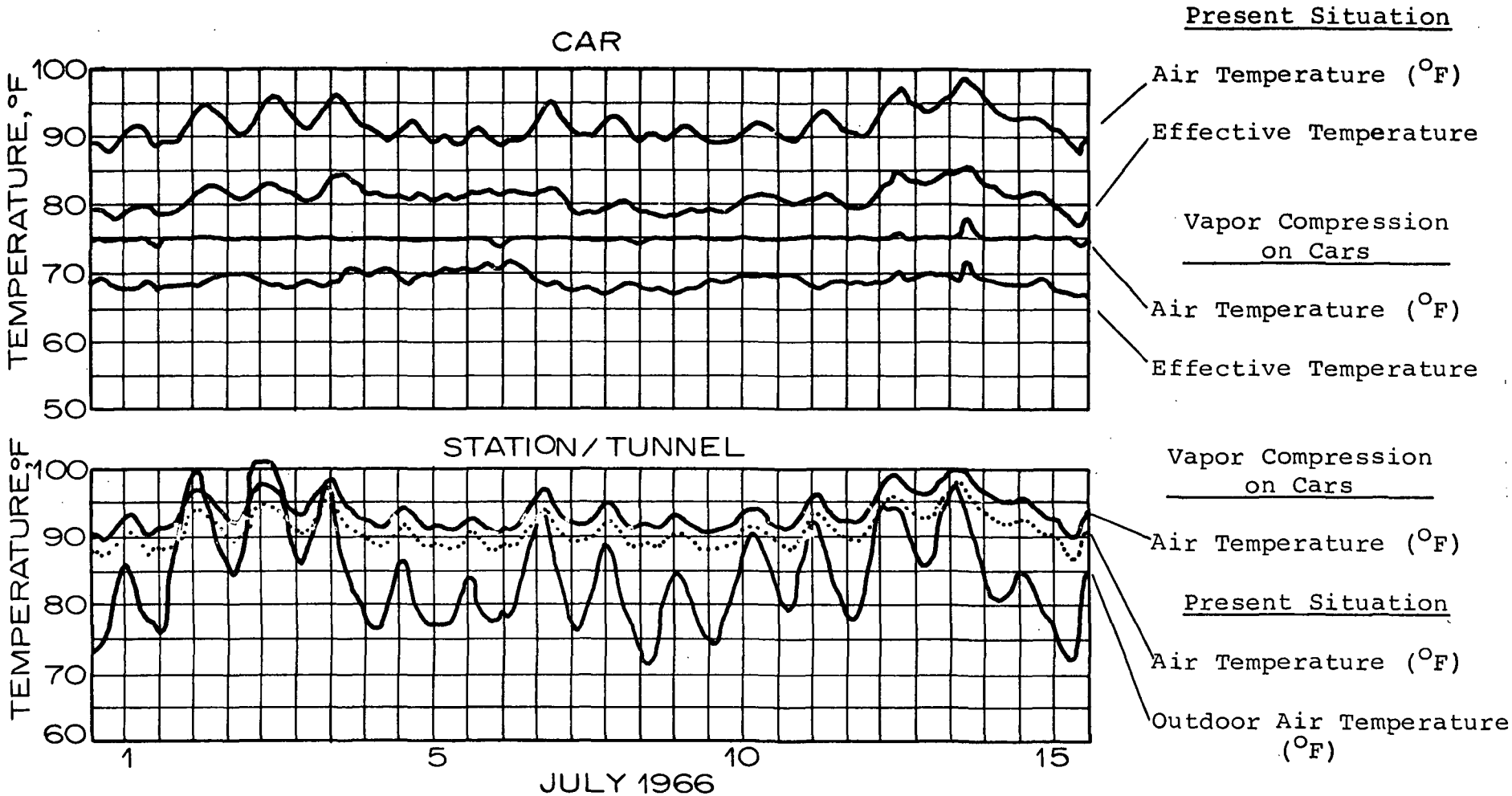

Figure 1. Model Predictions--Present Situation Versus Air Conditioning on Cars for New York City Subway, (1).

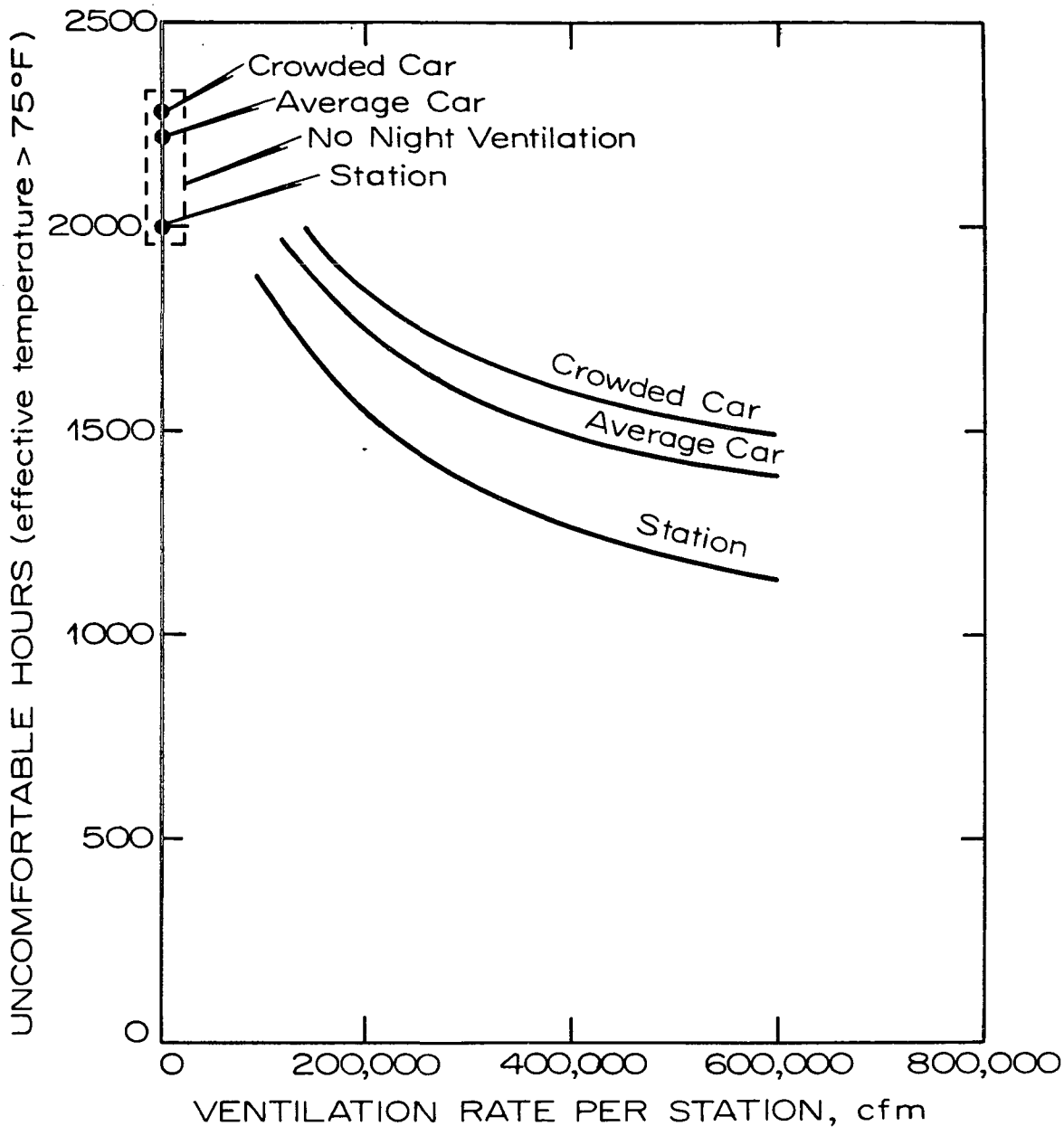

Figure 2. Effect on Nighttime Ventilation on Comfort in New York City Subway, (1).

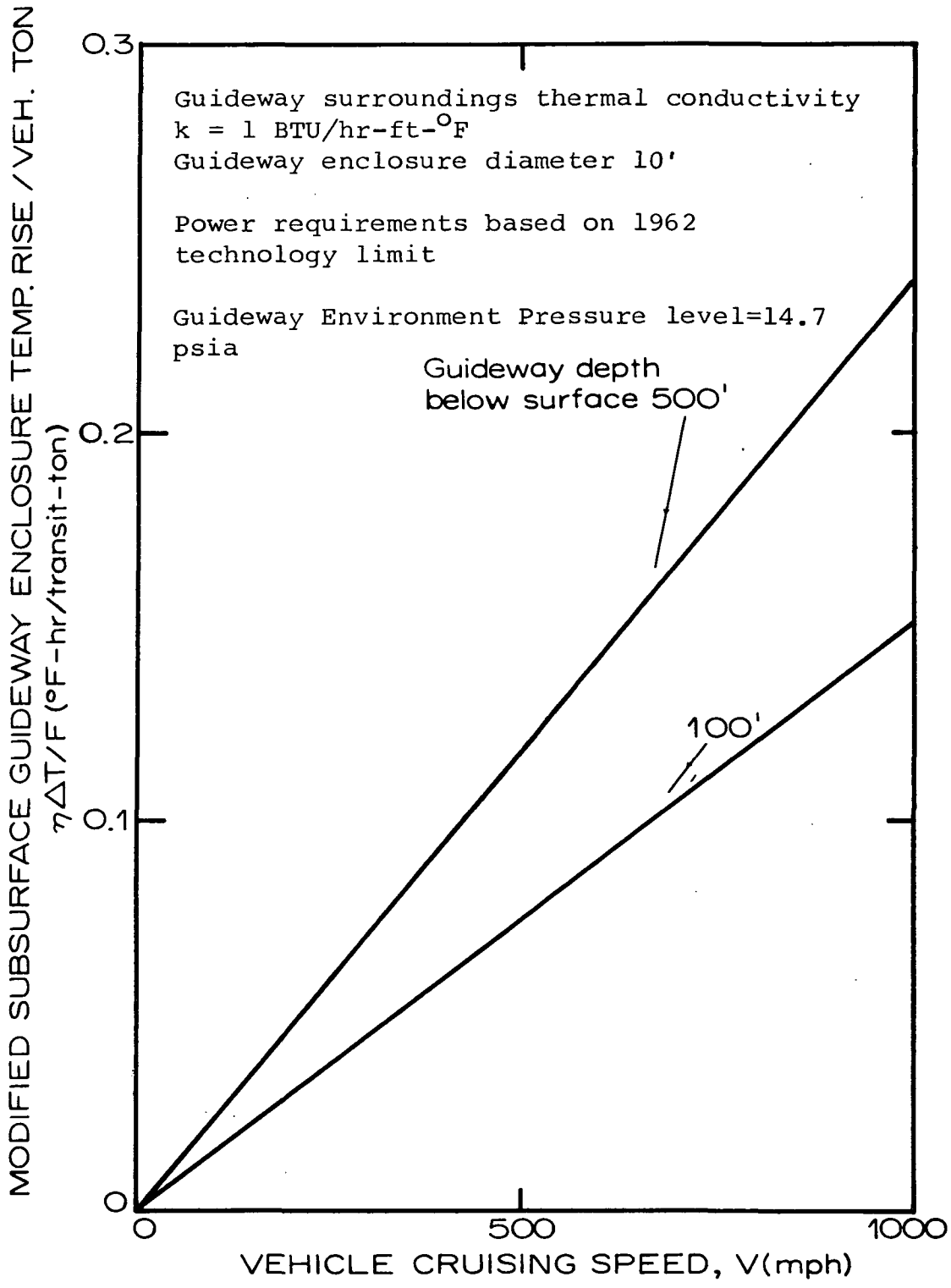

Figure 3. Modified Steady Subsurface Guideway Enclosure Temperature Rise per Ton of Vehicle Versus Vehicle Speed, (2).

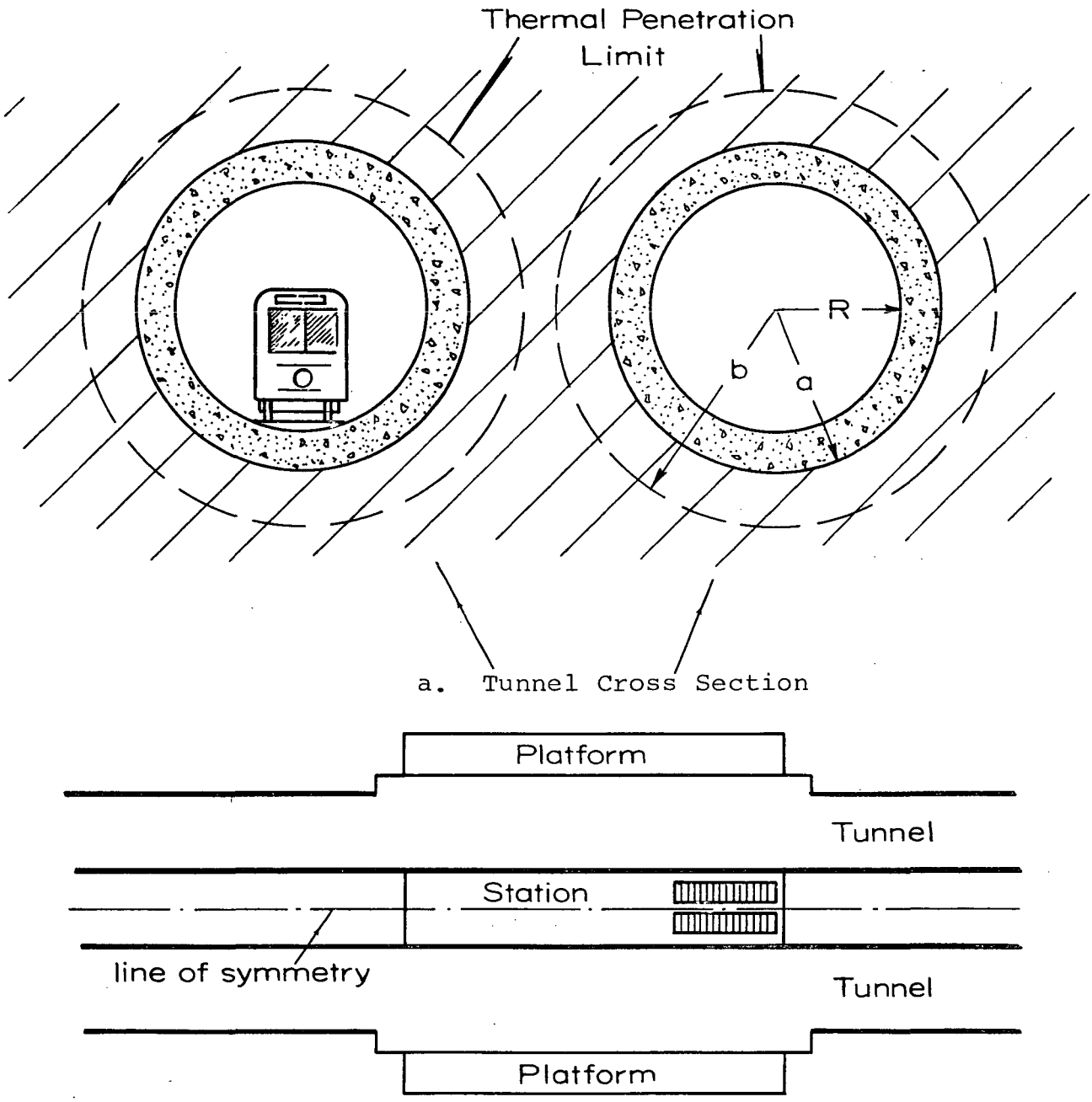

a. Tunnel Cross Section

b. Station and Tunnel Plan

Figure 4. Underground Rapid Transit-Physical Model.

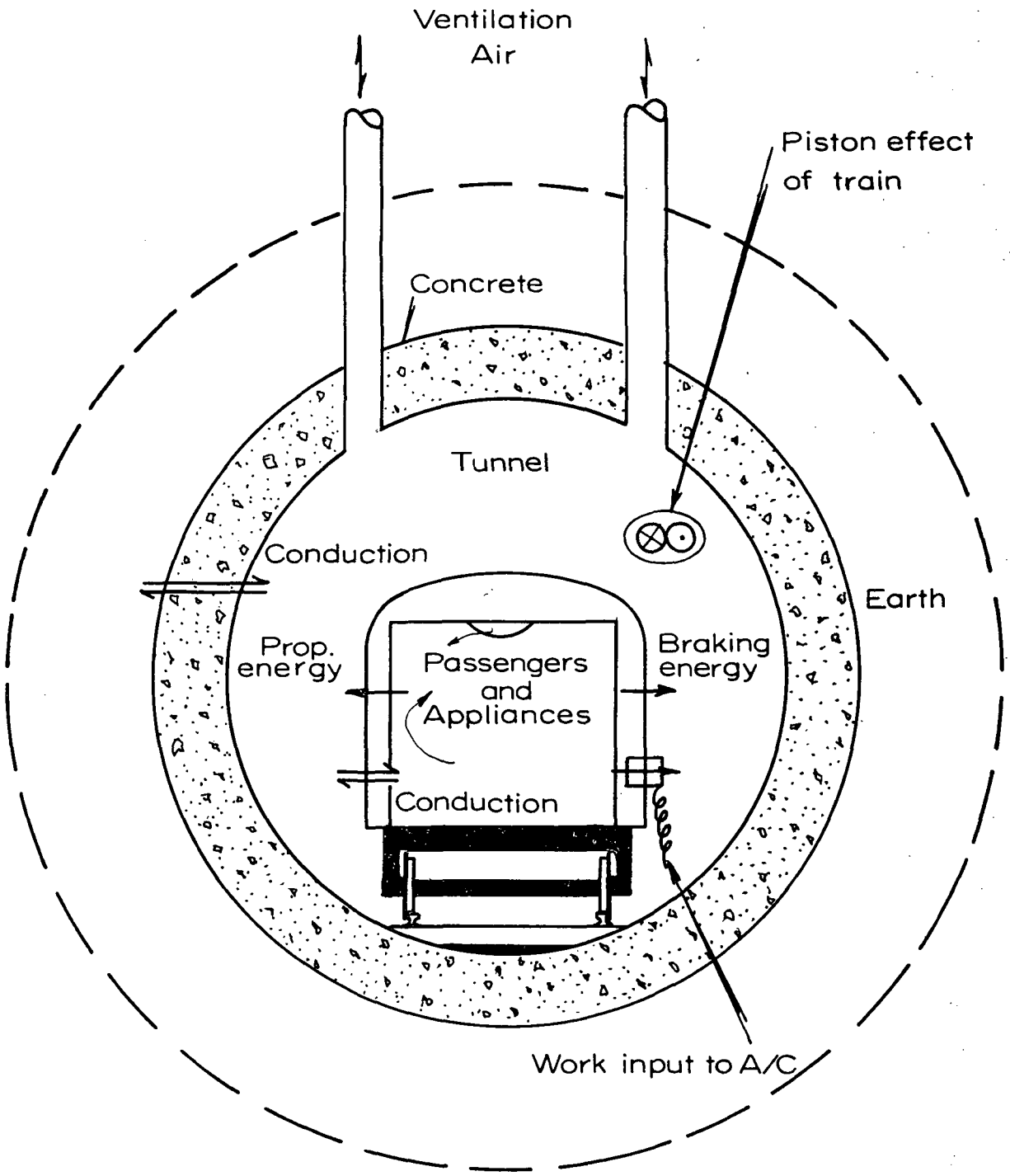

Figure 5. Heat Energy Exchanges in Tunnel.

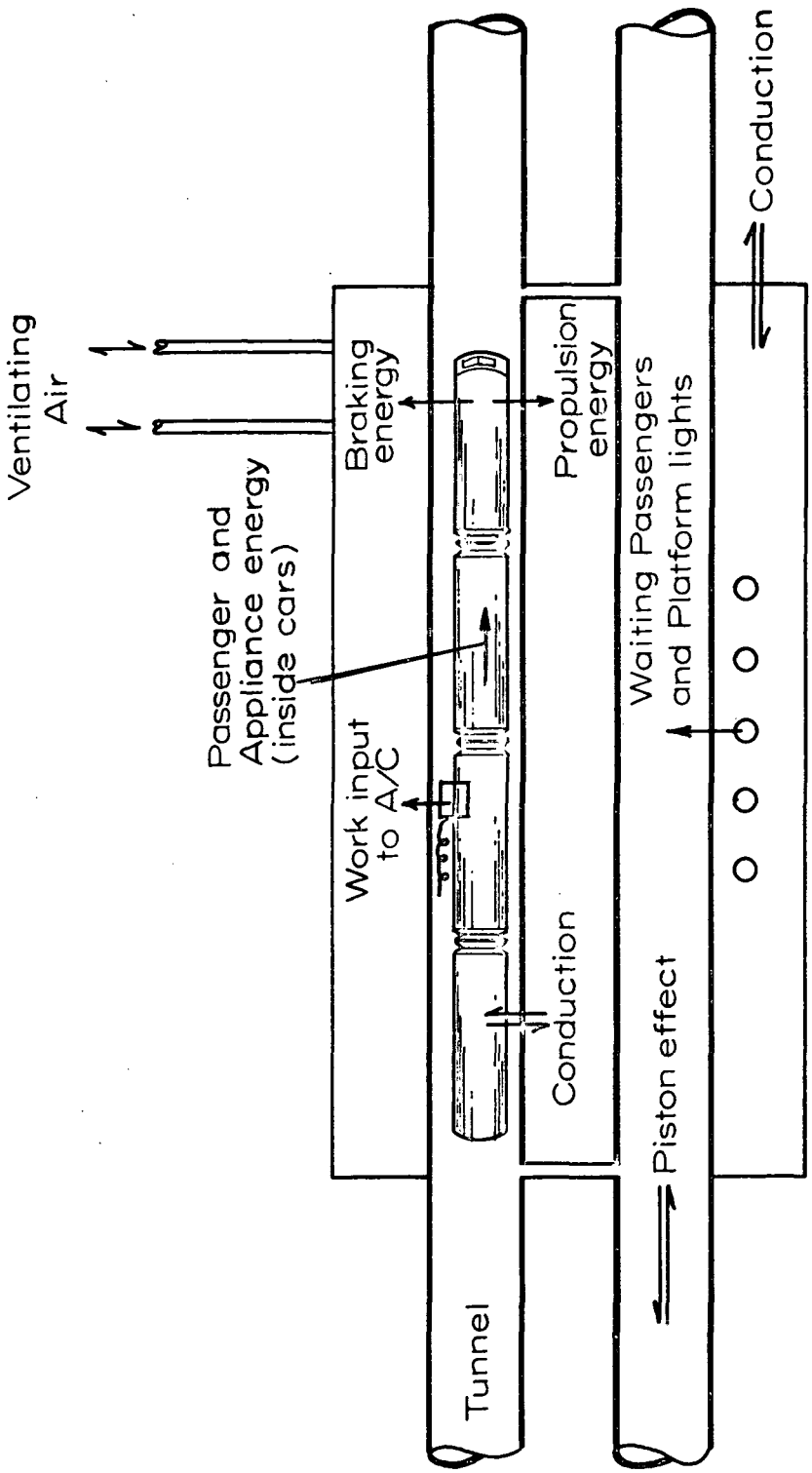

Figure 6. Heat Energy Exchanges in Station.

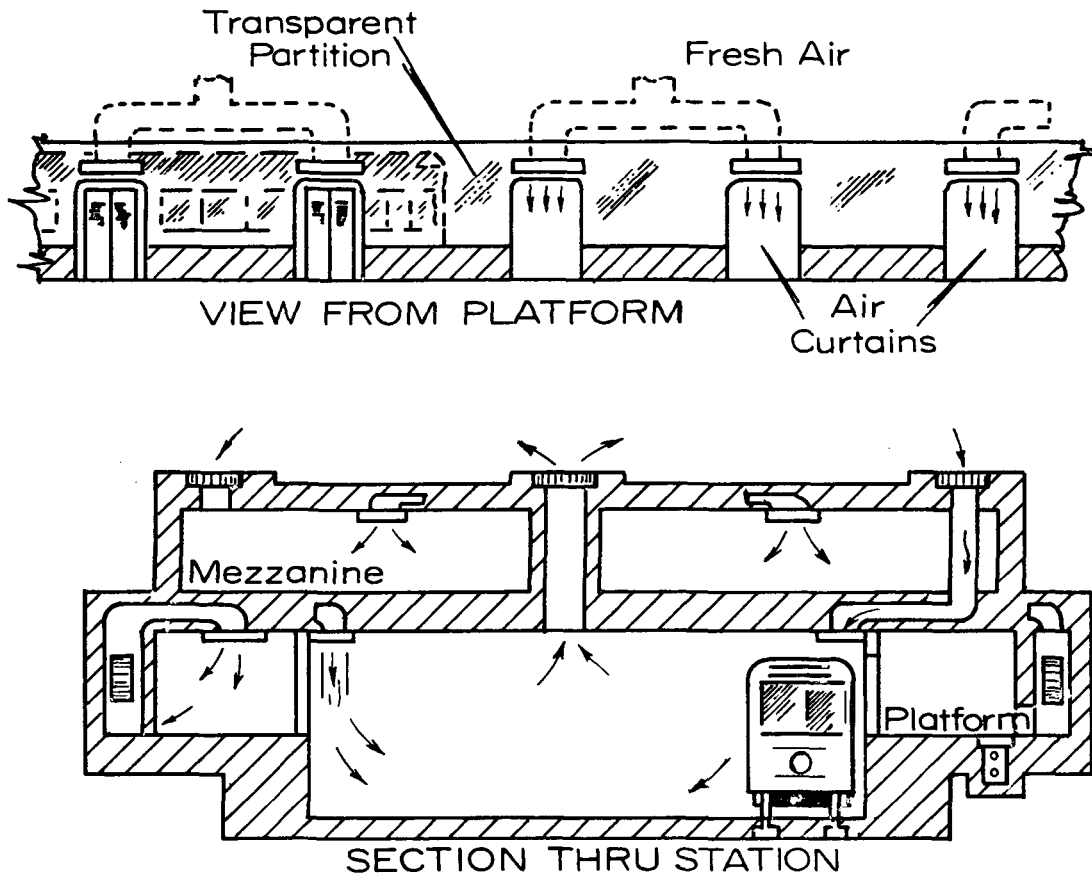

Figure 7. Station Air Conditioning and Ventilation Layout, (1).

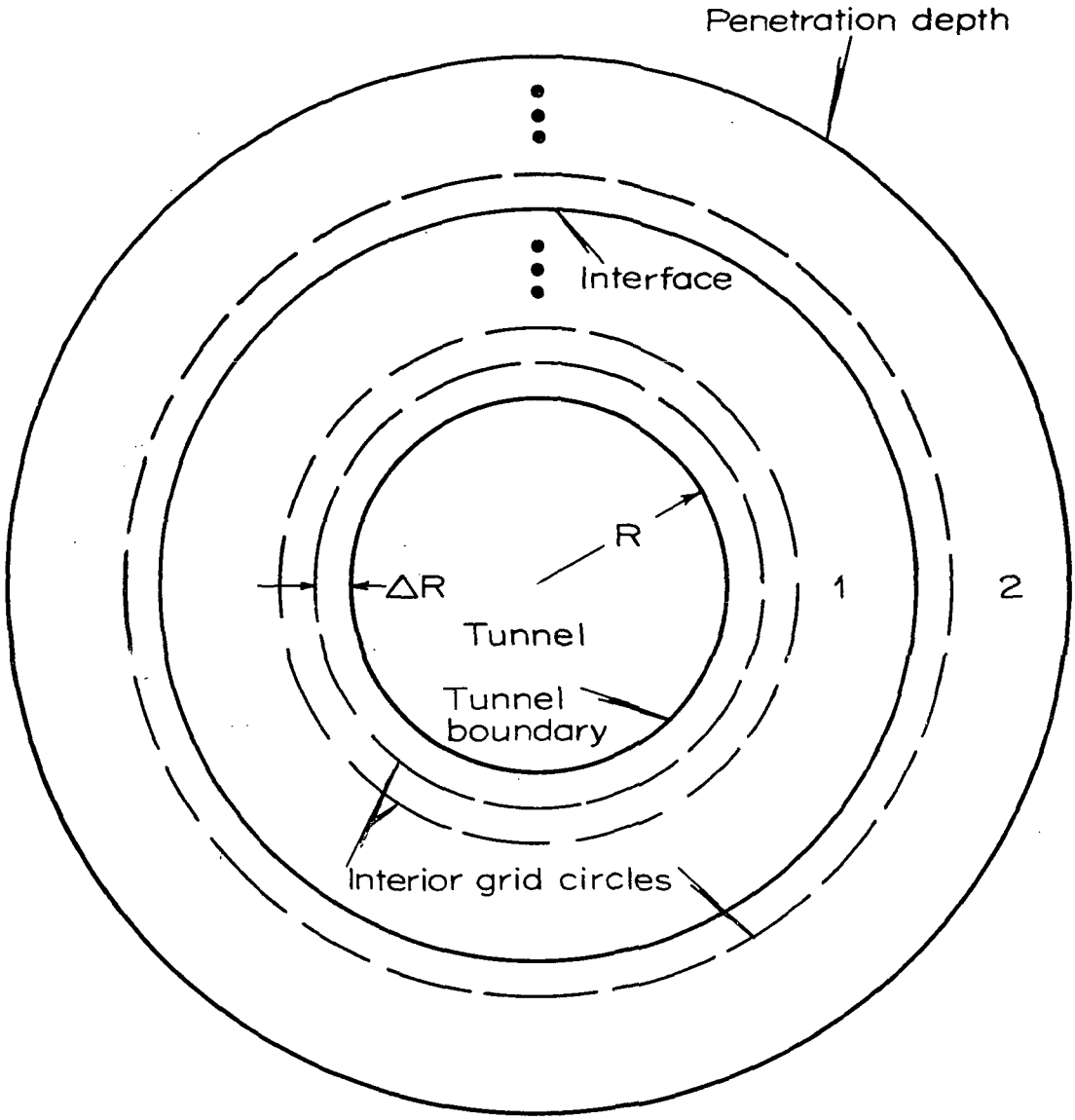

Figure 8. Grid Pattern for Difference Equations.

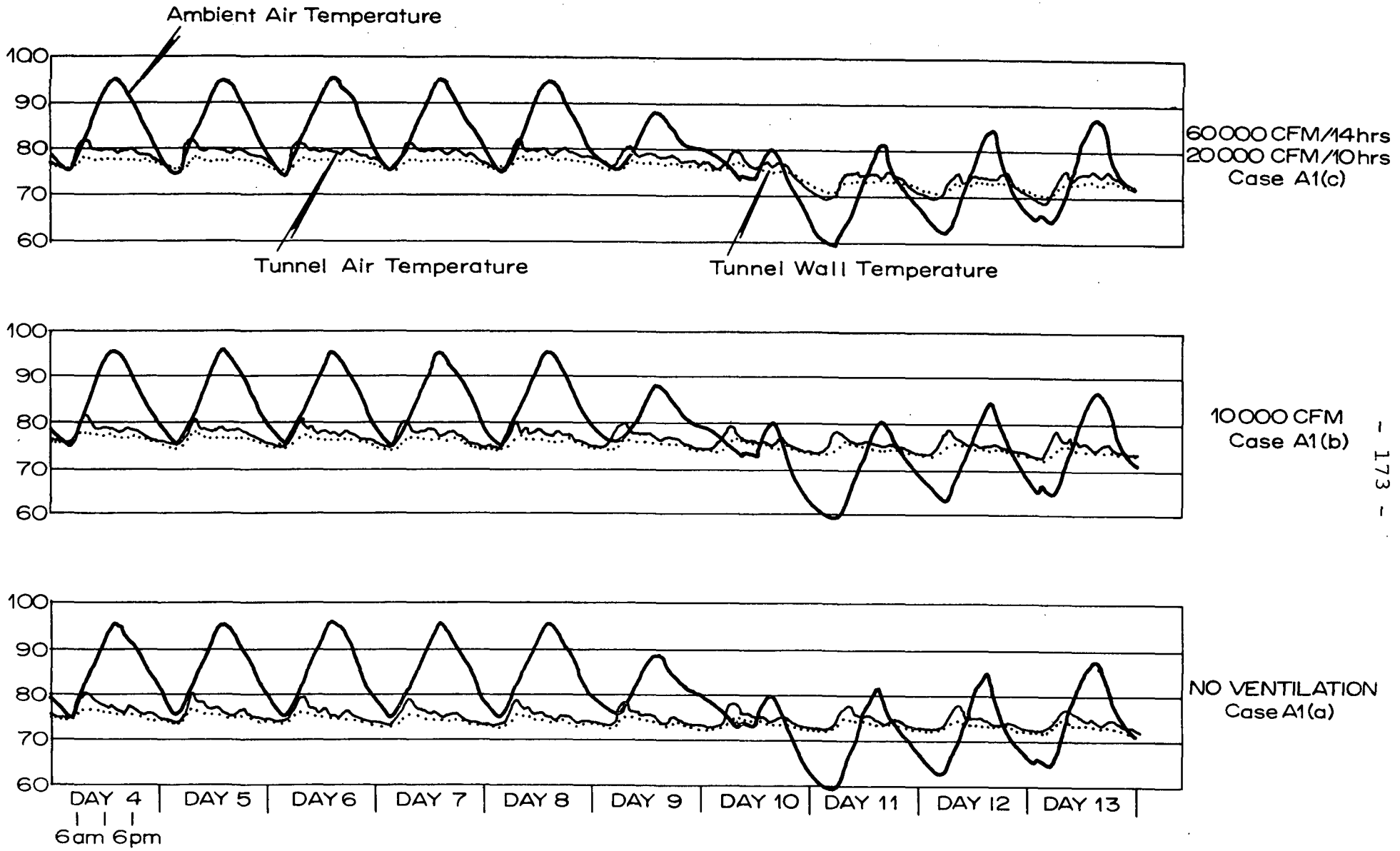

Figure 9. Tunnel Air and Wall Temperatures for Normal Traffic Density (Single Track).

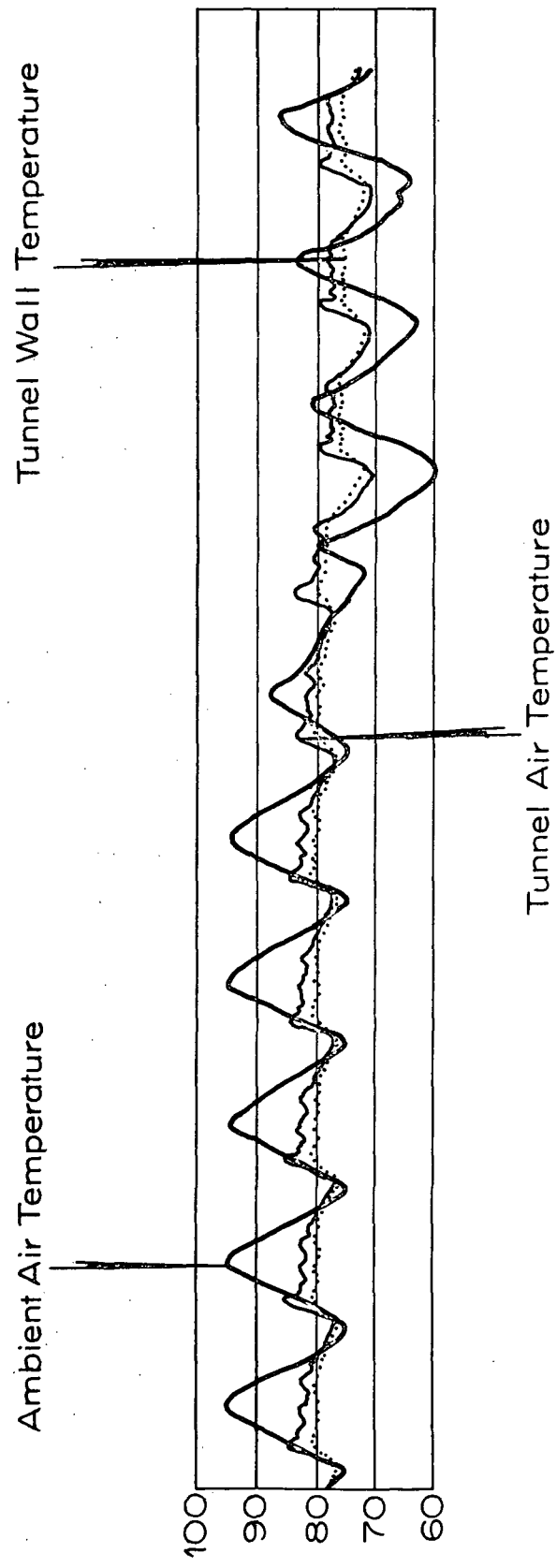

Figure 10. Tunnel Air and Wall Temperature for Heavy Traffic Density.

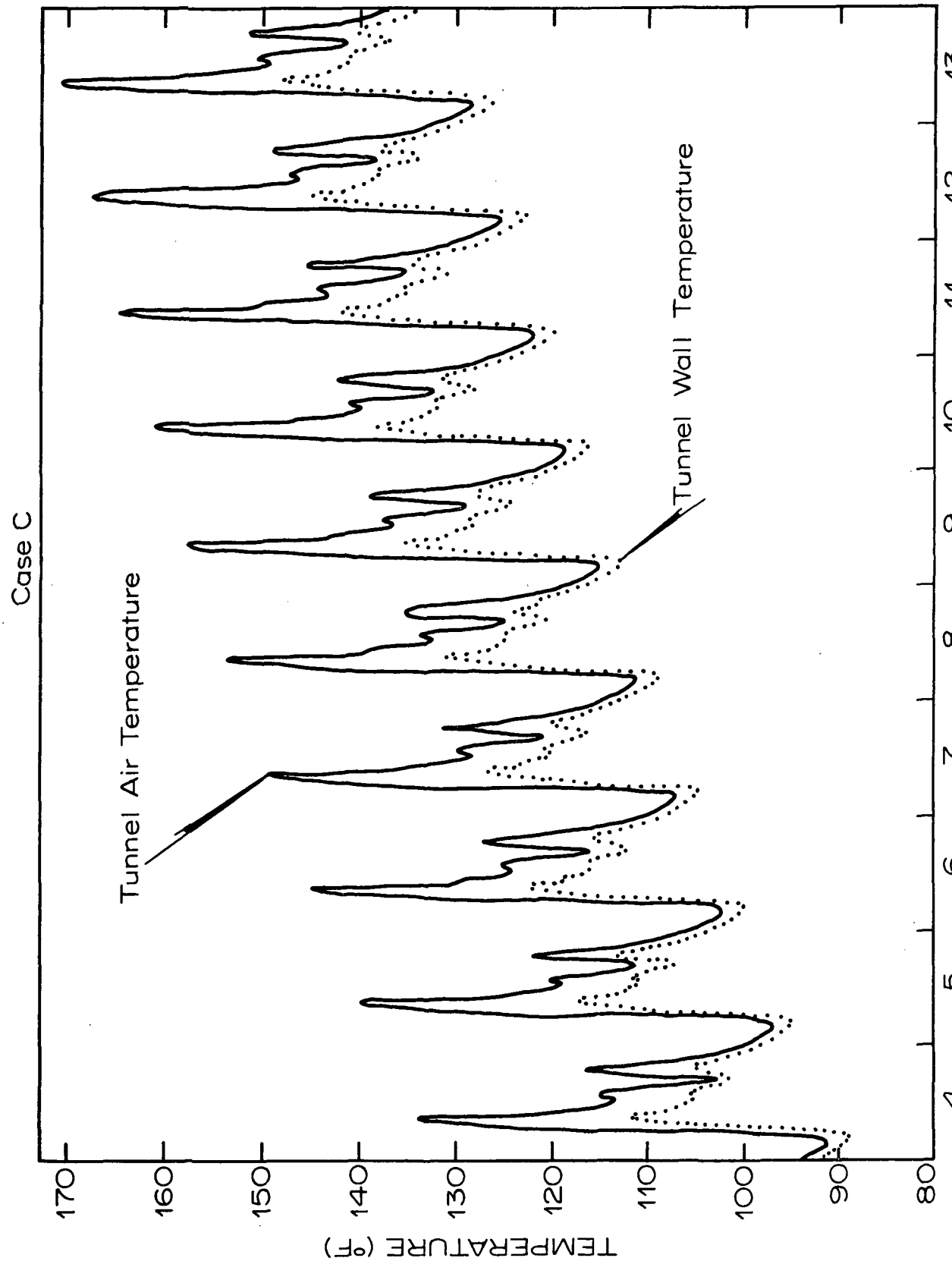

Figure 11. Tunnel Air and Wall Temperature for HSGT Simulation.

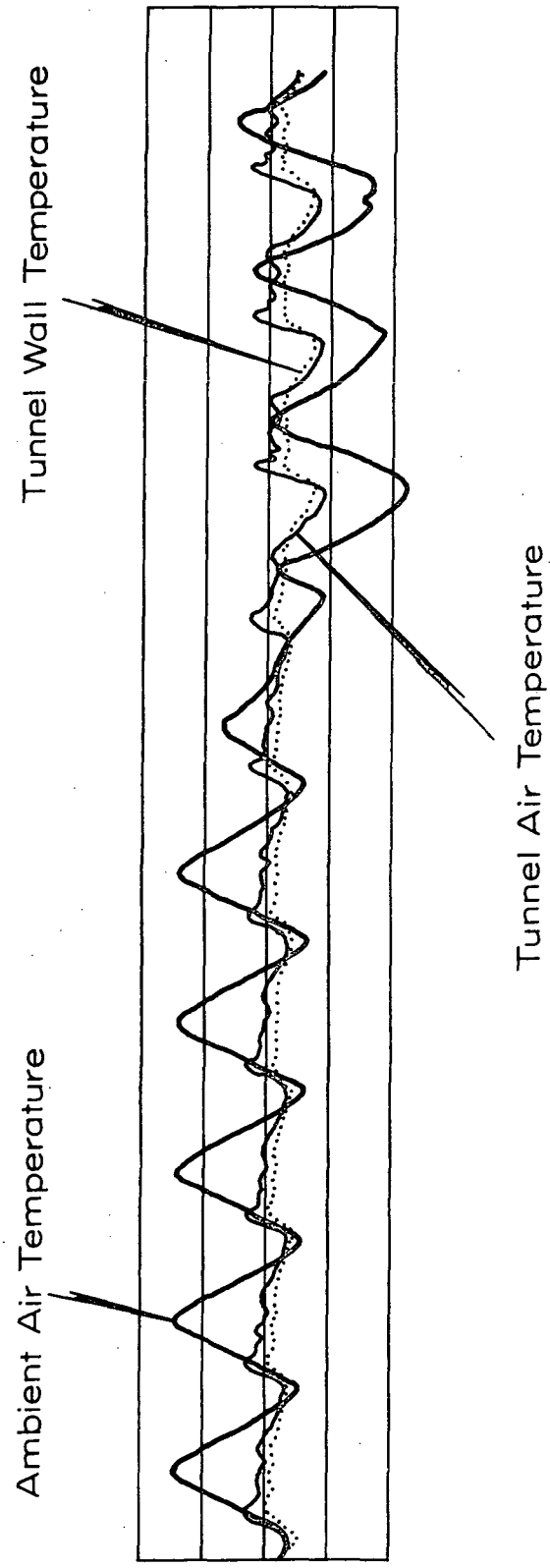

Figure 12. Tunnel Air and Wall Temperature for Double Track Tunnel.

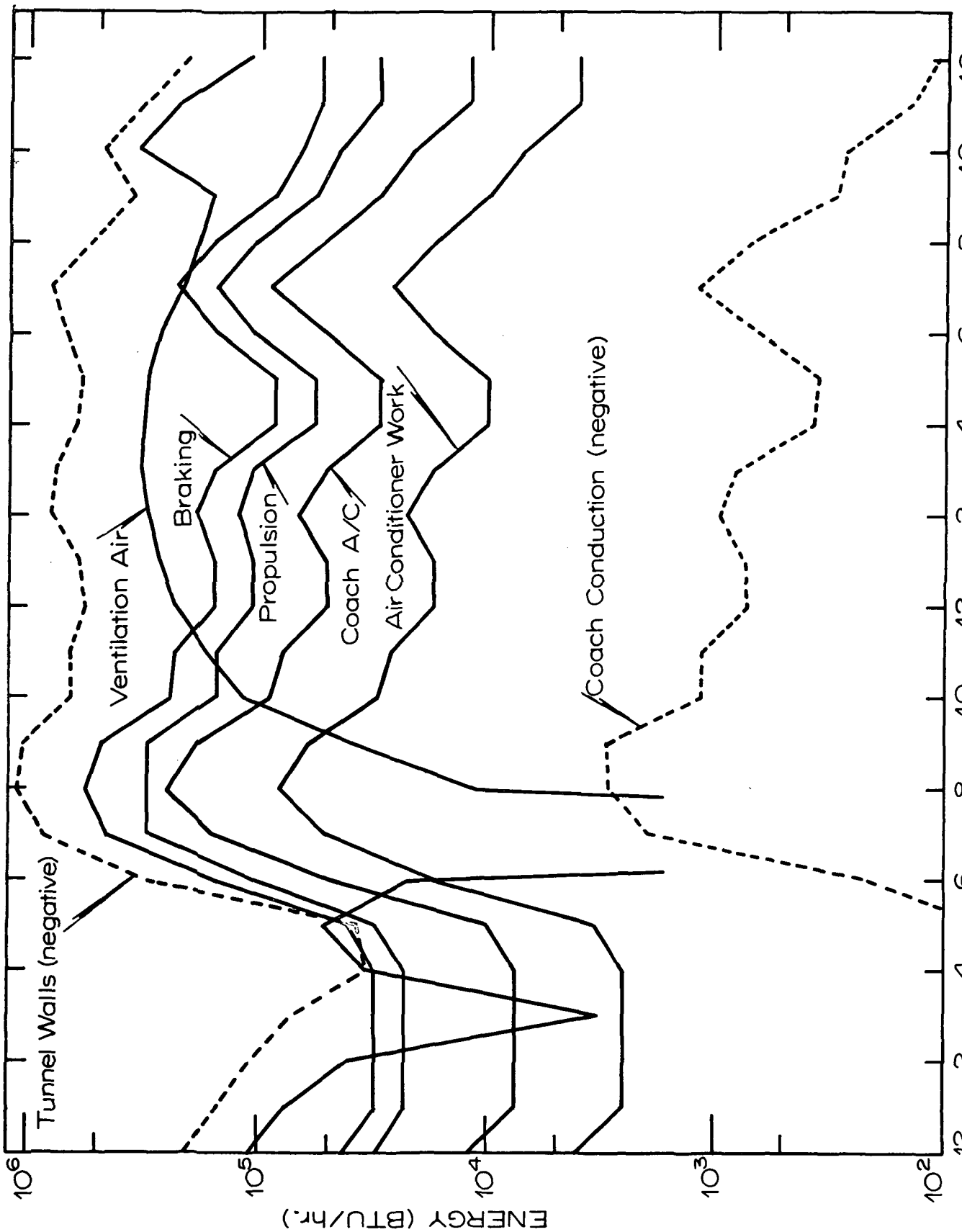

Figure 13. Energy Transfer Levels for a Subway.

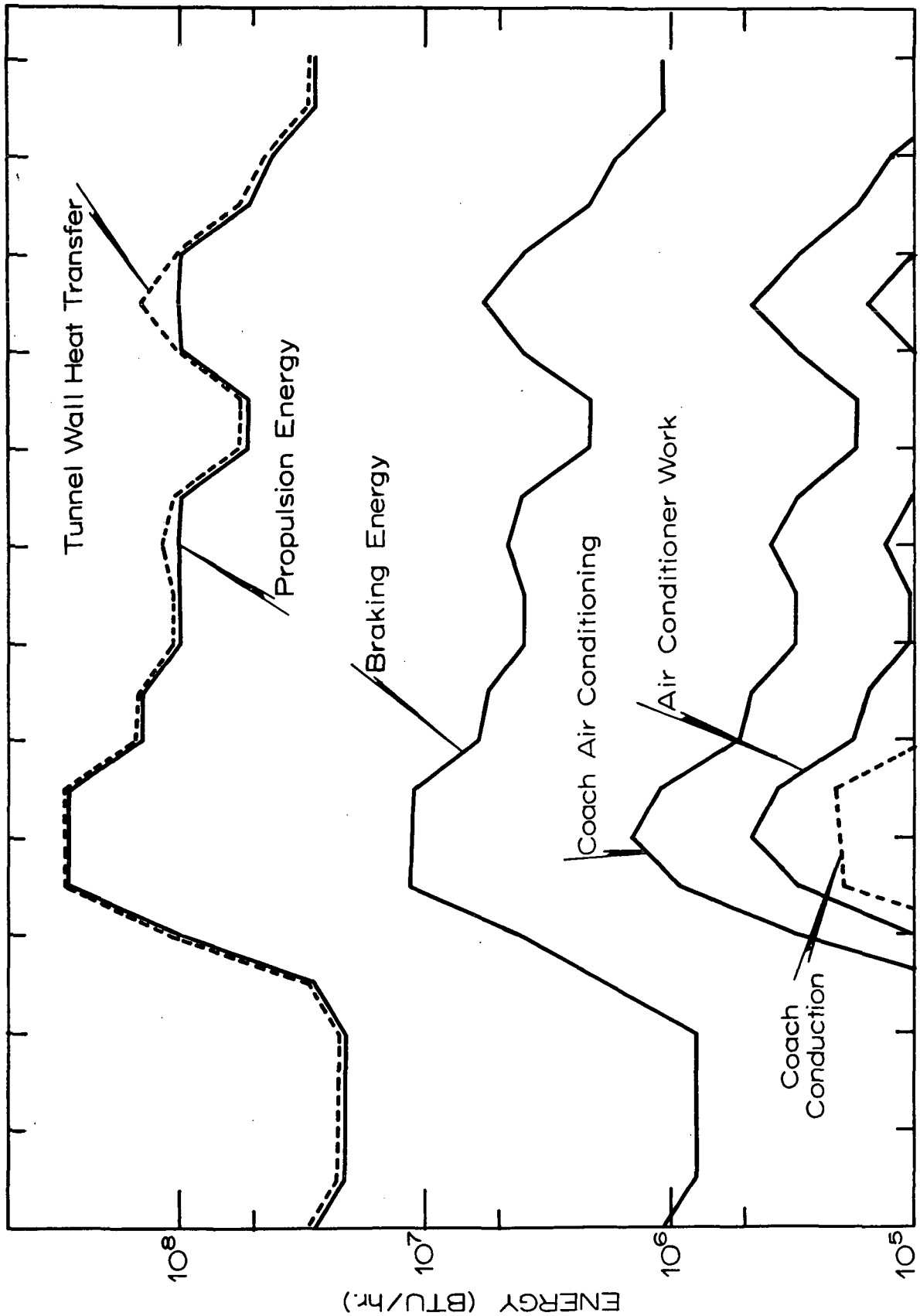

Figure 14. Energy Transfer Levels for High Speed Underground Transportation.

LIST OF REFERENCES

1. New York City Transit Authority, An Air Conditioning Study of the New York City Transit System, Part I "A Thermal System Model and Equipment Valuation."

2. Survey of Technology for High Speed Ground Transportation, Massachusetts Institute of Technology, PB 168-648, June 1965.

3. Chaddock, J. B., and Sud, I., "Energy Study of Underground Rapid Transit," Department of Mechanical Engineering, Duke University.

4. New York City Transit Authority, An Air Conditioning Study of the New York City Transit System, Part II "Feasibility of a Thermoelectric Air Conditioner for Subway Cars."

5. Irvin, L.A., and Asmus, J.R., "The Bay Area Rapid Transit Vehicle System," SAE Transactions, 1968.

6. Thon, J.G. and McLaren, M.W., "Power Supply for the BART System," Transportation Engineering Journal of ASCE, Vol. 95, Feb. 1969.

7. Carnahan, B., Luther, H.A., Wilkes, J.O., Applied Numerical Methods, John Wiley & Sons, Inc., 1969.

8. Douglas, J., Jr., "Round off Error in the Numerical Solution of the Heat Equation," Journal of the Association for Computing Machinery, Vol. 6, 1959.

9. Conte, S.D., Elementary Numerical Analysis, McGraw-Hill Book Co. 1965.

10. Hoppe, R.G. and Gouse, S.W., Jr., "Fluid Dynamic Drag on Vehicles Travelling through Tubes," Department of Mechanical Engineering, Carnegie-Mellon University.

11. Handbook of Air Conditioning System Design, Carrier Air Conditioning Company, McGraw-Hill Book Co., 1965.

12. Meyer, R.J., Kien, J., "Technology and Urban Transportation," Federal Clearinghouse Report PB 168 070, June 1962.

13. Aeronautical Labs, California Institute of Technology, Pasadena, Cal., "Theoretical Scaling Laws for Subway Modeling," March 71, PB 206 779.

14. Parsons, Brinkerhoff, Quade and Douglas, New York, "Single Track Subway Environmental Simulation Model, Phase I," Aug. 71, PB 206 895.

15. Kaiser Engineers, Oakland, Cal., "Subway Environmental Design Criteria, Sept. 71, PB 206 896.

16. Kaiser Engineers, Oakland, Cal., "Research Bibliography Ventilation and Environmental Control in Subway Rapid Transit Systems, Phase I," Aug. 71, PB 205 996.

EXPERIMENTAL INVESTIGATION OF TUBED VEHICLE AERODYNAMIC CHARACTERISTICS

Bruce R. Munson and Leslie D. Smith
Department of Mechanical Engineering
Duke University

Introduction

One of the many alternative systems for effective mass transportation that have been proposed involves vehicles traveling within the confines of a tube. Advantages of the tubed systems include isolation of noise and noxious odors. Such systems would also be unaffected by weather and require minimum right of way. The proposed systems involve propulsion by gravity, pressure differential or self-contained propulsion units.

Due to the extremely high cost of a prototype of any of these systems, it is necessary to fully investigate the proposals in order to properly evaluate cost and feasibility. In the development of many previous ground transportation systems, evaluation of the aerodynamic problems was a refinement to be considered after a working model or system was constructed. In the tubed vehicle systems proposed, the aerodynamic forces are much larger than in non-tubed systems and thus present one of the predominant problems. Before continuing development of these systems, there must be accurate information concerning the aerodynamic characteristics, including drag, moments, and preferred orientation within the tube.

Any accurate analysis of the theoretical problem is very involved. From a fluid mechanics point of view, the problem is that of a compressible viscous flow, with troublesome geometry and boundary conditions. Likewise, experimental evaluations in conventional wind or water tunnels present problems. Proper modeling must include the vehicle moving with respect to the tube; i.e. a boundary enclosing the vehicle that is capable of moving at speeds very close to the speed of the free stream area. In addition, water tunnels fail to include compressibility effects.

As shown by both involved theoretical analysis and intuitive application of basic fluid dynamic principles, tubed vehicles are

inherently unstable. As the vehicle is moving down the tube, if its center line becomes misaligned with the center line of the tube, a moment is developed which tends to further misalign the vehicle. This situation leads to unwanted oscillations and, in the extreme, catastrophic failure.

Foa (1) has proposed a self-propelled tubed transit system and has carried out theoretical analysis of some of the problems. Theoretical and experimental evaluation of pneumatic propulsion tubed systems has been performed by Cudlin, Harman, and Murray (5). Gouse and his associates (2,3,4) have made theoretical and experimental evaluations of the drag of vehicles traveling in a tube. They also noticed and commented on the instabilities mentioned above.

Goodman (6) has performed a theoretical analysis of the incompressible flow field around a tubed vehicle using potential flow theory for slender bodies. He evaluated the aerodynamic forces for an ellipsoid of revolution and with Lehman (7) has experimentally checked his theoretical predictions using a water tunnel in which the vehicles occupy up to fifty percent of the cross sectional area of the tube. Goodman (8) has also considered corrections to the above to account for compressibility.

For the present study, a water filled vertical tube and gravity drop vehicles were used to evaluate stability and drag of near cylindrical bodies. Vehicles with ogive shaped noses and short cone tail sections were investigated for three different vehicle diameter to tube diameter ratios, and three vehicle length to vehicle diameter ratios. A three-inch inside diameter guideway tube filled with water provided Reynolds numbers based on vehicle diameter of the order of magnitude of 10^4 with vehicle velocities of one to five feet per second. An electromagnetic sensing system consisting of a vehicle mounted magnet and sensing coils mounted on the outside of the guideway tube made it possible to determine the vehicle velocity and the existence of oscillatory instability of the vehicle. The aluminum vehicle ends were connected by a tubular plastic center section. A weight that could be moved fore and aft within the vehicle allowed the center of gravity to be moved. The large buoyant force of a vehicle in water, combined with the

variable center of gravity allowed the achievement of a statically neutral stability condition - the boundary between stable (not oscillating) and unstable (oscillating) vehicle motion. Knowledge of the magnitude of the buoyancy, the position of the center of gravity for the neutral condition, and vehicle velocity allowed the evaluation of the principal stability derivative, the change in moment about the center of gravity for a change in angle between the center lines of the vehicle and guideway tube.

Hence stability and drag information was obtained using a model system that has the correct boundary conditions. That is, a system in which the vehicle moves within a stationary tube. The experimental results show that operation of a vehicle within an enclosed guideway does indeed increase the aerodynamic problems (drag and stability) compared to operation of a vehicle in an open space.

Experimental Apparatus

Vehicles with a movable center of gravity were dropped in a vertical, water filled tube. An electromagnetic instrumentation system allowed the evaluation of vehicle speed and stability. The movable center of gravity allowed the achievement of a statically neutral stability condition. Details of the guideway tube assembly and vehicles are shown in Figures 1 and 2.

The guideway consisted of a sixteen-foot vertically mounted plastic tube (Figure 1). Figure 2 shows the construction details and shape of the vehicles. The front end was made in the shape of an ogive while the rear section ended in a steep cone with a steel cap. Vehicles were constructed with diameters of 1.6 inches, 1.9 inches, and 2.375 inches. Between the ends were fitted plastic center sections of various lengths. Thus, each of the three diameter end pairs could be used with three different length tubular center sections, giving nine possible vehicles, with length to diameter ratios of 10, 15, and 20.

A small magnet was mounted in the rear perpendicular to the longitudinal center line of the vehicle. An electromagnetic sensing system consisting of the vehicle mounted magnet, a set of coils

mounted on the outside of the guideway tube, and appropriate amplifiers and recorder was used to measure vehicle speed and determine stability. As the vehicle mounted magnet passed the two diametrically opposed rows of coils mounted on the guideway tube, a sinusoidal signal was induced in each row of coils. The strength of these signals is proportional to the velocity of the vehicle and the distance of the vehicle mounted magnet from each row of voils. If the vehicle did not oscillate or rotate as it passes through the instrumented section of the guideway, a constant amplitude sinusoidal signal was obtained from each of the two rows of coils mounted on the guideway tube. However, if the magnet has a lateral motion (due to oscillation of the vehicle) while passing through the instrumented section of the guideway, sinusoidal waves of changing amplitude are induced. This is illustrated in Figure 3. Sometimes the vehicle rotated while in the instrumented section, but this could be differentiated from oscillation as shown in Figure 3. As the distance between each coil is known, examination of the period of sinusoidal output gave the vehicle velocity. The output of each row of coils was sent to a pair of linear amplifiers with gains of 10^3, and then to a two-channel strip chart recorder. The traces from the recorder provide a record of the vehicle velocity and stability. A longer instrumented section would have been useful, but ten coils on each side gave satisfactory results.

Test Procedure

The general method used to determine stability and drag for the vehicles was as follows. The chosen vehicle was held at the top of the water filled guideway tube by the electromagnet. The magnet current was turned off to drop the vehicle. The strip chart output was examined to determine vehicle velocity and the existence of vehicle oscillation as previously explained in connection with Figure 3. Several drops were made, changing the position of the movable weight in the vehicle to determine the neutral stability condition, i.e., the dividing line between regions of oscillation and non-oscillation. The position of the

center of gravity for the neutral vehicle was determined by balancing the vehicle on a knife edge. The drag, equal to the weight of the vehicle in water, was measured by suspending the vehicle into the water filled tube from a spring scale.

The drag coefficient was based on vehicle base area and is defined by

$$C_{DB} = \frac{D}{\frac{1}{2}\rho V^2 A_V} \tag{1}$$

where D is drag in pounds, ρ is fluid density in slugs per cubic foot, V is velocity in feet per second, and A_V is the cross sectional area of the vehicle in square feet.

The Reynolds number was based on vehicle diameter D_V and defined by

$$Re = \frac{VD_V}{\nu} \tag{2}$$

Stability information was obtained by considering a moment balance about the center of gravity of the vehicle. The forces involved in static stability in these tests are the buoyancy and the drag. The neutral point obtained from testing is the center of gravity position at which the sum of the moments about the center of gravity is zero, i.e., when the buoyancy and drag moments cancel each other. The analysis of the problem is helped by the introduction of the center of pressure, i.e., the point at which the aerodynamic forces can be represented completely by linear forces. About the center of pressure the aerodynamic forces create no moment. In the case of tubed vehicles, this theoretical center of pressure is well forward of the geometric center, sometimes beyond the nose of the vehicle as shown in Figure 4. For the problem at hand, the aerodynamic force of importance is the drag. The buoyancy acts at the center of mass of the displaced water, and since the front and rear sections of the vehicles tested are not of the same geometry, this point lies a small distance behind the half-length position. The distance of the center of gravity from the nose of the vehicle for the neutral condition was measured and this subtracted from the distance from the nose to the point at which the buoyancy acts gives

d_1 in Figure 4.

The buoyancy was evaluated by subtracting the measured drag from the weight of the vehicle in air. This value was checked by evaluating the displacement of the vehicle geometrically and multiplying by the density of water; no discrepancies were found. The distance d_1 multiplied by the sine of the vehicle angle of attack δ gives the moment arm of the buoyant force about the center of gravity.

At neutral stability

$$|M_{CG}| = Bd_1 \sin \delta = DX_{Cp} \sin \delta \tag{3}$$

or, using the small angle approximation

$$M_{CG} = Bd_1 \delta \tag{4}$$

Where B is the buoyancy force, D the drag force, and δ is in radians.

A quantity of interest is the rate of change of moment with respect to angle of attack.

$$\frac{dM_{CG}}{d\delta} = Bd_1 \tag{5}$$

This is put in nondimensional form by using the moment coefficient which is defined by

$$C_{m\delta} = \frac{dM/d\delta}{\frac{1}{2}\rho V^2 A_v L} = \frac{Bd_1}{\frac{1}{2}\rho V^2 A_v L} \tag{6}$$

where L is the overall length of the vehicle.

Thus by adjusting the center of gravity of the vehicle until the neutral condition was obtained ($\Sigma M_{CG} = 0$, no wobble) and by measuring the buoyancy and speed it was possible to determine the longitudinal static stability derivative.

Results

The drag and moment coefficients for all tests performed are presented in Table 1 and Table 2. Figures 5 and 6 illustrate the drag coefficients for the nine vehicles tested as a function of vehicle length to diameter ratio and blockage ratio. The drag

Table 1

Drag Coefficients

α	L/D	V ft/sec	D_V in.	D oz.	C_D	R_e x 10^{-4}
.306	15	3.275	1.66	4.25	1.71	4.53
.306	15	2.82	1.66	3.5	1.90	3.9
.306	15	1.6	1.66	1.2	2.02	2.21
.306	15	2.78	1.66	3.5	1.95	3.84
.404	15	3.39	1.9	9.5	2.89	5.36
.404	15	2.32	1.9	5	3.04	3.67
.404	15	1.05	1.9	1	2.99	1.66
.404	15	2.32	1.9	5.2	3.16	3.67
.404	15	1.26	1.9	1.5	3.12	1.995
.404	15	2.27	1.9	4.75	3.03	3.59
.625	15	.98	2.375	6.25	13.7	1.94
.625	15	1.515	2.375	13.25	12.2	3.0
.625	15	1.96	2.375	22	12.1	3.88
.625	15	2.78	2.375	42	11.5	5.5

Table 2

Moment Coefficients and Drag Coefficients

α	L/D	L in.	X_{CG} in.	δ_{CB} in.	X_{CB} in.	d_1 in.	W oz.	D oz.	B oz.	$C_{m\delta}$	V ft/sec	D_v in.	R_e x 10^{-4}	$C_{m\delta}$ corr	C_D	C_D corr
.306	10	16.5	7.45	.477	8.73	1.28	28	8.5	19.5	.260	5.0	1.66	6.91	.284	1.46	1.6
.306	15	24.8	11.5	.476	12.88	1.38	34	4.5	29.5	1.76	3.28	1.66	4.54	.670	1.80	1.84
.306	20	33.6	14.25	.478	17.28	3.03	46	5	41.0	1.76	3.0	1.66	4.15	1.77	2.39	2.41
.404	10	18.8	8.6	.54	9.94	1.34	39	9.5	29.5	.490	3.75	1.9	5.94	.523	2.22	2.37
.404	15	27.95	13.25	.546	14.52	1.27	46	2	44.0	2.44	1.64	1.9	2.60	2.27	2.87	2.65
.404	20	40.1	16.0	.549	20.60	4.6	72	8	64.0	3.49	2.63	1.9	4.16	3.51	3.8	3.83
.625	10	23.6	11.25	.678	12.48	1.23	68	10.5	57.5	2.89	1.48	2.375	2.93	2.74	10.15	9.59
.625	15	35.35	12.85	.685	18.36	5.51	116	30	96.0	5.32	2.3	2.375	4.55	5.42	11.9	12.1
.625	20	48.0	21.95	.684	24.68	2.73	176	56	120.0	7.04	1.43	2.375	2.83	6.05	57.5	54.3

results from this study are compared with those obtained by Gouse (4) in Figure 5. Figure 7 presents the drag coefficients versus Reynolds number for the three vehicle diameters with an L/D_v of fifteen. These test results are from a series of drops with various vehicle weights, i.e., different drag forces for the same vehicle.

Figures 8 and 9 illustrate the moment coefficient results for the nine vehicles tested. The results are presented as the derivative of moment with respect to angle of attack versus vehicle length to diameter ratio and blockage ratio. Figure 10 shows a comparison of the measured moment coefficient with the theoretical inviscid results for straight constant area vehicles and for ellipsoidal vehicles.

Discussion of Results

Drag

Gouse et al. (3) present experimentally determined drag coefficient for vehicles of the same shape as used in the present study. Hoppe and Gouse (4) present slightly different drag data accompanied by a theoretical prediction using tube wall and vehicle wall friction factors. They present their data in terms of C_D, drag coefficient, versus L/D_v, vehicle length to diameter ratio, and a parameter β, the ratio of guideway tube diameter to vehicle diameter, i.e., $\beta = D_T/D_v$ where D_T is the tube diameter and D_v the vehicle diameter.

It is stated in reference (4) that the drag coefficient is proportional to the Reynolds number to the minus one-sixth power. Data from the present study shows this dependence to be valid (Figure 9). Hence, to give a consistent set of results, the drag coefficients were normalized to $R_e = 4 \times 10^4$ by using the minus one-sixth power rule. The data from (4) is for polished vehicles at a Reynolds number of approximately 1×10^5. Although the vehicles of this study were not polished and the Reynolds number was slightly different, the results here agree quite well with those of Gouse (4).

Moment Coefficient

Figures 8 and 9 represent the principal results of this investigation, in terms of the longitudinal static stability derivatives for the nine vehicles. Not all of the trends were expected from previous theoretical (inviscid) calculations, but they are believed to be valid. As the forces affecting stability are similar to those affecting drag, a similar correction for Reynolds number variation was used; that is, the stability derivatives data were adjusted to represent a Reynolds number of 4×10^4 by ratioing the Reynolds number raised to the minus one-sixth power. This correction was never large since all of the vehicles were tested at Reynolds numbers close to 4×10^4. It can be seen from Table 2 and Figures 8 and 9 that the confinement of a vehicle within a tube, $\alpha \neq 0$, does indeed increase the instability of the vehicle and further, that the length of the vehicle affects the stability. That is, vehicles which occupy a larger portion of the guideway tube or long vehicles tend to be less stable, i.e., have larger values of $C_{m\delta}$.

Goodman (5) performed a theoretical analysis of the stability problem using incompressible potential (inviscid) flow theory. The problem at hand is clearly very much a viscous problem. Using potential flow theory with a system of sources and sinks, Goodman solved the inviscid, small perturbation problem by using cross-flow potentials to obtain the flow field for small vehicle oscillations. Using this flow field, he was able to evaluate the pressure coefficient at the body surface and to evaluate the angle of attack derivative of the moment coefficient for the body. The results, in integral form, are

$$\frac{\partial}{\partial \delta}\frac{M}{q} = \frac{-2}{S_R}\int_0^L \frac{(x-a)^2(1+\alpha)\ S_o{}^2\ dx}{(1-\alpha)^5}$$

$$- \frac{2}{3}\ S_R \int_0^L \frac{(3-3\alpha\ +\ 2\alpha^2)dx}{(1-\alpha)^3}$$

where L is vehicle length, $\alpha = \alpha(x)$ is the ratio of vehicle cross sectional area to tube cross sectional area, S_R is the area of

the guideway tube, $S_o = \frac{dS_o}{dx}$ is the derivative of vehicle area with respect to vehicle center line distance, and dx is the incremental center line distance. When evaluated for an ellipsoid of revolution these give what appears to be reasonable results. With Lehman (6), Gouse has experimentally repeated these findings for an ellipsoid of revolution using a stationary vehicle in a water tunnel. When applied to the vehicle shape used in these tests the prediction is not very good. It should be noted that the moment coefficient blockage ratio dependence is essentially the same for both the theoretical and experimental results. Also, the experimental results agree more favorably with the theoretical predictions as the vehicle length to diameter ratio is increased.

Conclusions

The drag coefficients have been defined experimentally at a Reynolds number of 4×10^4 for a series of nine vehicles traveling within a guide tube. These compare well with other published results.

The longitudinal static stability derivatives for the nine vehicles have been experimentally determined at a Reynolds number of 4×10^4. These were determined with the proper boundary conditions (vehicle moving in the tube) and with a viscid but incompressible fluid. Goodman's theory using either an ellipsoid of revolution or a constant area vehicle gives moment coefficient values higher than measured, although the trends are similar.

It is seen that for higher values of blockage ratio the drag and stability values are quite different from free stream values (no confinement in a tube). Both the drag coefficient and the moment coefficient increase with blockage ratio and vehicle length to diameter ratio.

The unstable moment, while increasing with vehicle length and blockage ratio, is not extremely high. Rear fins should solve the stability problem for tubed vehicles.

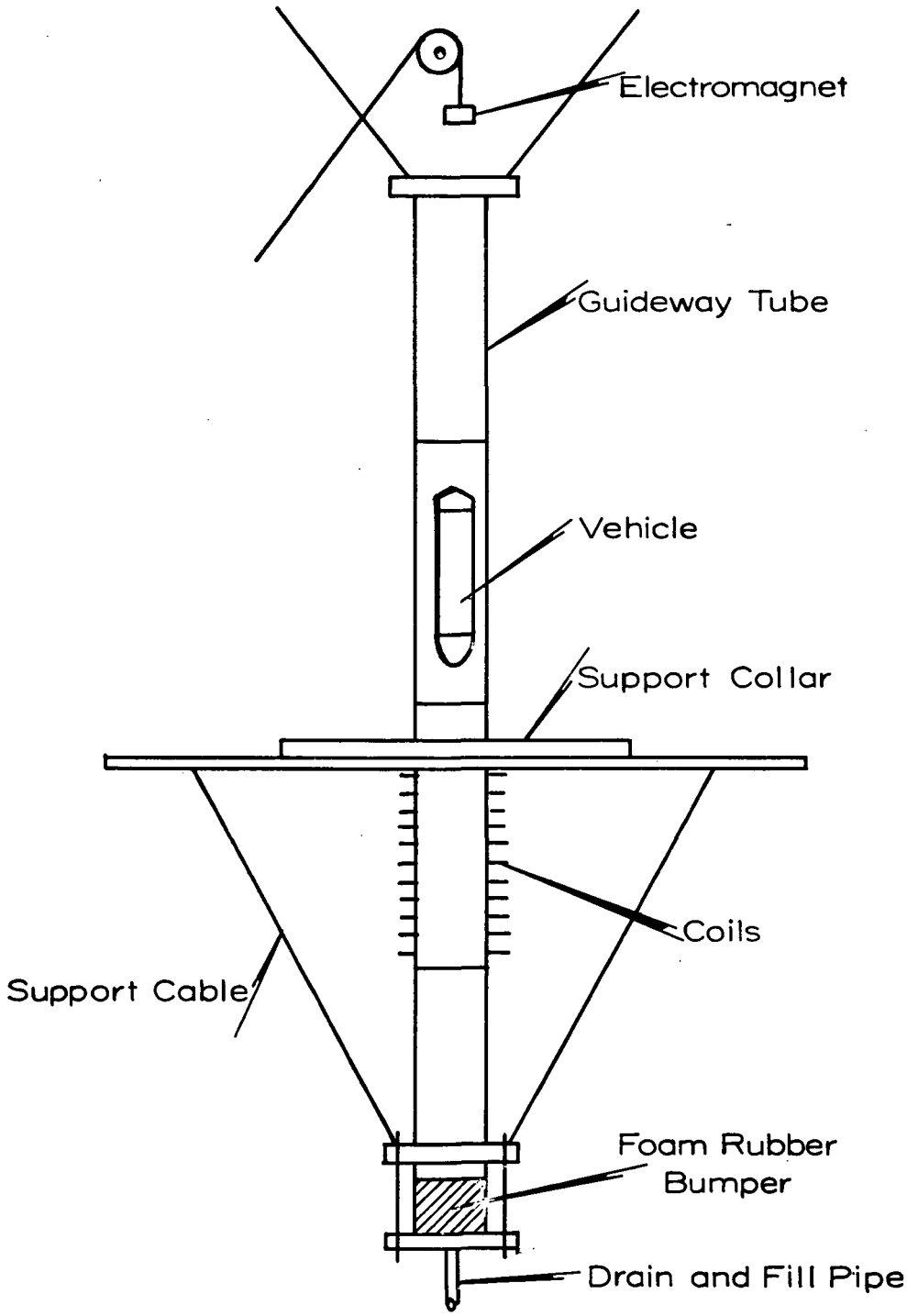

Figure 1. Guideway System.

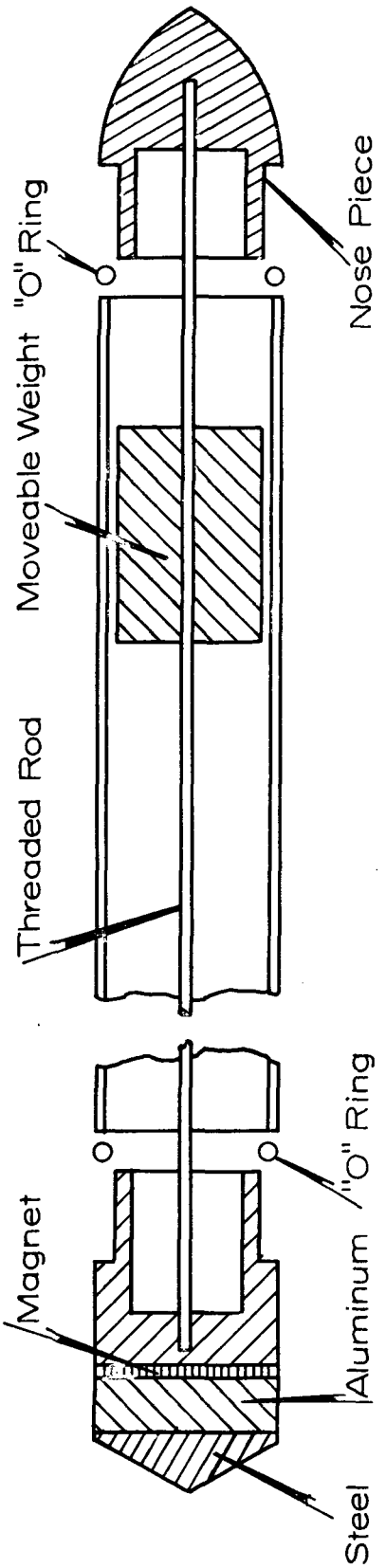

Figure 2. Construction of Vehicles.

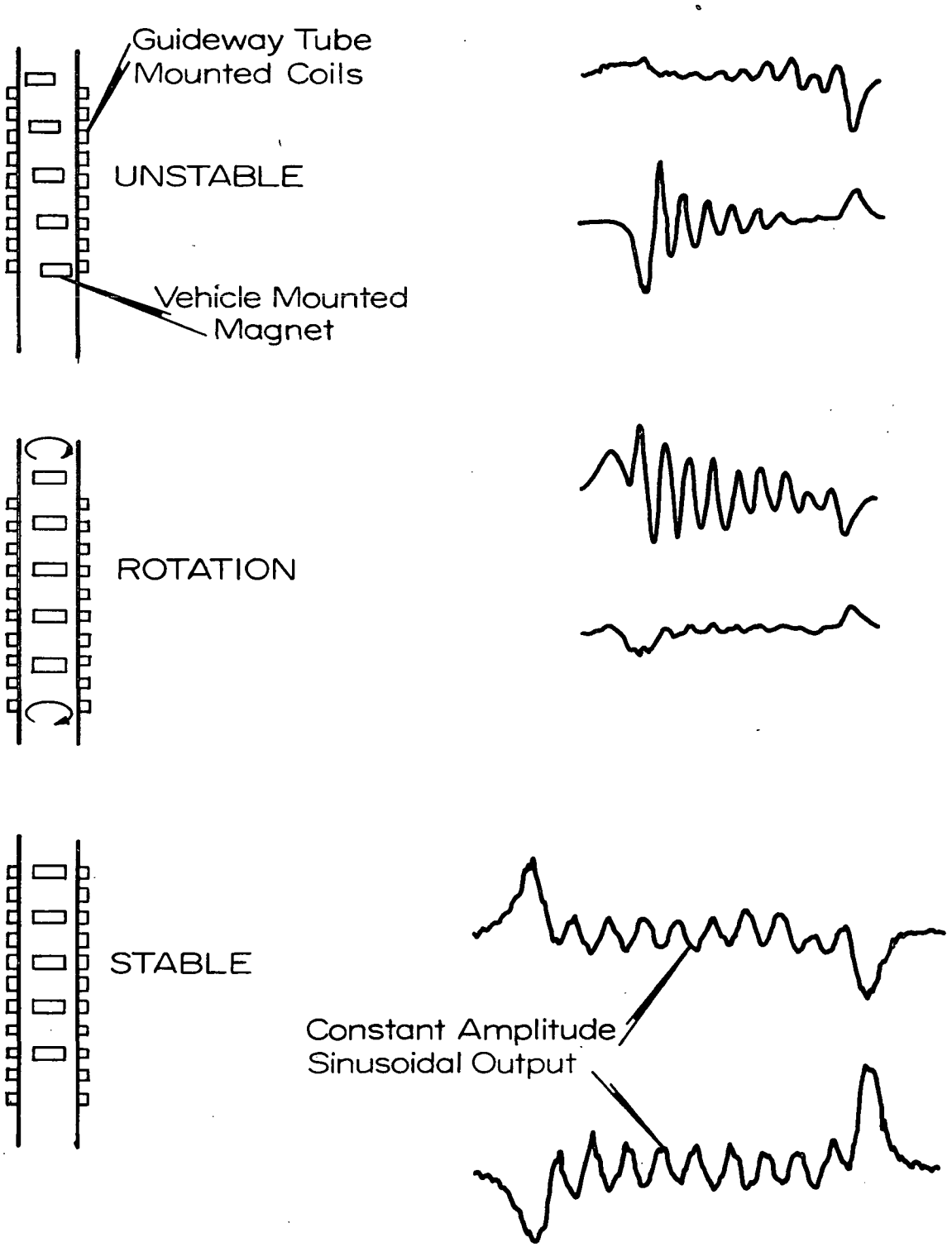

Figure 3. Strip Chart Comparison.

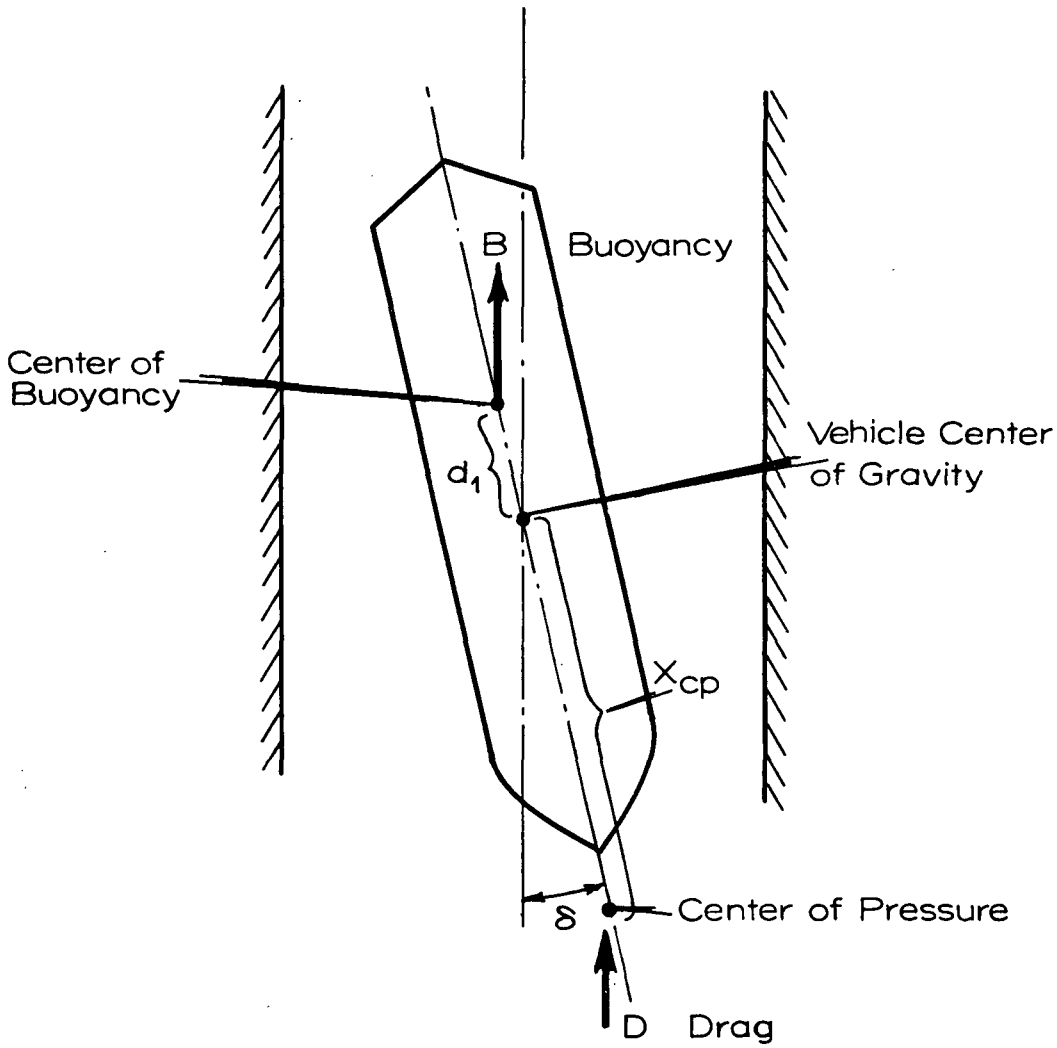

Figure 4. Illustrating the Location of the Center of Buoyancy and Center of Pressure.

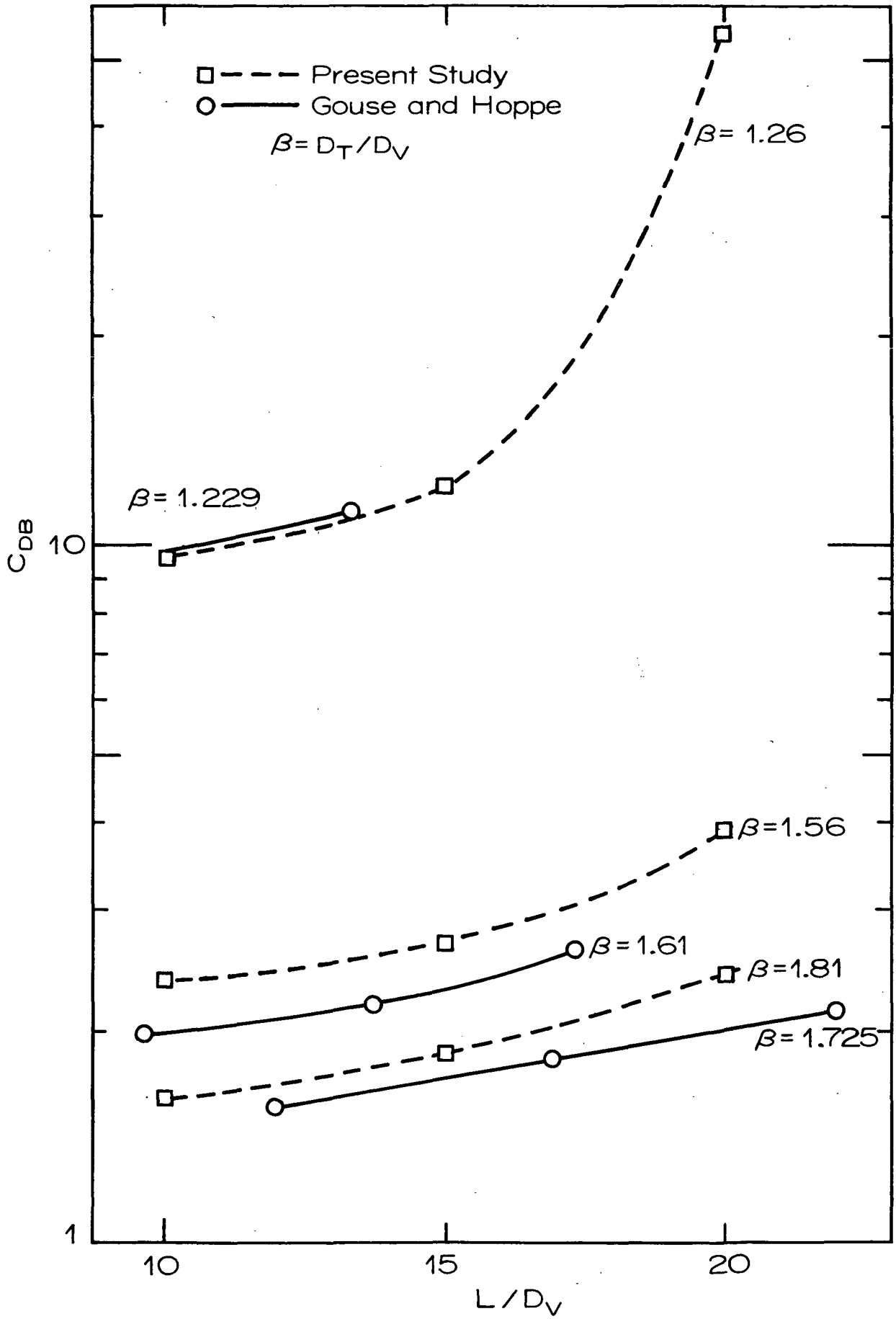

Figure 5. Drag Coefficient vs L/D_V.

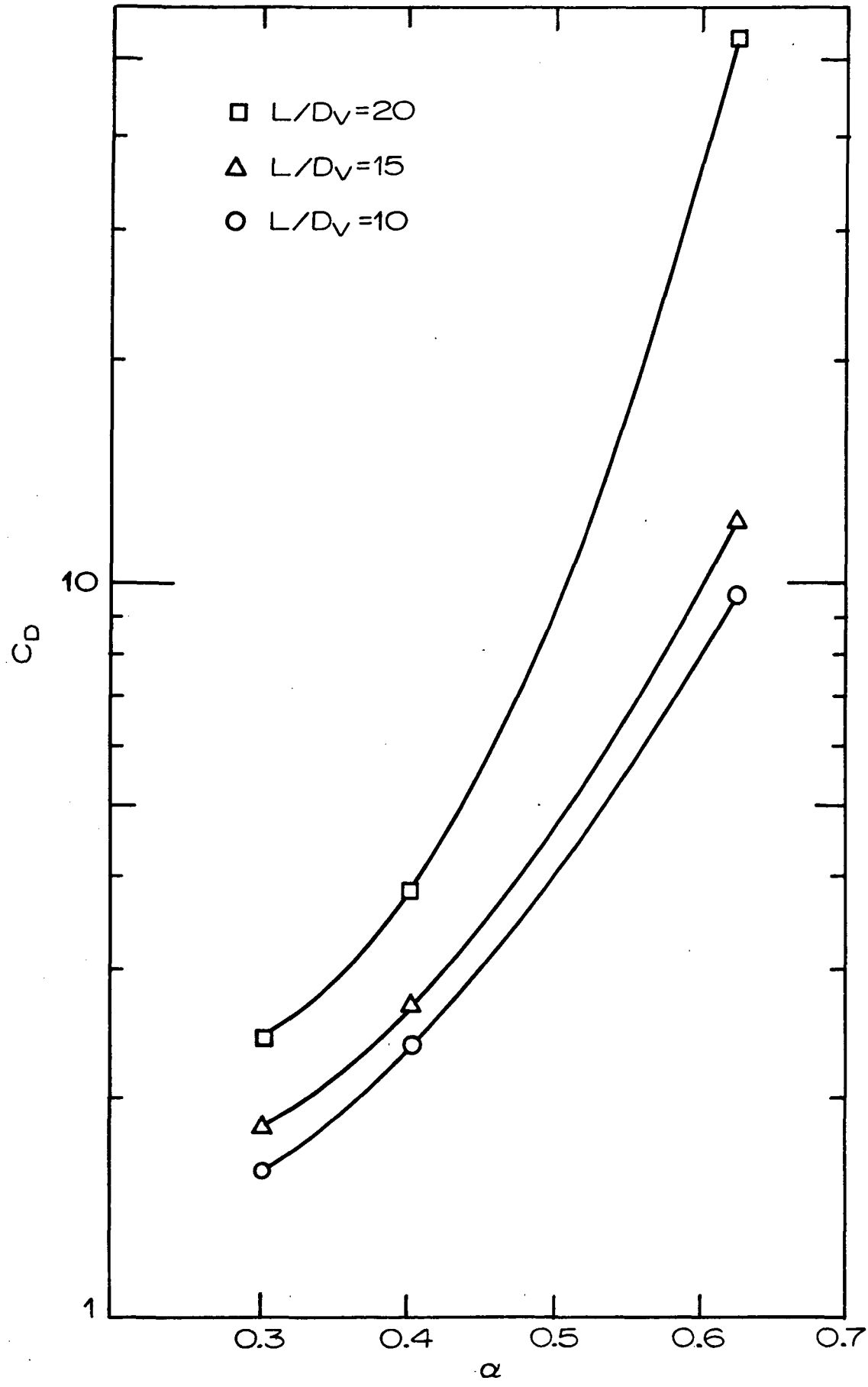

Figure 6. Drag Coefficient vs α.

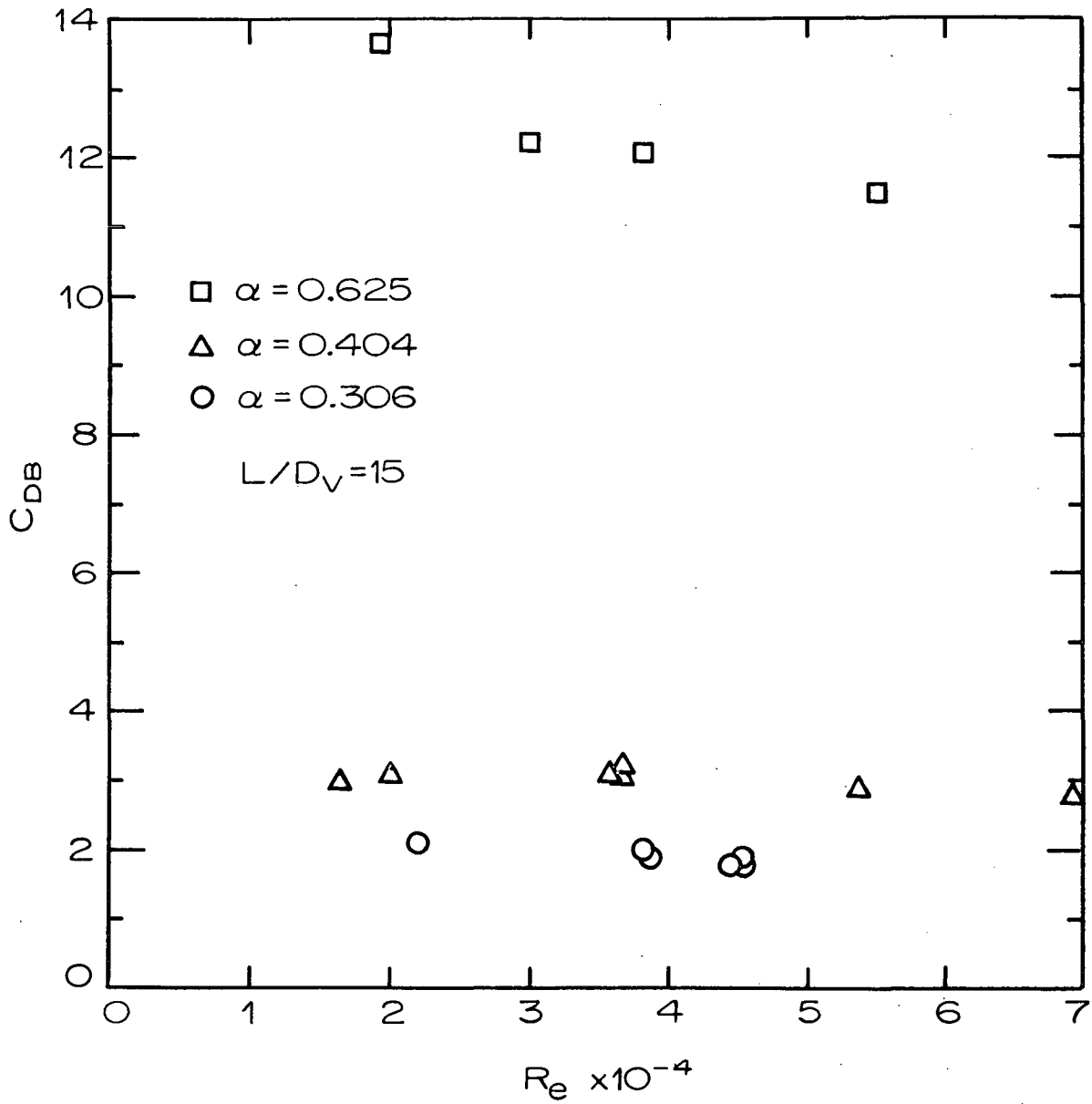

Figure 7. Drag Coefficient vs R_e.

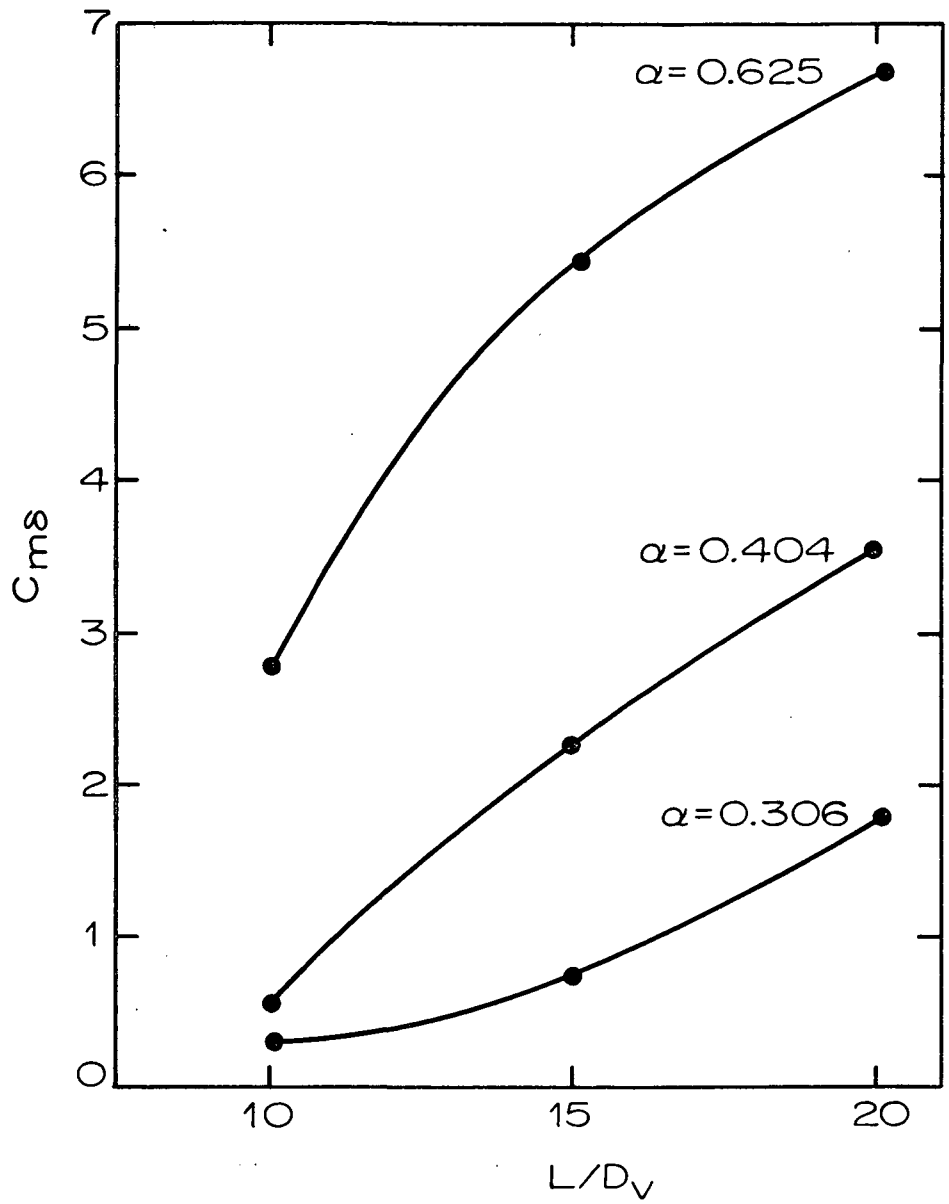

Figure 8. $C_{m\delta}$ vs L/D_v.

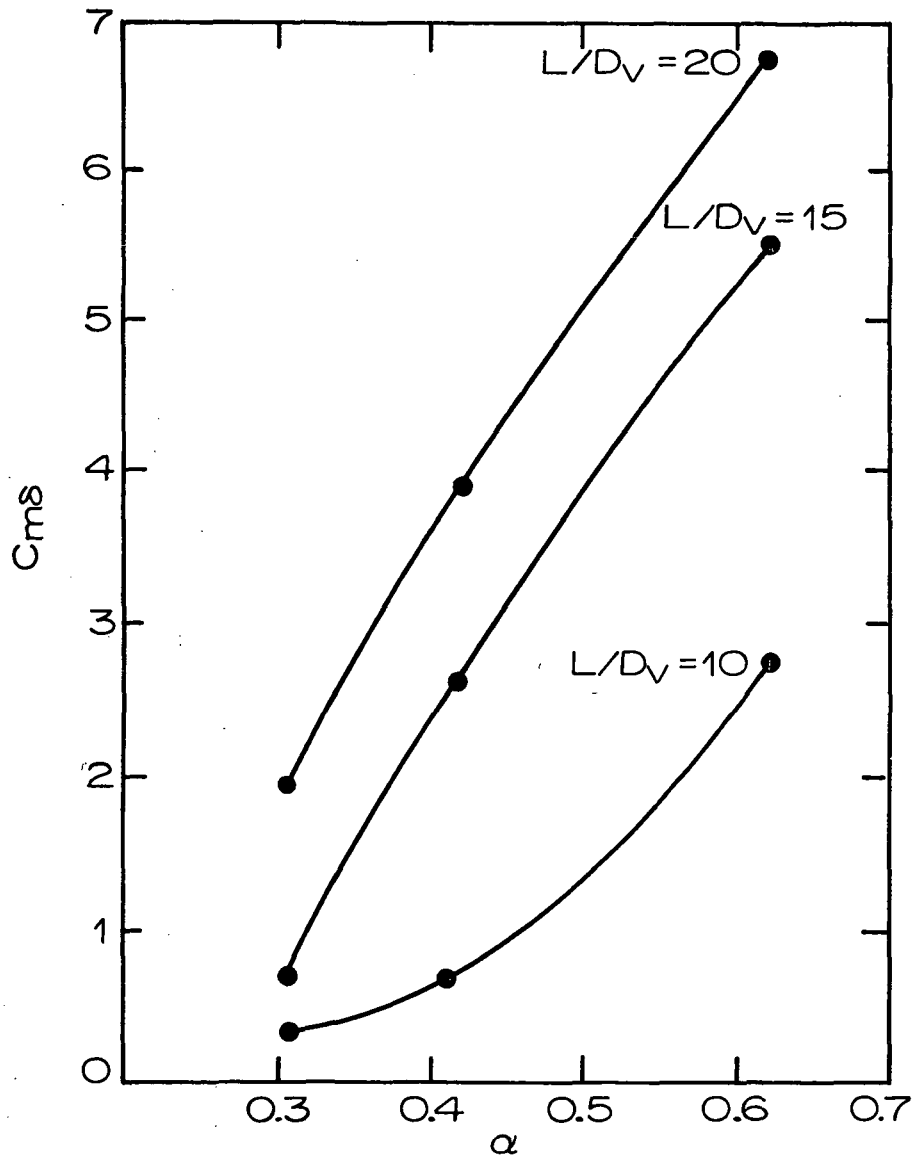

Figure 9. C_{m_δ} vs α.

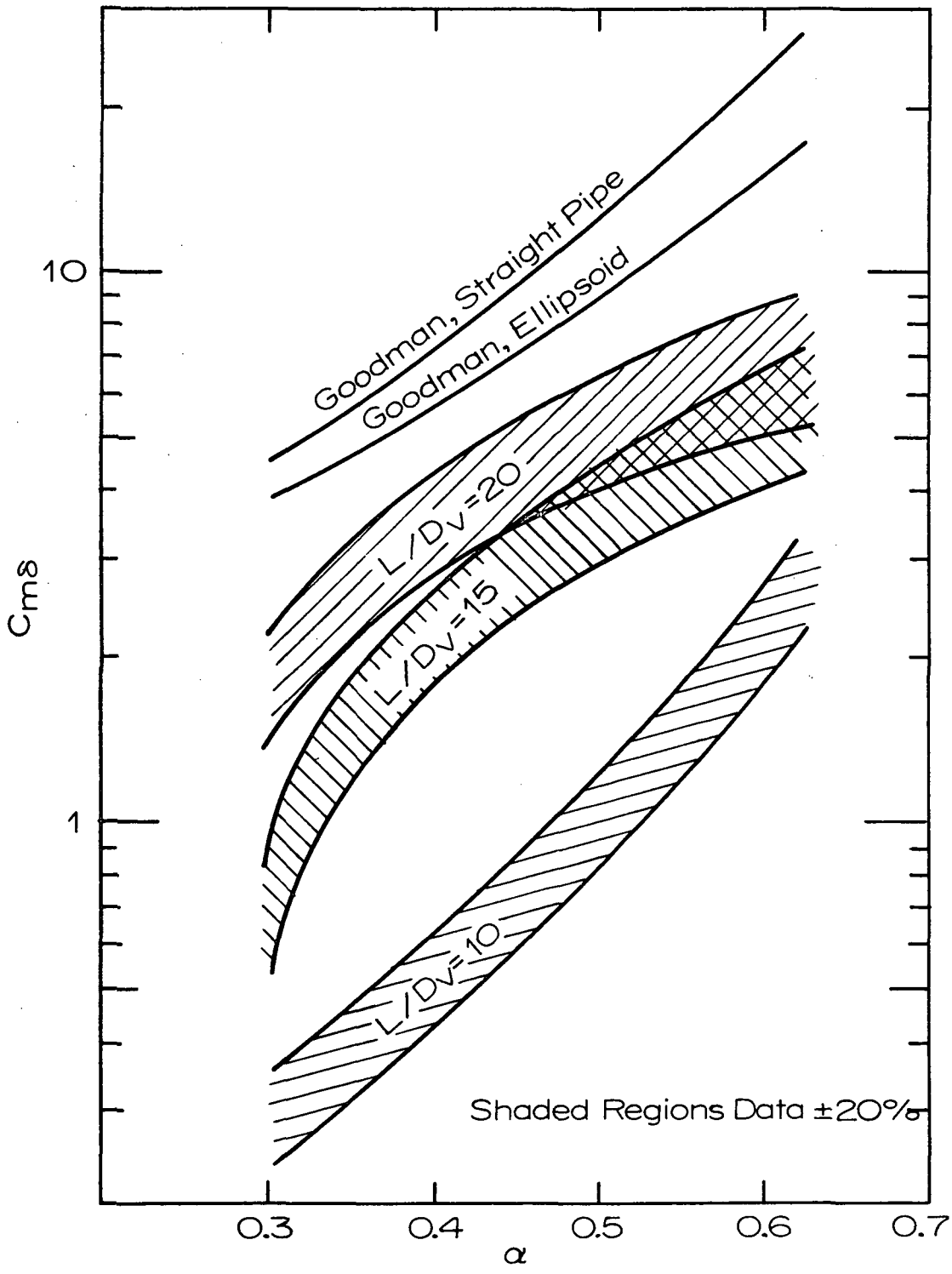

Figure 10. Graph Comparing C_{m_δ} Data and Predictions.

List of References

1. Foa, J. V., et al., "Project Tubeflight-Phase I, Feasibility Study," R. P. I., Troy, N. Y., Sept. 1966.

2. Gouse, S. W., Jr., and Swarden, M., "Universal Drag Law," MIT, EPL, Cambridge, Mass., Dec. 1966, PB 173 C47.

3. Gouse, S. W., Jr., Noyes, B. S., and Swarden, M., "Aerodynamic Drag on a Body Traveling in a Tube," MIT, EPL, Cambridge, Mass., Oct. 1967, PB 177 211.

4. Hoppe, R. G., and Gouse, S. W., Jr., "Fluid Dynamic Drag on Vehicles Traveling Through Tubes," Carnegie-Mellon University, Pittsburgh, Penn., August 1969.

5. Cudlin, J. J., Harman, C. M., and Murray, J. J., "Numerical Analog for a Model Vacuum-Air Transport System," U. S. Army Research Office-Durham, Durham, N. C., Jan. 1970.

6. Goodman, T. R., "The Aerodynamic Characteristics of a Slender Body Travelling in a Tube," Oceanics, Inc., Plainview, N. Y., January 1967, PB 173-997.

7. Goodman, T. R., and Lehman, A. F., "Static Aerodynamic Force Measurements of Bodies in Tubes," Oceanics, Inc., Plainview, N. Y., April 1968, PB 177-671.

8. Goodman, T. R., "Effects of Compressibility and the Resistance of Slender Cylinders Travelling in a Tube," Oceanics, Inc., Plainview, N. Y., November 1967, PB 176-204.

A DYNAMIC MODELING METHOD OF UNSTEADY FLOWS IN FLUID LINES WITH LARGE BIAS VELOCITIES

Donald Wright and O. L. Mercier
Department of Mechanical Engineering, Duke University

Introduction

Fluid line dynamics has been a subject of intense interest to control engineers for over a decade. A useful model for a fluid line would be a transfer function matrix relating dynamic behavior at end points, without considering flow phenomena at all points along the tube.

Finite difference techniques and methods of characteristics are common tools for dealing with the highly nonlinear fluid flow equations. These procedures yield numerical or graphical solutions to specific problems, but do not result in an analytic model relating end conditions.

The majority of published research, [1 to 8][1], has been concerned with the dynamic response of fluid lines with negligible (or small) bias-velocity, laminar flows. A notable exception by F. T. Brown [9] deals with the acoustic frequency response of fluid lines with turbulent flow.

The purpose of this paper is to present a direct, analytical method of integrating the equations of unsteady gas flow in a circular tube with non-negligible bulk flow velocity. The nonlinear character of the flow equations is overcome by judicious choice of integrating variables and by subsequent linearization. The method yields a transfer function matrix of the fluid line. The solution or simulation of the result is beyond the scope of this paper, but O. Mercier [10] has incorporated the transmission matrix in a model describing the behavior of a semi-passive vehicle operating in a partially evacuated circular tube. The pneumatic tube concept is under preliminary study as a high speed ground transportation application.

[1] Numbers in square brackets refer to references at end of paper.

Assumptions and Basic Unsteady-Flow Equations

The following assumptions are made to simplify the mathematical formulation of a viscous, compressible fluid flow through a long, circular tube:

1. The flow field is turbulent, fully developed with slowly varying bulk flow velocity. Consequently, end conditions are also slowly varying.
2. The flow is one-dimensional, adiabatic, and behaves according to the perfect-gas law with constant specific heats.
3. The tube friction factor is constant.
4. The flow is shock free.
5. The tube is circular, constant area, and horizontal.

Four basic equations describe this flow. Written for an infinitesimal control volume of length dx, they are:

Continuity Equation

$$\frac{\partial}{\partial x}(\rho VA)dx + \frac{\partial}{\partial t}(\rho A dx) = 0 \tag{1}$$

Momentum Equation

$$\frac{\partial}{\partial x}(PAdx) + \frac{\partial}{\partial x}(\tau_{xx}Adx) + \frac{\partial}{\partial x}(\rho AV^2dx) + \frac{\partial}{\partial t}(\rho VAdx) = 0 \tag{2}$$

Energy Equation

$$\frac{\partial}{\partial x}\left[\rho VAdx\left(u + \frac{P}{\rho} + \frac{V^2}{2}\right)\right] + \frac{\partial}{\partial t}\left[\rho Adx\left(u + \frac{V^2}{2}\right)\right] = 0 \tag{3}$$

Perfect Gas Law

$$P = R\,\rho\,T.$$

The normal viscous stress, τ_{xx}, can be related to the wall shearing stress, τ_w, by

$$\tau_{xx} = \tau_w \frac{RDdx}{A}$$

and

$$\tau_w = f\frac{\rho V^2}{2}$$

where f is the Fanning friction factor. Noting that $\partial A/\partial x = 0$ and applying the perfect-gas law, with $R = C_p - C_v$ and $k = C_p/C_v$,

Equations (1), (2) and (3) reduce to

$$\frac{\partial}{\partial x}(\rho V) + \frac{\partial \rho}{\partial t} = 0 \tag{4}$$

$$\frac{\partial P}{\partial x} + \frac{\partial}{\partial x}(\rho V^2) + \frac{\partial}{\partial t}(\rho V) + \frac{2f}{D}\rho V^2 = 0 \tag{5}$$

$$c_p \frac{\partial}{\partial x}(\rho V T) + \frac{1}{2}\frac{\partial}{\partial x}(\rho V^3) + \frac{1}{k-1}\frac{\partial P}{\partial t} + \frac{1}{2}\frac{\partial}{\partial t}(\rho V^2) = 0. \tag{6}$$

Equations (4), (5) and (6) and the perfect-gas law equation constitute complete information about the considered fluid line. These equations involve multiple products of variables and are consequently strongly nonlinear. The main goal of this paper is to demonstrate how, by proper choice of new variables, these equations can be matrically integrated.

The choice of integrating variables makes possible the separation of position and time derivatives, and allows linearization which leads to a matrix form of the differential equations. The choice also facilitates the linearization of some residual nonlinear coefficients about a desired mean quantity (the time averaged bulk flow velocity, previously assumed to be slowly changing). The final result is a matrix differential equation, with constant coefficients.

Choice of Integrating Variables

In the case of a uniform one-dimensional distributed system, F. T. Brown [11] has shown how the dynamic equations can be reduced by selecting variables in pairs; the number of pairs being equal to the number of types of transmitted powers. Within a pair, one of the variables is symmetrical, such as a pressure or a voltage, and the other is asymmetrical, such as a volume flow rate or an electric current. The requirement is that power or its time integral, or derivative, is proportional to the product of the two variables.

In the case of a non-uniform system, as in the present problem, the non-negligible bias velocity makes the choice of variables far less straightforward. Many combinations of variables must be considered and tested until a reduced form of the basic equa-

tions is obtained, allowing satisfactory linearization. Two variables of a given pair can no longer be required to have their product proportional to a power and the resulting matrix should not necessarily be symmetric. Simplicity of this matrix and ultimate convenience in the evaluation of its exponential are the only criteria to be considered in testing a candidate set of integrating variables. Although a more systematic approach would be highly desirable, patience and luck are still factors of importance for a successful variable search.

Reduction to a Linear Form

Continuity Equation. Substitution of the Perfect Gas Law into Equation (4) yields

$$\frac{\partial \dot{m}}{\partial x} + \frac{A}{RT}\frac{\partial P}{\partial t} - \frac{A\rho}{T}\frac{\partial T}{\partial t} = 0. \tag{7}$$

The term $\partial T/\partial t$ could be expanded in terms of $\partial \dot{m}/\partial t$ and $\partial H_f/\partial t$ but would increase the nonlinearity of the equation. However, for a slowly varying bulk flow velocity, preventing massive local flow accelerations,

$$R\rho\frac{\partial T}{\partial t} << \frac{\partial P}{\partial t} \tag{8}$$

Justification of this approximation is given elsewhere [10]. The approximation applies to non-negligible bulk flows, and situations of very small bias velocities must be treated by other available methods [3,5,7,8]. Applying Equation (8), the continuity equation becomes

$$\frac{\partial m}{\partial x} + \frac{A}{RT}\frac{\partial P}{\partial t} = 0. \tag{9}$$

Momentum Equation. Expressing ρV^2 in terms of P and F, Equation (5) becomes

$$\frac{\partial F}{\partial x} + \frac{\partial \dot{m}}{\partial t} + \frac{2f}{D}F - \frac{2fA}{D}P = 0. \tag{10}$$

Energy Equation. Expansion of the residual nonlinear term ρV^3 gives

$$d(\rho V^3) = d\frac{(\rho V^2)^2}{\rho V} = \frac{2V}{A}dF - 2VdP - \frac{V^2}{A}d\dot{m},$$

and substitution of the 4 integrating variables in Equation (6) then yields the new form

$$\frac{1}{A}\frac{\partial H_f}{\partial x} + \frac{V}{A}\frac{\partial F}{\partial x} - V\frac{\partial P}{\partial x} - \frac{V^2}{2A}\frac{\partial \dot{m}}{\partial x} + \frac{3-k}{2(k-1)}\frac{\partial P}{\partial t} + \frac{1}{2A}\frac{\partial F}{\partial t} = 0 \qquad (11)$$

The Perfect-Gas Law equation can also be written as a partial differential equation in x.

$$dP = R\,d(\rho T) = R\,d\frac{(\rho VT)(\rho V)}{\rho V^2} = \frac{RT}{AV}d\dot{m} + \frac{R}{AC_pV}dH_f - \frac{RT}{AV^2}dF + \frac{RT}{V^2}dP,$$

or
$$(1 - \frac{RT}{V^2})\frac{\partial P}{\partial x} - \frac{RT}{AV}\frac{\partial \dot{m}}{\partial x} + \frac{RT}{AV^2}\frac{\partial F}{\partial x} - \frac{R}{AC_pV}\frac{\partial H_f}{\partial x} = 0. \qquad (12)$$

The four basic equations, expressed in (9), (10), (11) and (12) in terms of P, m, F and H_f and their derivatives are expressed in terms of $\partial P/\partial x$, $\partial \dot{m}/\partial x$, $\partial F/\partial x$ and $\partial H_f/\partial x$. The following matrix equation is obtained:

$$\begin{bmatrix} \frac{\partial P}{\partial x} \\ \frac{\partial F}{\partial x} \\ \frac{\partial \dot{m}}{\partial x} \\ \frac{\partial H_f}{\partial x} \end{bmatrix} = \begin{bmatrix} C_1 & -C_2 & 0 & 0 \\ C_3 & -C_4 & 0 & 0 \\ 0 & 0 & 0 & 0 \\ C_5 & -C_6 & 0 & 0 \end{bmatrix} \begin{bmatrix} P \\ F \\ \dot{m} \\ H_f \end{bmatrix} + \begin{bmatrix} T_1 & T_2 & -T_3 & 0 \\ 0 & 0 & -1 & 0 \\ -T_4 & 0 & 0 & 0 \\ -T_5 & -T_6 & -T_7 & 0 \end{bmatrix} \begin{bmatrix} \frac{\partial P}{\partial t} \\ \frac{\partial F}{\partial t} \\ \frac{\partial \dot{m}}{\partial t} \\ \frac{\partial H_f}{\partial t} \end{bmatrix} \qquad (13)$$

where
$$C_1 = \lambda\frac{1 + (k-1)M^2}{1-M^2} \qquad C_4 = \lambda$$

$$C_2 = \frac{C_1}{A} \qquad C_5 = \frac{\lambda AV^3}{RT(1-M^2)}$$

$$C_3 = \lambda A \qquad C_6 = \frac{C_5}{A}.$$

Also,

$$T_1 = \frac{V}{2kRT}\,\frac{k+3+(k-1)kM^2}{1-M^2} \qquad T_5 = \frac{A(k-1)}{2}\,\frac{3-k-2kM^2-(k-1)k^2M^4}{1-M^2}$$

$$T_2 = \frac{(k-1)V}{2AkRT(1-M^2)} \qquad T_6 = \frac{1-kM^2}{1-M^2}$$

$$T_3 = \frac{1}{A}\,\frac{1+(k-1)M^2}{1-M^2} \qquad T_7 = \frac{V^3}{RT(1-M^2)},$$

$$T_4 = \frac{A}{RT}$$

where $M = \dfrac{V}{\sqrt{kRT}}$ = local Mach Number

and $\lambda = \dfrac{2f}{D}$.

Inspection of Equation (13) reveals that $\partial P/\partial x$, $\partial F/\partial x$ and $\partial \dot{m}/\partial x$ are independent of $\partial H_f/\partial x$. H_f can therefore be deleted as an integrating variable with no loss of information. This reduction of the order of the matrix differential equation was made possible by the earlier approximation, Equation (8), in the continuity equation.

Defining a 3-dimensional vector $\underline{z}(x,t)$,

$$\underline{z}(x,t) = \begin{bmatrix} P(x,t) \\ F(x,t) \\ \dot{m}(x,t) \end{bmatrix}, \tag{14}$$

and introducing the linear time-derivative operator $D \equiv \partial/\partial t$, Equation (13) can be rewritten

$$\frac{\partial}{\partial x}\,\underline{z}(x,t) = [R]\,\underline{z}(x,t) \tag{15}$$

with $$[R] = \begin{bmatrix} C_1+T_1D & -C_2+T_2D & -T_3D \\ C_3 & -C_4 & -D \\ -T_4D & 0 & 0 \end{bmatrix}.$$

Some of the elements of the matrix [R] are not constant but, rather, are functions of the local velocity and temperature. Peano-

Baker's method of integration (see Pipes [12]) would provide a means to integrate the matrix differential equation (15) with variable coefficients but its implementation involves series expansion and, thus, is essentially numerical. It is, consequently, highly desirable to consider the matrix [R] as a constant by evaluating the varying terms about their time-averaged mean value and solve as a differential equation with constant coefficients.

Simple evaluation of the coefficients about the time-averaged bulk flow velocity, V_m, and mean temperature[2], T_m, gives a matrix of constant coefficients. Notationally,

$$[R_m] = [R]_{\substack{T \longrightarrow T_m \\ V \longrightarrow V_m,}}$$

and

$$\frac{\partial}{\partial x} \underline{z}(x,t) = [R_m]\, \underline{z}(x,t) \qquad (16)$$

The coefficients of this 3 x 3 matrix have been previously defined in (13). The position- and time-derivatives are completely separated in Equation (16) and, considering D as an independent operator, the differential equation (16) can be considered as an ordinary differential equation and integrated with respect to x (see, for instance, Pipes [12] for justification of this procedure of operational calculus).

Integration of the Fluid Line Equations

The solution of Equation (16) is straightforward and, in general, is given by

$$\underline{z}(x,t) = [G(x-x_o,D)]\, \underline{z}(x_o,t)$$

with

$$[G(x-x_o,D)] = e^{[R_m](x-x_o)}.$$

[2] For a slowly varying bulk flow, free of massive local pressure disturbances, the relative variation of absolute temperature is extremely small.

Integrating Equation (16) from $x_o = 0$ to $x = \ell$, the solution matrix $[G(\ell,D)]$ represents the transmission matrix of a length of tube ℓ (i.e., a linear dynamic model of the frictional adiabatic gas flow in the tube, expressing analytically the relationship between the vectors $\underline{z}$ at both ends). The transmission matrix $[G(\ell,D)]$ can be calculated directly by means of the inverse Laplace transformation in the x-domain.

$$[G(\ell,D)] = e^{[R_m]\ell} = \mathcal{L}^{-1}\{[sI-R_m]^{-1}\}, \tag{17}$$

where s is the Laplace operator in the x-domain and I is the identity matrix.

The inverse matrix $[sI-R_m]^{-1}$ is readily obtained as

$$[G(s,D)] = [sI-R_m]^{-1} = \begin{bmatrix} G_{11}(s) & G_{12}(s) & G_{13}(s) \\ G_{21}(s) & G_{22}(s) & G_{23}(s) \\ G_{31}(s) & G_{32}(s) & G_{33}(s) \end{bmatrix} \tag{18a}$$

or, in expanded form,

$$[sI-R_m]^{-1} = \frac{1}{|sI-R_m|} \begin{bmatrix} s(s+C_4) & s(T_2D-C_2) & -T_3Ds-T_2D^2 \\ C_3s+T_4D^2 & s^2-(C_1+T_1D)s-T_3T_4D^2 & -Ds+T_1D^2 \\ -T_4D(s+C_4) & C_2T_4D-T_2T_4D^2 & \begin{matrix} s^2+(C_4-C_1-T_1D)s + \\ -(C_4T_1D+C_3T_2D) \end{matrix} \end{bmatrix} \tag{18b}$$

with $$|sI-R_m| = s^3 + (C_4-C_1-T_1D)s^2 -$$

$$- (C_3T_2D - C_4T_1D + T_3T_4D^2)s - T_2T_4D^3. \tag{19}$$

Extraction of the roots of this determinant, which is also the characteristic polynomial of the matrix differential equation (16), is a necessary step before taking the inverse Laplace transform of each element of $[G(s,D)]$. Because of the presence of the independent operator D, this extraction is not simple and no exact

analytical solution, involving only polynomials in D, can be found to the equation $|sI-R| = 0$.

Information can be obtained, however, from the limiting condition of zero bulk flow velocity. Indeed, as V_m approaches zero, some coefficients of $[R_m]$ vanish and the determinant takes the reduced form

$$|sI-R| = s^3-T_3T_4D^2s = s(s+\sqrt{T_3T_4}D)(s-\sqrt{T_3T_4}D).$$

When V_m is no longer negligible, a similar form can be predicted for the roots of Equation (19) but with complementary terms proportional to V_m and functions of the operator D. A relatively simple factored expression of the determinant has been found to be

$$|sI-R| = (s+a+bD+cD)(s+a+bD-cD)(s+d+eD) \qquad (20)$$

where a, b, c, d and e are functions of the coefficients of $[R_m]$. This factorization approximates Equation (19) with an error on the term in s^o of order $V_mD^3/(RT_m)^2$, which is small relative magnitude. More elaborate factorization of the determinant does not significantly reduce the magnitude of the error, even though cumbersome functions of D would be added in the roots. The roots of the determinant $|sI-R|$ are taken to be

$$\begin{aligned} s_1 &= -a-bD-cD \\ s_2 &= -a-bD+cD \\ s_3 &= -d-eD. \end{aligned} \qquad (21)$$

The nine elements $G_{ij}(s)$ of $[G(s,D)]$, are ratios of polynomials in s; to take their inverse Laplace transform requires an expansion in partial fractions,

$$G_{ij}(s) = \frac{A_{ij}(D)}{s-s_1} + \frac{B_{ij}(D)}{s-s_2} + \frac{C_{ij}(D)}{s-s_3}$$

where $A_{ij}(D)$, $B_{ij}(D)$ and $C_{ij}(D)$ are ratios of polynomials in D. Space limitation precludes the enumeration of the polynomials, but their derivation is elementary, although tedious [10].

Each element $G_{ij}(\ell,D)$ of the transmission matrix is the

inverse Laplace transform of the corresponding element $G_{ij}(s,D)$ of $[G(s,D)]$, Equation (18):

$$G_{ij}(\ell,D) = A_{ij}(D)e^{s_1\ell} + B_{ij}(D)e^{s_2\ell} + C_{ij}(D)e^{s_3\ell}$$

where s_1, s_2 and s_3 are also polynomials in D and are given in Equation (21).

$$G_{ij}(\ell,D) = A_{ij}(D) \times e^{-a\ell} \times e^{-(b+c)\ell D} +$$

$$+ B_{ij}(D) \times e^{-a\ell} \times e^{-(b-c)\ell D} + C_{ij}(D) \times e^{-d\ell} \times e^{-e\ell D}.$$

D is the linear time derivative operator. It can now be replaced by the Laplace operator p, in the time-domain. The elements of the transmission matrix of the fluid line are then, written in operational form,

$$G_{ij}(\ell,p) = A_{ij}(p) \times e^{-a\ell} \times e^{-(b+c)\ell p} + B_{ij}(p) \times e^{-a\ell} \times e^{-(b-c)\ell p} +$$

$$+ C_{ij}(p) \times e^{-d\ell} \times e^{-e\ell p}, \text{ with } i, j = 1, 2, 3. \qquad (22)$$

A physical significance can be attached to the terms of Equation (22): the exponentials $e^{-a\ell}$ and $e^{-d\ell}$ are constants and represent an attenuation along the tube, proportional to its length ℓ; the exponentials in e^{-Tp} correspond in the time domain to pure time-delays of T seconds. The delays T are seen to be proportional to the length of tube; they also depend on the speed of propagation of a flow disturbance in the direction of the bulk flow and against it.

Reduction to a 2-dimensional model -

The transmission matrix $[G(\ell,p)]$ derived above is a 3-dimensional dynamic model of the gas flow through a length of tube ℓ and is associated with the vector

$$\underline{z} = \begin{bmatrix} P \\ F \\ \dot{m} \end{bmatrix}.$$

The 3 variables P, F, and $\dot{m}$ were necessary to avoid excessive

linearization of the flow equations before their integration. But once the transmission matrix obtained, it is advantageous to reduce the order of the model to 2-dimensional. According to end conditions, the variable F(o,t), especially, can be variously expressed in terms of P(o,t) and $\dot{m}$(o,t), for instance

$$F(o,t) \cong A\ P(o,t) + V_m\ \dot{m}(o,t), \tag{23}$$

if V is little changing at the tube inlet, or

$$F(o,t) = A(1+kM_o^2)P(o,t) \cong A\ P(o,t), \tag{24}$$

if $M^2 << 1$ at the tube inlet which is common with frictional gas flows in long tubes. Generally, F(ℓ,t) is not a quantity of interest and can be deleted from the dynamic model. A reduced 2-dimensional transmission matrix can then be readily obtained:

$$\begin{bmatrix} P\ (\ell,t) \\ \dot{m}\ (\ell,t) \end{bmatrix} = [G'(\ell,p)] \begin{bmatrix} P(o,t) \\ \dot{m}(o,t) \end{bmatrix} \tag{25}$$

with, in the case expressed by Equation (24), if $M^2 << 1$ at the air inlet,

$$[G'(\ell,p)] = \begin{bmatrix} G'_{11}(p) & G'_{12}(p) \\ G'_{21}(p) & G'_{22}(p) \end{bmatrix} = \begin{bmatrix} G_{11}(p)+A\ G_{12}(p) & G_{13}(p) \\ G_{31}(p)+A\ G_{32}(p) & G_{33}(p) \end{bmatrix} .$$

Natural end causalities, defining at each end which variable is input and which is output, lead to a modification of the non-causal transmission matrix [G'(ℓ,p)], Equation (25), into a causal transfer function matrix. To illustrate this, considering a length of tube where the flow is induced by a pump at the outlet, the mass-flowrate at the outlet and the atmosphere pressure at the inlet are causal inputs; the input-output relationship thus reads

$$\begin{bmatrix} P(\ell,t) \\ \dot{m}(o,t) \end{bmatrix} = [T(\ell,p)] \begin{bmatrix} P(o,t) \\ \dot{m}(\ell,t) \end{bmatrix} \tag{26}$$

$$\text{with } [T(\ell,p)] = \begin{bmatrix} T_{11}(p) & T_{12}(p) \\ T_{21}(p) & T_{22}(p) \end{bmatrix} = \begin{bmatrix} G'_{11} - \frac{G'_{12}G'_{21}}{G'_{22}} & \frac{G'_{12}}{G'_{22}} \\ -\frac{G'_{21}}{G'_{22}} & \frac{1}{G'_{22}} \end{bmatrix} .$$

Expressed in terms of the elements $G_{ij}(\ell,p)$ of the transmission matrix, Equation (22), the 4 transfer functions of the fluid system are

$$T_{11} = G_{11}+A\,G_{12} - \frac{G_{13}(G_{31}+A\,G_{32})}{G_{33}} \qquad T_{12} = \frac{-G_{13}}{G_{33}}$$

$$T_{21} = -\frac{G_{31}+A\,G_{32}}{G_{33}} \qquad T_{22} = \frac{1}{G_{33}} \qquad (27)$$

Implementation of the result -

1. By replacing in the four transfer functions $T_{ij}(p)$ the Laplace operator p by the imaginary frequency $j\omega$, the frequency response in attenuation and phase of the fluid line can be readily investigated.

2. Analog or digital simulation of the fluid line can be directly implemented from the transfer function matrix $[T(\ell,p)]$. Replacing the quantities G_{ij} by their expansion, Equation (22), the elements of [T] can be expanded in terms of A_{ij}, B_{ij} and C_{ij}, associated with exponentials terms.

A practical significance can be attached to each of these terms. a) Terms in $e^{-a\ell}$ represent attenuation of the disturbance wave increasing with the length of tube. b) Terms in $e^{-T\ell p}$ represent elementary time-delays of duration $T\ell$ seconds, then directly proportional to the length of tube; they also depend on the speed of propagation of a perturbation in the direction of the flow and against it. c) Terms A_{ij}, B_{ij} and C_{ij} are lags and account for the dispersive behavior of the line.

Limiting Case of Negligible Bulk-Flow Velocity

Although a non-negligible bulk-flow velocity was assumed to enable one-dimensional flow analysis and to allow approximation (8), it is interesting to evaluate the transmission matrix of the fluid line when the mean flow velocity vanishes and to see how the resulting stationary flow matrix approaches the known result of a uniform transmission line.

As $V_m \longrightarrow 0$, the coefficients of $[R_m]$ become

$$C_1 = C_4 = \lambda \qquad T_1 = T_2 = 0$$
$$C_2 = \lambda/A \qquad T_3 = 1/A$$
$$C_3 = \lambda A \qquad T_4 = A/RT_m.$$

The roots of the characteristic polynomial become

$$s_1 = -s_2 = -cD = -D/\sqrt{RT_m}$$
$$s_3 = 0.$$

These roots yield a reduced transmission matrix

$$[G'(\ell,D)]_o = \begin{bmatrix} \frac{1}{2}(e^{\Gamma}+e^{-\Gamma}) & \frac{-1}{2Ac}(e^{\Gamma}-e^{-\Gamma}) \\ \frac{-Ac}{2}(e^{\Gamma}-e^{-\Gamma}) & \frac{1}{2}(e^{\Gamma}+e^{-\Gamma}) \end{bmatrix}$$

with $$\Gamma = c\ell D = \frac{\ell}{\sqrt{RT_m}}D.$$

$[G'(\ell,D)]_o$ is the transmission matrix of a uniform transmission line of characteristic impedance $\underline{z}_c = 1/Ac$ and of propagation operator $\Gamma = c\ell D$. This corresponds to a distributed series impedance $\underline{z} = \ell D/A$ and a distributed shunt admittance $Y = Ac^2\ell D$. This comparison with the known results of a uniform transmission line partially establishes the validity of the dynamic model represented by the matrices [G] and [T].

Further comparison of the linearized equations (15) with the equations describing a uniform transmission line shows [10] partial correspondence between their respective terms. Series

resistance and inductance and shunt capacitance per unit length of tube can be identified as

$$R^* = \frac{\lambda V_m}{A}(1+kM_m^2)$$

$$I^* = \frac{1}{A}(1+kM_m^2)$$

$$C^* = \frac{A}{RT_m}.$$

Conclusion

An original analytical method of solution has been presented for the equations of unsteady, adiabatic, frictional gas flow in a tube with large bias velocity. Proper choice of integrating variables and linearization about time-averaged bulk-flow velocity and mean temperature allows integration as an ordinary matrix differential equation. The integration results in an analytic dynamic model of the fluid line, in the form of a transmission matrix, only a function of the length of the line and of the linear time-derivative operator, p.

Implementation of this model is simple and requires little additional calculations, regardless of variations of the end-conditions. It also allows direct simulation of the fluid line.

Validity is, as yet, only partially established by comparing the zero bulk-flow velocity limit of the derived model with the known results of uniform transmission lines.

Limitations include slowly varying end-conditions and non-negligible, shock-free bulk flows.

Nomenclature

a	attenuation term, L^{-1}
A	tube cross sectional area, L^2
A_{ij}	quotient of polynomials in D, or p
b	time delay per unit length of line, $L^{-1}T$
B_{ij}	quotient of polynomials in D, or p
c	time delay per unit length of line, $L^{-1}T$
C_1, C_2, C_3, C_4	positive constants, elements of $[R_m]$
C_{ij}	quotient of polynomials in D, or p
C_p, C_v	fluid specific heats per unit mass at constant pressure, constant temperature, $L^2T^{-2}\theta^{-1}$
D	-tube diameter, L -time-derivative operator ($\equiv \partial/\partial t$)
e	= 2.718...
$F(x,t)$	impulse function = $A(P+\rho V^2)$, MLT^{-2}
f	Fanning friction factor (=1/4 × D'arcy-Weisbach friction factor)
$[G(\ell,D)]$	3 × 3 non-causal transmission matrix
$G_{ij}(\ell,D)$, $G_{ij}(\ell,p)$	elements of $[G(\ell,D)]$
$[G'(\ell,p)]$	2 × 2 reduced transmission matrix
$G'_{ij}(p)$	elements of $[G'(\ell,p)]$
$[G(s,D)]$	3 × 3 matrix, Laplace transform of $[G(\ell,D)]$ in x-domain
$G_{ij}(s)$	elements of $[G(s,D)]$
h	enthalpy per unit mass (= C_pT), L^2T^{-2}
$H_f(x,t)$	enthalpy flow = $h\dot{m}$ = $AC_p\rho VT$, ML^2T^{-3}
I	identity matrix
j	= $\sqrt{-1}$
k	= C_p/C_v
ℓ	length of tube, L

M	Mach number = $V/\sqrt{kRT}$
$\dot{m}(x,t)$	mass flowrate, MT^{-1}
$P(x,t)$	static pressure, $ML^{-1}T^{-2}$
p	parameter for Laplace transformation in time-domain
$[R]$, $[R_m]$	3 x 3 matrix with variable coefficients, with constant coefficients, evaluated about V_m and T_m
R	gas constant, $L^2T^{-2}\theta^{-1}$
s	parameter for Laplace transformation in x-domain
s_1, s_2, s_3	roots of the characteristic polynomial
T	-local absolute fluid temperature, θ -in e^{-TD}, time delay, T
$[T]$	transfer function matrix
T_{ij}	elements of $[T]$
T_m	time-averaged mean flow temperature, θ
T_1, T_2, T_3, T_4	positive constants, elements of $[R_m]$
t	time, T
u	local internal energy per unit mass, L^2T^{-2}
V	local flow velocity, LT^{-1}
V_m	time-average bulk flow velocity, LT^{-1}
x	axial coordinate, L
$\underline{z}$	3 x 1 vector
π	= 3.14159...
ρ	local fluid density, ML^{-3}
τ_{xx}	normal viscous stress on a cross section, $ML^{-1}T^{-2}$
τ_w	wall shearing stress, $ML^{-1}T^{-2}$

References

1. Nichols, N. B., "The Linear Properties of Pneumatic Transmission Lines," ISA Transactions, Vol. 1, January 1962, pp. 5-14.

2. Brown, F. T., "The Transient Response of Fluid Lines," Journal of Basic Engineering, Trans. ASME, Vol. 84, No. 4, December 1962, pp. 547-553.

3. Ansari, J. S., and Oldenburger, R., "Propagation of Disturbance in Fluid Lines," Journal of Basic Engineering, Trans. ASME, Vol. 89, No. 2, June 1967, pp. 415-422.

4. Karam, J. T., Jr., and Franke, M. E., "The Frequency Response of Pneumatic Lines," Journal of Basic Engineering, Trans. ASME, Vol. 89, No. 2, June 1967, pp. 371-378.

5. Reid, K. N., "Dynamic Models of Fluid Transmission Lines," Proceedings of Symposium on Fluidics and Internal Flow, October 1968, Vol. I, pp. 143-172.

6. Tijdeman, H., "Remarks on the Frequency Response of Pneumatic Lines," Journal of Basic Engineering (Technical Briefs), Trans. ASME, Vol. 91, No. 2, June 1969, pp. 325-327.

7. Orner, P. A., "Linear Dynamic Modeling of Plowing Fluid Lines," Journal of Basic Engineering, Trans. ASME, Vol. 91, No. 4, December 1969, pp. 740-749.

8. Kantola, R., "Transient Response of Fluid Lines Including Frequency Modulated Inputs," Journal of Basic Engineering, Trans. ASME, Vol. 93, No. 2, June 1971, pp. 274-282.

9. Brown, F. T., Margolis, D. L., and Shah, R. P., "Small-Amplitude Frequency Behavior of Fluid Lines with Turbulent Flow," Journal of Basic Engineering, Trans. ASME, Vol. 91, No. 4, December 1969, pp. 678-693.

10. Mercier, O. L., "Dynamic Modeling and Control of Pneumatic Tube-Vehicle Systems," M. S. Thesis, Duke University, Durham, N. C., 1972.

11. Brown, F. T., "A Unified Approach to the Analysis of Uniform One-Dimensional Distributed Systems," Journal of Basic Engineering, Trans. ASME, Vol. 89, No. 2, June 1967, pp. 423-432.

12. Pipes, L. A., "Applied Mathematics for Engineers and Physicists," McGraw-Hill Book Company, Inc., New York, New York, 1958.

III. FINANCIAL REPORT

NASA Sustaining University Grant

URBAN TRANSPORTATION SYSTEMS

Expenditures February 1, 1969 - June 30, 1972

A.	Salaries and Wages		
	1. Faculty	$48,800.44	
	2. Technical	2,596.34	
	3. Secretarial	2,397.10	
	4. Graduate Students	17,777.95	
	Total Salaries and Wages		$ 71,571.83
B.	Fringe Benefits		5,398.51
C.	Overhead		38,039.75
D.	Supplies and Equipment		5,218.50
E.	Computer and Equipment Rentals		1,799.56
F.	Travel		4,570.81
		TOTAL	$126,598.96*

*Renewal Grant 1969 of $100,000 plus $26,598.96 carryover project funds from 1968-69.